SYNTHESIS, CHARACTERIZATION, AND APPLICATION OF LOW AND REDUCED BAND GAP THIENO[3,4-*b*]PYRAZINE-BASED MATERIALS

A Dissertation
Submitted to the Graduate Faculty
of the
North Dakota State University
of Agriculture and Applied Science

by

Michael Edward Mulholland

In Partial Fulfillment of the Requirements
For the Degree of
DOCTOR OF PHILOSOPHY

Major Department:
Chemistry and Biochemistry

July 2013

Fargo, North Dakota

North Dakota State University
Graduate School

Title

Synthesis, Characterization, and Application of Low and Reduced Band Gap Thieno[3,4-*b*]pyrazine-based Materials

By

Michael Edward Mulholland

The Supervisory Committee certifies that this ***disquisition*** complies with North Dakota State University's regulations and meets the accepted standards for the degree of

DOCTOR OF PHILOSOPHY

SUPERVISORY COMMITTEE:

Seth Rasmussen
Chair

Pinjing Zhao

Sivaguru Jayaraman

Victoria Gelling

Approved:

10/23/2013
Date

Gregory Cook
Department Chair

ABSTRACT

Conjugated polymers are a class of materials receiving significant interest due to their unique combination of optical and electronic properties found in inorganics with the flexibility and processability of traditional organic plastics. These materials have become popular in application to electronic devices such as organic photovoltaics (OPVs), organic light-emitting diodes (OLEDs), sensors, electrochromics and field effect transistors (FETs). As the energetic gap between frontier orbitals, the band gap (E_g) is largely responsible for the energetic transitions of these materials and thus tuning of this parameter is of great interest. A popular method to reducing E_g is through the use of fused ring systems such as thieno[3,4-*b*]pyrazines (TPs). These TP-based materials have been previously applied to solar cells. However, all exhibited limited efficiency (<5% PCE). In an effort to improve the efficacy of TPs in electronic devices, the scope of available TP materials was expanded in an effort to study the effect of changing both side chain and comonomer has on the material properties.

In an effort to study the effect of side chains Rasmussen and coworkers introduced a new method in 2008 toward synthesis of 2nd generation TPs with expanded electronic tuning. To further develop this work, preparation of new electron-withdrawing TPs were generated. Application of 1st and 2nd generation TPs in the production of homopolymeric and copolymeric materials was performed, along with characterization of their optical and electronic properties. Select materials with altering side chain and comonomeric unit were then applied to OPV devices and efficiencies were evaluated based on the changed parameter.

ACKNOWLEDGEMENTS

I would first like to thank my advisor, Prof. Seth Rasmussen, for his significant assistance over past the five years. Whether discussing chemistry, video games, or Game of Thrones, Seth had an open door and was willing to assist in the furthering of my career in chemistry. I would like to thank the rest of my committee for their help and advice over the course of my graduate career. Without excellent lab members, the journey through graduate school would be significantly more challenging. I was fortunate to have such lab members working with me daily, assisting in my work and making the lab an enjoyable place to work. I would particularly like to mention Dr. Sean Evenson and Ryan Schwiderski who both worked with me for many years.

I would like to make special thanks to my family, particularly my mom and dad who were always supportive of my goals and helping me along the way. I would also like to thank my sister, Sarah and her husband, Josh. Whether listening to me talk about my research, helping me pick an apartment in Fargo, or going to rock concerts, they provided support I greatly appreciated and made my time here much more enjoyable. My grandparents, Russ and Kathy, have been instrumental in helping me, both through good and bad times, when all other lights go out.

As I am an avid gamer I would like to thank Bioware and Bethesda for making excellent games which I sank far too much time into. Through the course of my graduate career playing games allowed me to relax and recharge before going to do more chemistry. My friends Nicholas Youngs, Jon Powell, and Ashley Ward also have been a source of enjoyment and support for many years. Finally I would like to thank my Dungeons and Dragons group: Eric (Ooze) Uzelac, Eric Jannsen, Seth Adrian, Anthony Clay, Alisa Fairweather, Dillon Hofsommer, Sammy Silbert, and Kristine Konkol. The time was short, but it was fun.

DEDICATION

Dedicated to my mother:

Dorothy Jean Mulholland

TABLE OF CONTENTS

LIST OF TABLES

LIST OF FIGURES

LIST OF SCHEMES

LIST OF CHARTS

LIST OF ABBREVIATIONS AND ACRONYMS

BDT.....benzodithiophene

BHJ .....bulk heterojunction

br .....broad

BTD.....2,3,1-benzothiadiazole

BuLi .....butyllithium

CP.....conjugated polymer

CT .....charge-transfer

CV .....cyclic voltammetry

DA.....donor-acceptor

dba.....dibenzylideneacetone

DCM .....dichloromethane

DIO 1,8-diiodooctane

DMEDA.....*N,N'*-dimethylethylenediamine

DMF.....*N,N*-dimethylformamide

DP .....degree of polymerization

DTP.....dithieno[3,2-*b*:2',3'-*d*]pyrrole

EDOT.....3,4-ethylenedioxythiophene

E_g.....band gap

E_{pa}.....anodic peak potential

EtOAc .....ethyl acetate

EW .....electron-withdrawing

eV.....electron volt

FF .....fill factor

GPC.....gel permeation chromatography

GRIM .....Gignard metathesis

H.....hour

HH.....head-to-head

HOMO .....highest occupied molecular orbital

HT .....heat-to-tail

ITO.....indium tin oxide

IV .....current-voltage

J_{sc}.....short circuit voltage

LUMO.....lowest unoccupied molecular orbital

min .....minute

MO .....molecular orbital

mp .....melting point

M_n.....number average molecular weight

M_w .....weight average molecular weight

NBS.....*N*-bromosuccinimide

NIR.....near infrared

NMR .....nuclear magnetic resonance

OFET.....organic field effect transistor

OLED.....organic light-emitting diode

OPV.....organic photovoltaic

P3AT.....poly(3-alkylthiophene)

P3HT .....poly(3-hexylthiophene)

PC_6TP.....poly(2,3-dihexylthieno[3,4-*b*]pyrazine

$PC_{61}BM$.....phenyl-C_{61}-butyric acid methyl ester

PCE .....power conversion efficiency

PDI .....polydispersity index

PEDOT.....poly(3,4-ethylenedioxythiophene)

PPV .....poly(phenylene vinylene)

PSS.....polystyrene sulfonic acid

PTH .....*N*-ocytlphthalimide

RB .....round bottom

RT .....room temperature

s .....second

S .....siemen

$TBAPF_6$.....tetrabutylammonium hexafluorophosphate

THF .....tetrahydrofuran

TLC .....thin-layer chromatography

TMEDA .....*N,N,N',N'*-tetramethylethylenediamine

TP .....thieno[3,4-*b*]pyrazine

TPBDT.....poly(thieno[3,4-*b*]pyrazine-*co*-benzodithiophene)

TPBTD.....poly(thieno[3,4-*b*]pyrazine-*co*-2,3,1-benzothiadiazole)

TPDTP .....poly(thieno[3,4-*b*]pyrazine-*co*-dithieno[3,2-*b*:2'3'-*d*]pyrrole)

TPFLO .....poly(thieno[3,4-*b*]pyrazine-*co*-fluorene)

TPPTH .....poly(thieno[3,4-*b*]pyrazine-*co*-*N*-octylphthalimide

TT.....tail-to-tail

UV-vis.....ultraviolet-visible

V.....volt

V_{oc}…….. ...open circuit voltage

CHAPTER 1. INTRODUCTION

1.1. Background of Conjugated Polymers

Conjugated polymers (CPs), often referred to as synthetic metals or conducting polymers, are a class of polymeric organic materials which feature extended pi orbital overlap along the backbone.[1] This overlap, shown in Figure 1.1, leads to an overall delocalization of electrons, creating a material which has conducting and optical properties similar to those of inorganic semiconductors. Combining these features with those of typical insulating plastics such as mechanical flexibility, ease of processing, and low density, produce materials[2,3] which have been used in a number of electronic devices including organic photovoltaics (OPVs),[2,4-6] organic light emitting diodes (OLEDs),[1,7-14] electrochromics,[15-19] sensors[20-25] and organic field effect transistors (OFETs).[9,26-33] Additionally these materials can be modified on a molecular level, allowing for specific tuning of the electronic and optical properties.[2,3,26,34,35.]

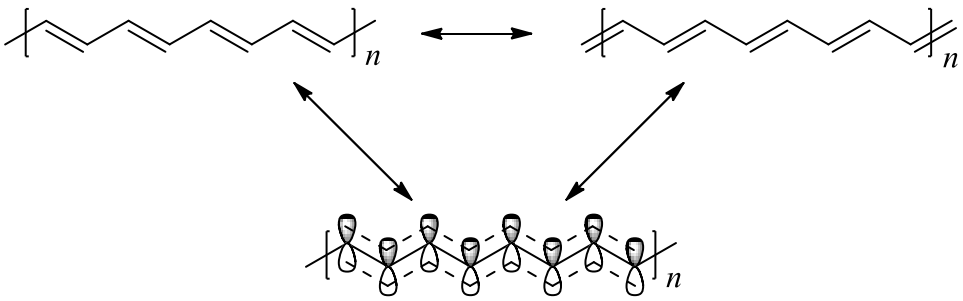

Figure 1.1. Conjugation via overlapping π orbitals illustrating π conjugation.

Although conjugated polymers had been in existence for many years, the first report of CPs featuring significant conductivity was in 1963 by the Australian group of Weiss and coworkers. In this report tetraiodopyrrole was heated, producing a cross-linked polypyrrole in the form of a black powder which displayed conductivities ranging from 0.005 – 1.0 S/cm.[36,37]

Further study showed that decreased iodine content led to a decrease in conductivity. However, at the time of the study the relationship between conductivity and iodine doping was not understood.[37-39] A second study by Jozefowicz and coworkers in 1968 found that the electronic properties of polyaniline could be manipulated by changing the pH of the environment.[37] In 1971 they were able to report conductivities as high as 30 S/cm from protonation of polyaniline by sulfuric acid.[37]

Conjugated polymers gained a great deal more attention upon the accidental generation of polyacetylene films in 1967 by Shirakawa and coworkers. The group had been studying the mechanism of Ziegler-Natta polymerization of acetylene when an error led to the addition of Ziegler-Natta catalyst at one thousand times the normal amount, leading to a silvery-film. Analysis of these films via IR spectroscopy showed that both *cis* and *trans* isomers were present (Figure 1.2) and that configuration was dependent on temperature. An irreversible isomerization of polyacetylene was found to occur at temperatures exceeding 145 °C.[40] Studies of the electronic properties of both isomers yielded a resistivity of 2.4×10^8 Ω cm eV for the *cis*-rich isomer and resistivity of 1.0×10^4 Ω cm for the *trans*.[40]

all *trans*-polyacetylene all *cis*-polyacetylene

Figure 1.2. *Cis* vs. *trans* isomers of polyacetylene.

While on a visit to Japan, Alan MacDiarmid observed the silver films Shirakawa had produced, and became interested in further studying these unique materials. In 1976, Shriakawa was invited to the University of Pennsylvania and met Alan Heeger, who had been collaborating

with MacDiarmid on conductivity studies of poly(sulfur-nitride).[41] Together, the three scientists combined MacDiarmid and Heeger's work on treating poly(sulfur-nitride) with bromine vapor to increase conductivity with Shirakawa's silver polymer films and found that, similar to the poly(sulfur-nitride), polyacetylene experienced a similar effect to four orders of magnitude.[41] However, it was noted that overexposure of the polymer film to bromine could lead to a decrease in conductivity. An additional study, doping *tran*-polyacetylene with iodine vapor gave conductivity over seven orders of magnitude higher, with a maximum conductivity of 38 S/cm.[42] This work was recognized in 2000 when Shirakawa, Heeger, and Macdiarmid were awarded the Nobel Prize in Chemistry for the discovery and development of conducting polymers.[43] Although this wording is often used to describe the accomplishment of these three individuals, as discussed, there were several other groups who had previously generated conducting polymers. The work of Shirakawa, Heeger, and Macdiarmid is, nonetheless, very significant in that materials of higher conductivities were generated and their work led to greater exposure of these types of materials, thus truly starting the expansion of work with CPs.

Since the initial studies discussed above, the field has grown substantially with new materials featuring a higher degree of electronic and optical tunability. Application of these materials to commercially-available electronic devices such as OLEDs and OPVs has been achieved, although a great deal more progress is required to develop efficient devices of the latter. A selection of common conjugated polymers which have been developed is shown below in Chart 1.1.

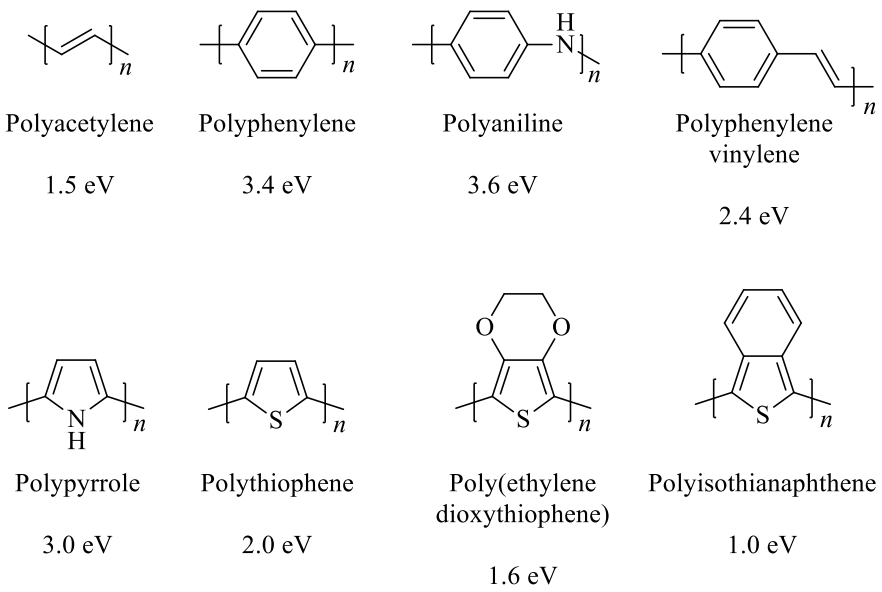

Chart 1.1. Commonly used conjugated polymers and their respective band gaps.[44]

1.2. Band Gap

One of the critical parameters which largely determines the optical and electronic properties for these materials is the band gap (E_g). The E_g is defined as the energetic separation between the filled valence and unfilled conduction bands of the bulk solid-state material. This is analogous to the HOMO-LUMO gap for molecular species. For an insulator this gap is large, typically over 2 eV. Conductors, such as metallic species, feature no gap between bands and thus electrons are able to feely move through the solid material. Between these two are semiconductors which typically have band gaps between 0 – 2 eV. A semiconductor with a band gap closer to 0 eV will often feature higher conducting behavior whereas ones closer to 2.0 eV will be more insulator-like. The conducting behavior is due to an increase of charge carriers existing in the conduction band. A lower band gap will allow excitation of electrons, through external sources of either induced potential or photon, to occur with a lower energy.

Additionally, lower energy between the two bands allows an enhanced thermal population of charge carriers in the conduction band.[45]

Within semiconducting materials there exists the sub classification of *low band gap* materials. This term has been used to define materials with a wide range of band gaps, including those with an E_g up to 2.0 eV. In 1998, Pomerantz proposed a definition of low band gap as materials featuring an E_g below 1.5 eV.[46] This E_g value is below that of polyacetylene (1.5 eV) which has the lowest band gap of the parent CPs. Thus the definition by Pomerantz retains the definition that no parent compounds are considered low band gap materials. While others have tried to redefine low band gap as < 2.0 eV, this definition has little meaning as most thiophene-based materials have band gaps around 2.0 eV. In support of Pomerantz's original definition, Rasmussen encourages this definition of low band gap materials. Additionally he has proposed materials featuring band gaps between 1.5 and 2.0 eV be called *reduced band gap* materials to give a more solid definition for those materials in this range.[45,47]

While metallic species feature true band-like energy structure, molecular systems such as conjugated polymers have bands which are derived from the combination of molecular orbitals (MOs). As previously discussed conjugated systems feature extended p orbital overlap which leads to greater π-conjugation through the material backbone and delocalization of electrons. This π-conjugation leads to a molecular structure which has narrowly spaced energy levels. As conjugation increases, the number of MOs increases and the spacing between MOs continues to decrease. Upon formation of a bulk solid-state material MOs become energetically indistinguishable and blend to form two bands, the filled π band being the valence band the empty π* band being the conduction band. The space between bands is then the E_g of the bulk material. A graphical representation of the generation of bands is shown in Figure 1.3.

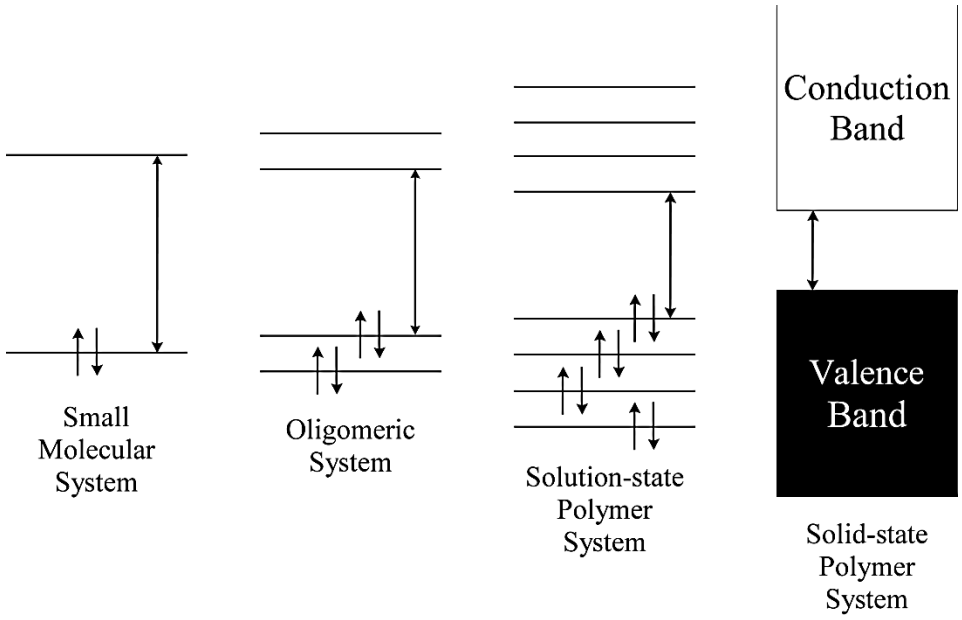

Figure 1.3. Band and molecular orbital (MO) structure in π-conjugated systems.

There are two basic methods to determine the band gap of a material, the first of which is via the solid state absorption of a film. Measurements of E_g in solution have been published, however solid state films give more accurate values, as in solution interchain coupling is limited. In this method the steepest slope of the lowest energy transition is extrapolated to the baseline, corresponding to a wavelength, illustrated in Figure 1.4A. This is then converted to an energy giving the optical band gap. Although this method is efficient toward the determination of E_g, its accuracy is not high. A second method toward determining band gap from an absorption profile plots hν vs. $(A \times h\nu)^2$, where hν is the photon energy and A is absorbance (Fig 1.4B).[44] This is the formally accepted method toward determining the optical band gap. Although absorption is useful in determining E_g, this method gives no information on oxidation or reduction potentials.

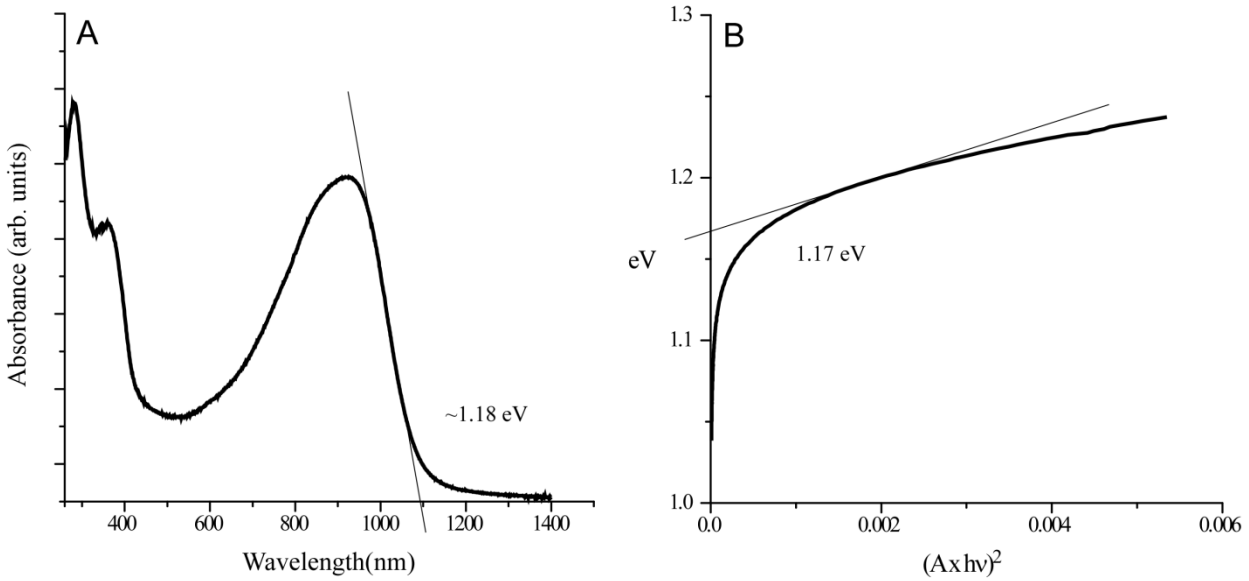

Figure 1.4. Determination of optical band gap by (A) extrapolation of transition edge to baseline and (B) plot of eV vs. (A x hν).[2]

Cyclic voltammetry (CV) is the second commonly used method to determine band gap. This method additionally provides data on the potential for oxidation and reduction potential. Additionally, the onset of oxidation and reduction may be determined which correspond to the HOMO and LUMO energies respectively. Electrochemical methods toward determination of the band gap utilize the separation between the onset of the potential of oxidation and reduction potential. Determination of HOMO and LUMO energies may be determined by first extrapolating the energy of where the oxidation and reduction onsets meet the background, as shown in Figure 1.5. This energy is then converted from the electrochemical standard to that of Fc/Fc^{+}. This energy may then be conveniently converted to reference against vacuum.[45] As many CPs have band gaps equal to or higher than 2 eV it is common that either oxidation or reduction may occur outside the solvent window. For low band gap materials this is less commonly an issue.

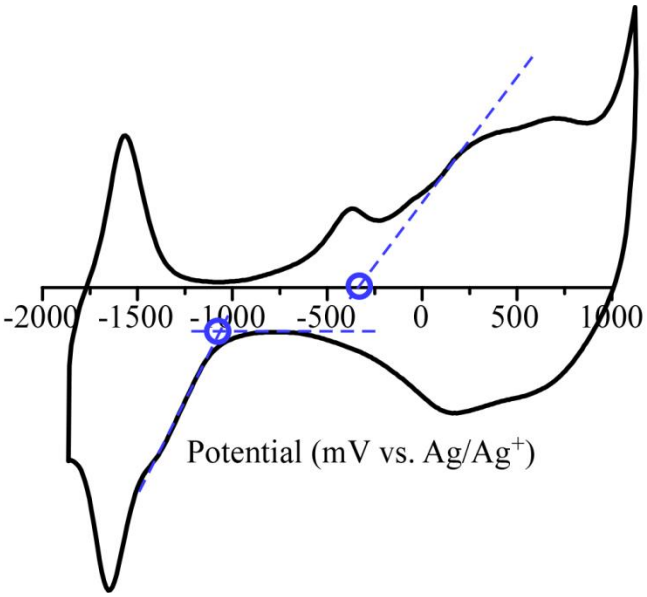

Figure 1.5. Determination of electrochemical band gap.

1.3. Control and Tuning of the Bang Gap

Given how instrumental band gap is in determining a material's optical and electronic properties, it is unsurprising that a great deal of effort is put forth in controlling the band gap along with HOMO and LUMO energies. There are several such methods aimed toward this end, the first of which is bond length alternation.

1.3.1. *Bond Length Alternation*

One of the features shown to be a large contributor to the band gap is bond length alternation. [48-52] As high conjugation is a result of overlapping p orbitals, bonds featuring higher symmetry in bond length character lead to increased delocalization of electrons. This is in contrast to large differences in alternating bond lengths, which feature more single-double or single-triple bond character, which thus leads to reduction in electron delocalization. Reduction in bond length alternation will thus cause a decrease in E_g whereas an increase will cause a larger E_g. One of the most efficient methods to observe this phenomenon is replacing a vinyl unit in a

polymer chain with an ethyne unit. The difference in double bond and triple bond lengths is large enough to observe the difference in bond length alternation. Once example of this is shown with thieno[3,4-*b*]pyrazine (TP) units (Figure 1.6) where the vinyl space polymer has a band gap of 0.88 eV and the ethyne space polymer has a band gap of 0.90 eV.[53]

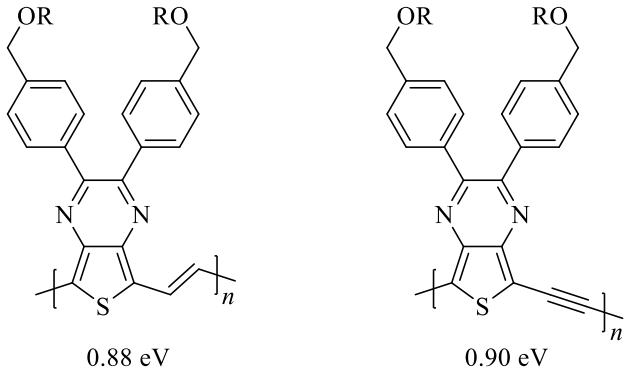

Figure 1.6. Example of bond length alternation and its effect on E_g.[53]

1.3.2. *Resonance Forms*

In contrast to polyacetylene, which features a degenerate ground state, aromatic-based CPs have non-degenerate resonance forms featuring a lower energy aromatic form and higher energy quinoidal form, shown in Figure 1.7.[44,48,49] While the afore mentioned bond length alternation has been shown to significantly affect the energy of the band gap, a much larger effect in aromatic CPs may be seen by promoting the system to the quinoidal form. Thus a transition from primarily the low-energy aromatic form to the higher energy quinoidal form, shown in Figure 1.8, will have a greater effect on reducing E_g.

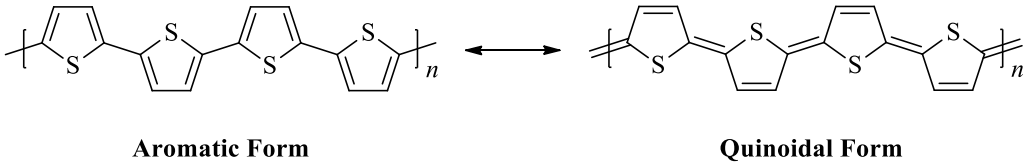

Figure 1.7. Alternation of aromatic and quinoidal forms of polythiophene.

Although the quinoidal form of thiophene is a higher energy state and thus more thermodynamically disfavored, methods toward increasing the propensity of the quinoidal form have been investigated. The primary method toward increasing the quinoidal nature of the thiophene backbone is implementation of a fused-ring system. In such fused-ring systems only one ring may accommodate the proper aromatic sextet in any resonance form and thus be aromatic. Thus, introduction of a fused ring, such as benzene, featuring higher aromaticity (empirical resonance energy of 25.0 kJ mol^{-1}) effectively limits the aromaticity of the thiophene (empirical resonance energy of 20.3 kJ mol^{-1}) backbone causing it to enter the quinoidal state.[47] Examples of the implementation of this include polyisothianaphthene (1.0 eV) and poly(thieno[3,4-*b*]pyrazine) (0.7 eV), which both feature band gaps lower than the parent polythiophene (2.0 eV).[44]

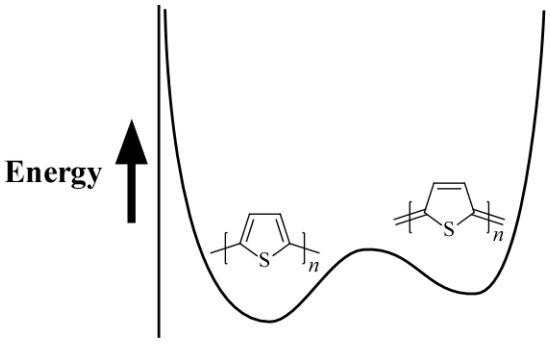

Figure 1.8. Energy diagram for polythiophene-based resonance structures.

1.3.3. *Planarity*

As band gap is highly reliant on the overlap of p orbitals, deviations from planarity of the polymer backbone can lead to significant increases in E_g. Theoretical studies have shown that torsional angles up to 30° will lead to minimal impact on π-overlap, however, larger deviations will cause significant increase in E_g.[54] The two most common causes toward deviations to planarity are β-hydrogen interactions amongst neighboring aromatic units and side chain interactions. Bond rotation due to β-hydrogen repulsion, as shown in Figure 1.9 A, is a larger issue for six-membered aryl polymers when compared to five-membered analogous systems.

One of the key advantages of organic electronics over their inorganic counterparts is solution processability, necessitating solubility of the polymer in common solvents. Most unfunctionalized CPs are completely insoluble due to strong interchain π stacking and thus functionalization via side chain addition is required. While addition of side chains provides solubility to the polymer, it also increases steric interactions via repulsion from side chains with the polymer backbone and neighbor side chains (Figure 1.9 B). Methods exist, however, aimed toward reducing the amount of steric repulsion.

One such method of reducing side chain interactions for asymmetric functionalized polymers is controlling the coupling mode. This method has been thoroughly investigated for poly(3-alkylthiophene)s (P3ATs) and thus will provide the primary example. For these systems there are three coupling modes: head-to-head (HH), head-to-tail (HT), and tail-to-tail (TT). It has been shown that in the case of HH coupling chain-chain interactions are maximized leading to increased rotation along the polymer backbone.[55] While TT coupling in one position of the polymer will increase separation of side chains at the coupled site, in a regioirregular polymer, this will always result in HH coupling.

In the case of HT coupling these chain-chain interactions are minimized thus leading to limited rotation. The selectivity of the HT mode over the others yields the regioregular polymer versus a regiorandom analogue. While side chain interactions with the sulfur lone pair still exist; these have a lower impact on torsional rotation than that of HH side chain interactions. Thus due to the advantages of regioregular P3ATs over regiorandom P3ATs via reduction of steric interactions, methods in improving the regioregularity of these P3ATs have been extensively investigated.[55-60]

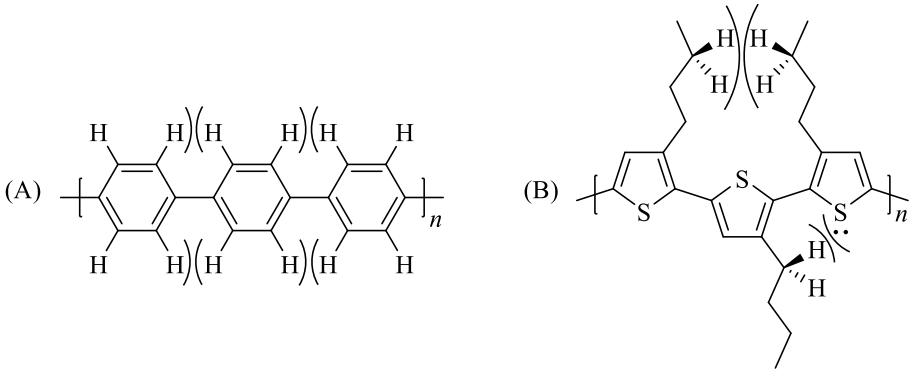

Figure 1.9. Torsional rotations stemming from (A) β-hydrogen repulsion and (B) side chain interactions.

A second method toward reducing side chain repulsion is exchange of heteroatoms in place of the α-methylene in the polymer side chain, Chart 1.2. The bulky α-methylene group can induce steric repulsion from a lone pain on neighboring monomer units, such as thiophene, causing twisting of the backbone. Exchanging a heteroatom in place of the methylene group can reduce the volume of this position and thus limit these steric repulsions, reducing band gap.[2,57] An added advantage to this strategy is the inductive effects of the heteroatom.[2,57,58] Electron donating heteroatoms, such as oxygen or nitrogen, destabilize the HOMO thus reducing the potential for oxidation and further reducing E_g. A limitation toward alkoxy side chain

substitution is reduced solubility due to fewer steric interactions. Intermediately-sized side chains such as amino groups yield improved solubility with similar electronic effects; however, with an increased steric bulk.[44]

Difunctionalized thiophenes have also been produced and shown to have advantageous characteristics by further modification of the electronics. One concern with these types of systems is the reintroduction of chain-chain interactions. To address this side chains featuring bridging alkyl groups were generated to reduce the chain-chain interactions. One of the most common of these is 3,4-ethylenedioxythiophene (EDOT) which features a bridging ethylene group.[61] The polymeric form of EDOT, PEDOT, has shown many beneficial properties, many of which are due to the lone pairs on the two oxygens featured on each unit. These electron-donating groups cause a destabilization of the polymer's HOMO, making it a good donor material.[45,62] One of the most common uses of this material is as a doped salt using poly(styrenesulfonate) (PSS) as a polyanion. This doped polymeric salt is commonly referred as PEDOT:PSS. This polymeric salt is commonly used to coat the bottom electrode of devices such as OLEDs and OPVs prior to addition of the active layer. [62,63]

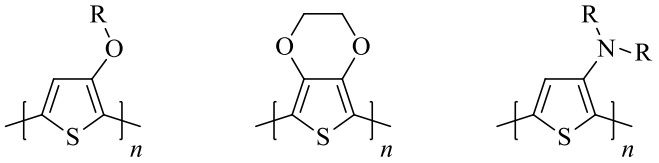

Chart 1.2. Polythiophenes featuring heteroalkyl side chains.

1.3.4. *Donor-Acceptor Copolymers*

One of the more popular approaches in recent years toward the generation of polymers featuring a low band gap is the combination of an electron deficient 'acceptor' (A) unit and an

electron rich ‘donor’ (D) unit in an alternating ‘donor-acceptor’ (DA) copolymer.[l,63] This approach was first presented by Havinga and co-workers based on the systems of polysquarains and polycroconains, both of which exhibited low band gaps.[64] In this approach it was thought that the donor material would modulate the polymer’s HOMO and the acceptor system would modulate the polymer’s LUMO. By combining these effects in a polymer featuring strong donor and acceptor units a reduction in E_g can occur.[64-70] An example of HOMO/LUMO gap reduction, with dimer systems of DD, AA, and DA in the ground state may be seen in Figure 1.10.[71] Initial thought behind this model also placed the first excitation state as a charge transfer from the HOMO-localized donor to LUMO-localized acceptor.

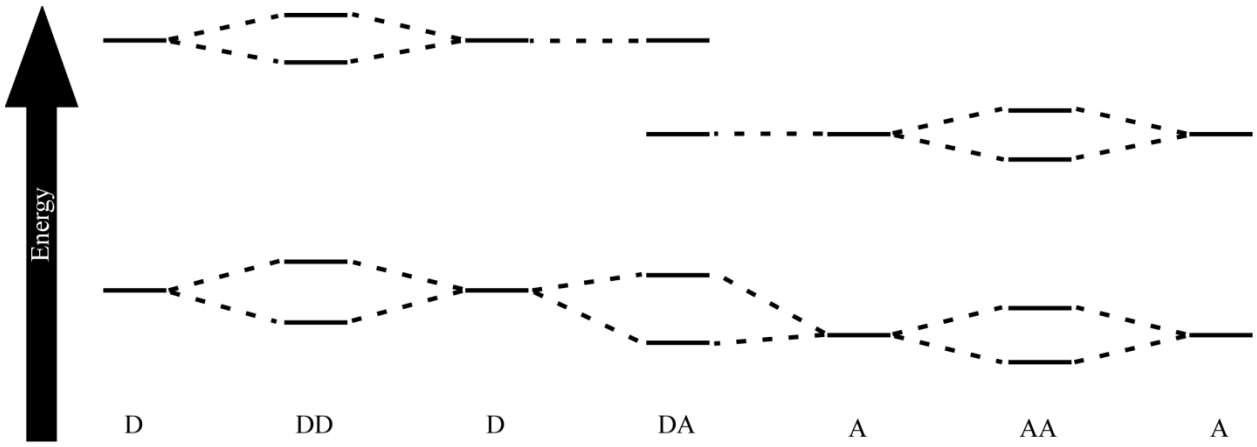

Figure 1.10. Energy scheme for donor-acceptor model showing dimer combinations of a donor with itself (DD), an acceptor with itself (AA) and the mixed system donor-acceptor (DA).[47]

While this method has been successfully used toward the design of numerous low and reduced band gap materials, this technique was initially generated for a specific class of materials, polysquaraines and polycroconains, but has since been implemented to a much broader scope of materials with little alteration to the theory behind it. More recent studies have indicated that rather than isolated donor and acceptor units throughout the backbone, the HOMO is

delocalized along the polymer backbone while the LUMO is located on isolated electron-deficient regions. Thus the primary excited state transition is a backbone to acceptor transition.[71] This also has the logic that for CPs to function delocalization is required, and thus having the HOMO spread over the polymer backbone leads to much further delocalization than that of an isolated donor unit. It has also been suggested that the lowering of E_g may be due to geometric mismatch of monomer units, where donor units are typically aromatic and acceptor units are more commonly quinoidal. Thus providing strong enough donor and acceptor character, a new resonance form might form showing double bond character between donor and acceptor units. Averaging of the two forms reduces bond length alternation, thus reducing band gap.[47,65]

Although units used to generate DA copolymers may fit conveniently as either strong electron donating or electron accepting, several systems have been shown to exhibit traits of both. These ambipolar units will often be the primary contributors to both HOMO and LUMO of the resulting polymers. It has been shown that when combined with typical "donor" units whose HOMO is stabilized in comparison to the ambipolar unit HOMO, E_g will increase. Thieno[3,4-*b*]pyrazine (TP) is one such ambipolar unit which has displayed these characteristics.[45] Combination of TPs with most other donor units will actually cause an increase in band gap from that of the homopolymeric material. This has been shown by Rasmussen and coworkers with combination of TP with EDOT and thiophene units in the generation of terthiophene systems.[72] In both cases, an increase of TP content in favor of either unit causes a red shift in absorption spectra and decrease in potential of oxidation.[71,72] This trend can also be seen in numerous copolymeric systems, where decreased TP content leads to a larger band gap.[45] Utilization of ambipolar materials, such as TPs, in the generation of DA copolymers is of interest for improved molecular design and developing new methods toward tuning the properties of DA. Design of

polymers may be adjusted to accommodate ambipolar units by utilizing the ambipolar unit to modulate the LUMO and selectively tune the HOMO.

1.4. Research Goals

Conjugated materials are of significant interest for application in electronic devices due to their electronic and optical properties. This class of materials has been thoroughly researched generating a wide variety of monomeric, oligomeric, and polymeric materials. Despite these advances significant research remains toward improving the design techniques used to construct new materials. The two most popular approaches in reducing band gap in recent years has been through inducing a quinoidal state by fused ring systems and generation of donor-acceptor copolymers. Thieno[3,4-*b*]pyrazine (TP) is a popular fused ring system used in creating low band gap polymers and has been used to generate reduced and low band gap copolymeric materials. Although numerous materials have been made using this TPs, most have used 1st generation alkyl or aryl analogues and not the more electronically tunable 2nd generation systems. Additionally TPs have commonly been used as traditional acceptor units even though they feature a higher HOMO than most common donors and thus act as ambipolar type units.

One goal of this research project is aimed toward providing insight into the nature of ambipolar units and how their electronic structure affects the overall electronics of generated polymers. Toward that end synthesis of new homopolymeric and copolymeric materials, using of both 1st and 2nd generation TPs will be discussed (Scheme 1.1), illustrating the unique properties of TP in selectively tuning both HOMO and LUMO energies. A second goal of this research is to expand the scope of available TP units, particularly by introduction of new electron-withdrawing side chains. Application of TP materials into solar cell devices will allow further study into how changing both TP-based side chains and comonomer unit affects solar cell efficiency.

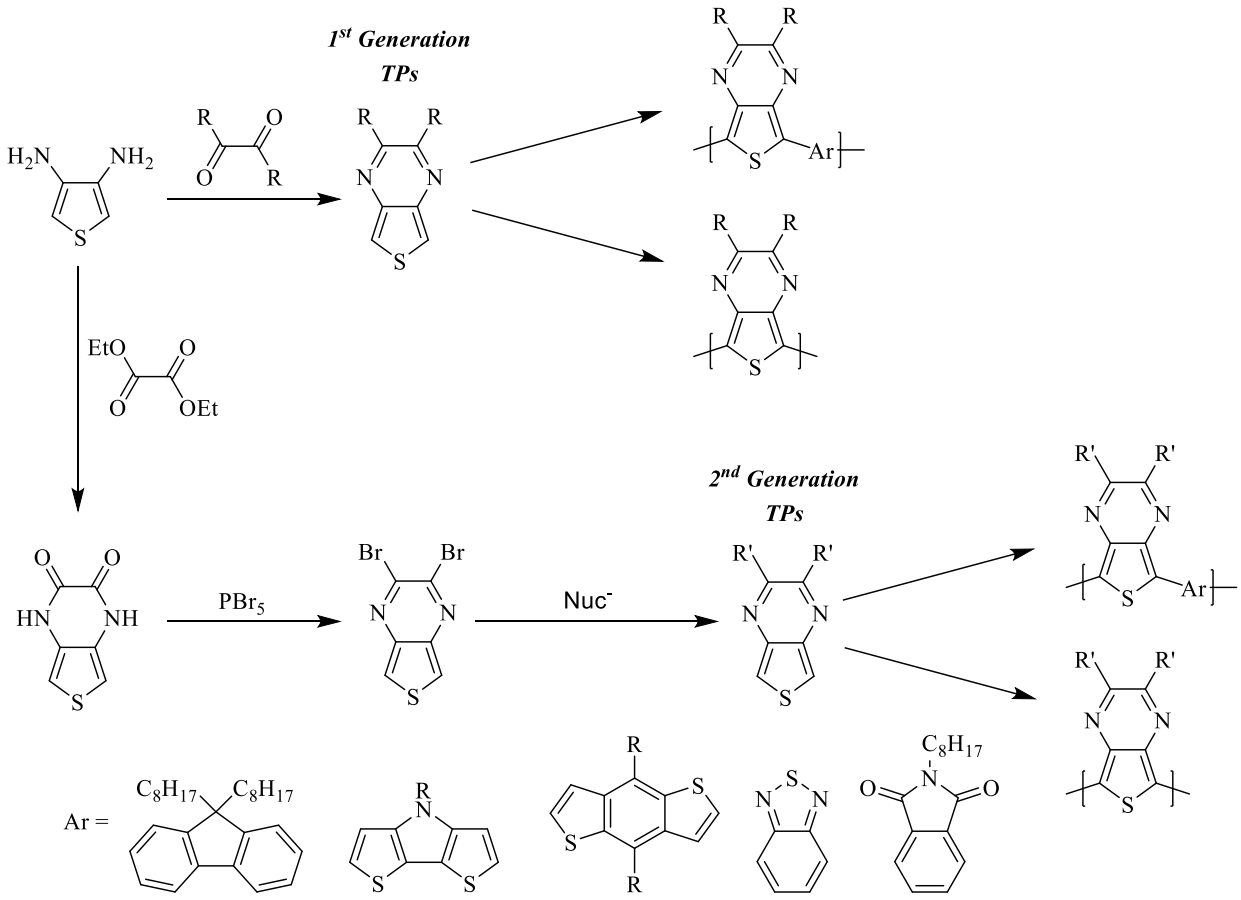

Scheme 1.1. Outline of proposed TP materials.

1.5 References

(1) Nyugen, T. P.; Destruel, P. Electroluminescent Devices Based on Organic Materials and Conjugated Polymers. In *Handbook of Luminescence, Display Materials, and Devices,* Inouye, H. S.; Rohwer, L. S., Eds; Organic, American Scientific Publishers, Sevenson Ranch, CA, 2003; Vol 1; p 5.

(2) Roncali, J. *Chem. Rev.* **1992**, *92*, 711-738.

(3) Roncali, J. *Chem. Rev.* **1997**, *97*, 173-205.

(4) Mozer, A. J.; Sariciftci, N. S. In *Handbook of Conducting Polymers: Processing and Applications,* 3rd ed.; Skotheim, T. A., Reynolds, R., Eds.; CRC Press: Boca Raton, FL, 2007; pp 10-1-10-37.

(5) Brabec, C. J.; Sariciftci, N. S. In *Semicondcuting Polymers: Chemistry, Physics, and Engineering*; Hadziioannou, G., van Hutten, P. F., Eds.; Wiley-VCH: Wienheim, 2000; pp 515-560.

(6) Barbella, G.; Melucci, M. In *Handbook of Thiophene-Based Materials: Applications in Organic Electronics and Photonics*; Perepichka, I. F., Perepichka, D. F., Eds.; Wiley: West Sussex, U. K., 2009; Vol. 1, pp 255-292.

(7) Friend, R. H.; Greenham, N. C. Electroluminescence in Conjugated Polymers. In Handbook of Conducting Polymers, 2nd Ed.; Skotheim, T. A., Elsenbaumer, R. L., Reynolds, J. R., Eds.; Marcel Dekker, Inc: New York, 1998; pp 823-880.

(8) Cui, T.; Liu, Y. In *Organic Electronics and Photonics: Electronic Materials and Devices*, Nalwa, H. H., Ed.; American Scientific: Stevenson Ranch, 2008; Vol. 1 pp 263-303.

(9) Christian-Pandya, H.; Vaidyanathan, S.; Galvin, M. In *Handbook of Conducting Polymers*, 3rd ed.; Skotheim, T. A., Reynolds, J. R., Eds.; CRC Press: Boca Raton, FL, 2007; Chapter 5.

(10) Grimsdale, A. C.; Chan, K. L.; Martin, R. E.; jokisz, P. G.; Holmes, A. B. *Chem. Rev.* **2009**, *109*, 897-1091.

(11) Epstein, A. J.; Wang, Y. Z. In *Semiconducting Polymer: Applications, Properties, and Synthesis*, Hsieh, B. R., Wei, Y., Eds.; American Chemical Society: Washington, DC, 1999; pp 160-173.

(12) Murray, M. M.; Holmes, A. B. In *Semiconducting Polymers: Chemistry, Physics, and Engineering*; Hadziioannou, G., van Hutten, P. F., Eds.; Wiley-VCH: Weinheim, 2000; pp 1-35.

(13) Campbell, I. H.; Smith, D. L. In *Semiconducting Polymer: Chemistry, Physics, and Engineering*; Hadziioannou, G., van Hutten, P. F., Eds.; Wiley-VCH: Weinheim, 2000; pp 333-364.

(14) Scott, J. C.; Malliaras, G. G. In *Semiconducting Polymers: Chemistry, Physics, and Engineering*; Hadziioannou, G., van Hutten, P. F., Eds.; Wiley-VCH: Weinheim, 2000; pp 411-462.

(15) Thomas, C. A.; Reynolds, J. R. In *Semiconducting Polymers: Applications, Properties, and Synthesis*; Hsieh, B. R., Wei, Y., Eds.; American Chemical Society: Washington, DC, 1999; pp 367-373.

(16) Meng, X. S.; Desjardins, P.; Wang, Z. Y. In *Semiconducting Polymers: Applications, Properties, and Synthesis*; Hsieh, B. R., Wei, Y., Eds.; American Chemical Society: Washington, DC, 1999; pp 61-75.

(17) Invernale, M. A.; Acik, M.; Sotzing, G. A. In *Handbook of Thiophene-Based Materials: Applications in Organic Electronics and Photonics*; Perepichka, I. F., Perepichka, D. F., Eds.; Wiley: West Sussex, U. K., 2009; Vol. 1, pp 757-782.

(18) Beaujuge, P. M.; Reynolds, R. *Chem Rev.* **2010**, *110*, 268-320.

(19) Beaujuge, P. M.; Amb, C. M.; Reynolds, J. R. *Acc. Chem. Res.* **2010**, *43*, 1396-1407.

(20) Guiseppi-Elie, A.; Wallace, G. G.; Matsue, T. In *Handbook of Conducting Polymers*, 2nd Ed.; Skothiem, T. A., Elsenbaumer, R. L., Reynolds, J. R., Eds.; Marcel Dekker, Inc.: New York, 1998; pp 963-992.

(21) Kossmehl, G.; Engelmann, G. In *Handbook of Oligo- and Polythiophenes*; Fichou, D., Ed.; Wiley-VCH: Weinheim, 1999; pp 491-524.

(22) Guiseppi-Elie, A.; Brahim, S.; Wilson, A. M. In *Handbook of Conducting Polymers: Processing and Applications*, 3rd Ed.; Skotheim, T. A., Reynolds, J. R., Eds.; CRC Press: Boca Raton, FL, 2007; pp 12-1-12-45.

(23) Nilsson, P.; Inganäs, O. In *Handbook of Conducting Polymers: Processing and Applications*, 3rd Ed.; Skotheim, T. A., Reynolds, J. R., Eds.; CRC Press: Boca Raton, FL, 2007; pp 13-1-13-24.

(24) MacDiarmid, A. G.; Huang, F.; Feng, J. In *Semiconducting Polymers: Applications, Properties, and Synthesis*; Hsieh, B. R., Wei, Y., Eds.; American Chemical Society: Washington, DC, 1999; pp 184-215.

(25) Ho, H.-A.; Leclerc, M. In *Handbook of Thiophene-Based Materials: Applications in Organic Electronics and Photonics*; Perepichka, I. F., Perepichka, D. F., Eds.; Wiley: West Sussex, U. K., 2009; Vol. 1, pp 813-832.

(26) Katz, H. E.; Dadabalapur, A.; Bao, Z. Oligo- and Polythiophenes; Fichous, D., Eds; Wiley-VCH, Germany, 1999; pp 490-495.

(27) Tessler, N.; Veres, J.; Globerman, O.; Rappaport, N.; Preezant, Y.; Roichman, Y.; Solomesch, O.; Talk, S.; Gershman, E.; Alder, M.; Zolotarev, V.; Gorelik, V.; Eichen, Y. In *Handbook of Conducting Polymers: Processing and Applications*, 3rd Ed.; Skotheim, T. A., Reynolds, J. R., Eds., CRC Press: Boca Raton, FL, 2007; pp 7-1-7-42.

(28) Bao, Z. In *Semiconducting Polymers: Applications, Properties, and Synthesis*; Hsieh, B. R., Wei, Y., Eds.; American Chemical Society: Washington, DC, 1999; pp 244-257.

(29) Horowitz, G. In *Semiconducting Polymers: Chemistry, Physics and Engineering*; Hadziioannou, G.; van Hutten, P. F., Eds.; Wiley-VCH: Weinheim, 2000; pp 463-514.

(30) Otsubo, T.; Takimiya, K. In *Handbook of Thiophene-Based Materials: Applications in Organic Electronics and Photonics*; Perepichka, I. F., Perepichka, D. F., Eds.; Wiley: West Sussex, U. K., 2009; Vol. 1, pp 321-340.

(31) Hotta, S. In *Handbook of Thiophene-Based Materials*; Perepichka, I. F., Perepichka, D. F., Eds.; Wiley: West Sussex, U. K., 2009; Vol. 1, pp 477-496.

(32) Fachetti, A. In *Handbook of Thiophene-Based Materials*; Perepichka, I. F., Perepichka, D. F., Eds.; Wiley: West Sussex, U. K., 2009; Vol. 1, pp 595-646.

(33) McCulloch, I.; Heeney, M. In *Handbook Thiophene-Based Materials*; Perepichka, I. F., Perepichka, D. F., Eds.; Wiley: West Sussex, U. K., 2009; Vol. 1, pp 647-672.

(34) Thompson, B. C.; Frechet, J. M. J. *Angew.Chem. Int. Ed.* **2008**, *47*, 58-77.

(35) Kim, J.; Lee, K.; Coates, N. E.; Moses, D.; Nguyen, T-Q.; Dande, M.; Heeger, A. J. *Science* **2006**, *317*, 222-225.

(36) McNeil, R.; Siudak, R.; Wardlaw, J. H.; Weiss, D. E. *Aust. J. Chem.* **1963**, *16*, 1056-1075.

(37) Rasmussen, S. C. *In 100+ Years of Plastics. Leo Baekeland and Beyond*; Strom, E. T., Rasmussen, S. C., Eds.; ACS Symposium Series, American Chemical Society: Washington, D.C., 2011; Chapter 10.

(38) Bolto, B. A.; Weiss, D. E. *Aust. J. Chem.* **1963**, *16*, 1076-1089.

(39) Bolto, B. A.; McNeill, R.; Weiss, D. E. *Aust. J. Chem.* **1963**, *16*, 1090-1103.

(40) Shirakawa, H. *Angew. Chem. Int. Ed.* **2001**, *40*, 2574-2580.

(41) Heeger, A. J. *Angew. Chem. Int. Ed.* **2001**, *40*, 2591-2611.

(42) Shirakawa, H.; Louis, E. J.; MacDiarmid, A. G.; Chiang, C. K.; Heeger, A. J. *Chem. Commun*. **1977**, 578-580.

(43) Dagani, R. *Chem. Eng. News* **2000**, *78*, 4-5.

(44) Rasmussen S. C.; Ogawa, K.; Rothstein, S. D. In *Handbook of Organic Electronics and Photonics: Electronic Materials and Devices*; Nalwa, H. S. Ed.; American Scientific Publishers; Stevenson Ranch, CA, 2008; Vol. 1, pp 1-50.

(45) Rasmussen, S. C.; Schwiderski, L.; Mulholland, M. E. *Chem. Commun.* **2011**, *47*, 11394-11410.

(46) Pomerantz, M. In *Handbook of conducting Polymers*, 2nd Ed.; Skotheim, T. A., Elsenbaumer, R. L., Reynolds, J. R., Eds.; Marcel Dekker Inc.: New York, 1998; pp 277-310.

(47) Rasmussen, S. C. Low Bandgap Polymers. In *The Encyclopedia of Polymeric Nanomaterials*, Muellen, K., Kobayashi, S., Eds.; Springer: Heidelberg, 2013; Chapter 57.

(48) Brédas, J.-L. *J. Chem. Phys*. **1985**, 82, 3808-3811.

(49) Brédas, J.-L. In *Electronic Properties of Polymers and Related Compounds*; Kuzmany, H., Mehring, M. S., Roth, S. Eds.; Springer-Verlang: Berlin, 1985.

(50) Dkhissi, A.; Louwet, F.; Groenendaal, L.; Beljonne, D.; LAzzaroni, r.; Brédas, J. L. *Chem. Phys. Lett.* **2002**, *359*, 466-472.

(51) Brédas, J. L.; Street, G. B.; Thémans, B.; André, J. M. *J. Chem. Phys.* **1985**, *83*, 1323-1329.

(52) Cary, F. A.; Sunberg, R. J. *Advanced Organic Chemistry part A: Structure and Mechanisms*, 4th Ed.; Kluwer Academic/Plenum Publisher, New York, 2000; pp 541-542.

(53) Chueh, C.-C.; LAi, M.-H.; Tsai, J.-H.; Wang, C.-F.; Chen, W.-C. *J. Polym. Sci., Part A: Polym. Chem.* **2010**, *48*, 74-81.

(54) Rasmussen, S. C.; Straw, B. D.; Hutchison, J. E. In *Semiconducting Polymers: Applications, Properties, and Synthesis*; Hsieh, B. R., Wei, Y., Eds.; American Chemical Society: Washington, DC, 1999; pp 347-366.

(55) McCullough, R. D.; Lowe, R. D. *J. Chem. Soc., Chem. Commun.* **1992**, 70-72.

(56) Chen, T. A.; Rieke, R. D. *J. Am. Chem. Soc.* **1992**, *114*, 10087-10088.

(57) Loewe, R. S.; Khersonksy, S. M.; McCullough, R. D. *Adv. Mater.* **1999**, *11*, 250-253.

(58) Daoust, G.; Leclerc, M. *Macromolecules* **1991**, *24*, 455-459.

(59) Wu, X.; Rieke, D. *J. Org. Chem.* **1995**, *60*, 6658-6659.

(60) Wu, X.; Chen, T. A.; Rieke, R. D. *Macromolecules* **1996**, *29*, 7671-7677.

(61) Heywang, G.; Jonas, F. *Adv. Mater.* **1992**, *4*, 116-118.

(62) Kirchmeyer, S.; Reuter, K.; Simpson, J. C. In *Handbook of Conducting Polymers: Theory, Synthesis, Properties, and Characterization*, 3rd ed.; Skotheim, T. A., Reynolds, J. R., Eds.; CRC Press: Boca Raton, FL, 2007; Chapter 10.

(63) Khan, R. U. A.; Hunziker, C.; Günther, P. *J. Mater. Sci.: Mater. Electron.* **2006**, *17*, 476-474.

(64) Amb, C. M.; Chen, S.; Graham, K. R.; Subbiah, J.; Small, C. E.; So, F.; Reynolds, J. R. *J. Am. Chem. Soc.* **2011**, *133*, 10062-10065.

(65) van Mulllekoma, H. A. M.; Vekemans, J. A. J. M.; Havinga, E. E.; Meijer, E. W. *Mater. Sci. Eng. R.* **2001**, *32*, 1-40.

(66) Helgesen, M.; Krebs, F. C. *Macromolecules* **2010**, *43*, 1253-1260.

(67) Steckler, T. T.; Zhang, X.; Hwang, J.; Honeyager, R.; Ohira, S.; Zhang, X.-H.; Grant, A.; Ellinger, S.; Odom, S. A.; Sweat, D.; Tanner, D. B.; Rinzler, A. G.; Barlow, S.; Brédas, J.-L.; Kippelen, B.; Marder, S. R.; Ryenolds, J. R. *J. Am. Chem. Soc.* **2008**, *131*, 2824-2826.

(68) Zhang, X.; Steckler, T. T.; Dasari, R. R.; Ohira, S.; Potscavage, W. J.; Tiwari, S. P.; Coppée, S.; Ellinger, Barlow, S.; Brédas, J.-L.; Kippelen, B.; Reynolds, J. R.; Marder, S. R. *J. Mater. Chem.* **2010**, *20*, 123-134.

(69) Zhang, X.; Shim, J. W.; Tiwari, S. P.; Zhang, Q.; Norton, J. E.; Wu, P.; Barlow, S.; Jenekhe, S. A.; Kippelen, B.; Brédas, J.-L.; Marder, S. R. *J. Mater. Chem.* **2011**, *21*, 4971-4982.

(70) Bundgaard, E.; Krebs, F. C.; *Sol. Energy. Mater. Sol. Cells* **2007**, *91*, 954-987.

(71) Wen, L.; Rasmussen, S. C.; *Polym. Prepr.* **2007**, *48*, 132.

(72) Wen, L. *PhD Dissertation*, North Dakota State University, Fargo, ND, 2008.

CHAPTER 2. SYNTHESIS AND CHARACTERIZATION OF NEW THIENO[3,4-*b*]PYRAZINES UTILIZING SIDE CHAINS TO TUNE THE ELECTRONIC PROPERTIES

2.1. Introduction

Due to their unique combination of electronic and optical properties typically associated to inorganic semiconductors with the processability and flexibility found in plastics, conjugated polymers have become an attractive class of materials for use in electronic devices. An advantage of these materials is the ability to tune the optical and electronic profiles via simple molecular design. One such method is through the use of a fused ring system. This induces a quinoidal state in the thiophene backbone of a polymer, reducing band gap.[1-3] Several such low band gap systems have been generated, including thieno[3,4-*b*]pyrazines (TPs) **2.1**, shown in Scheme 2.1.[4-40] These materials have been used to generate both homo- and copolymeric systems, displaying optical band gaps as low as 0.50 eV.[41]

The basic synthetic scheme for the production of TPs involves the condensation of 3,4-diaminothiophene **2.2** with an α-dione **2.3**.[42,43] This process has largely stayed a constant throughout TP's history; however, generation of the precursor **2.2** has undergone a great deal of modification. In every method this begins with bromination of thiophene to generate 2,5-dibromothiophene **2.4**. The halogens act to protect these positions for the subsequent nitration of the 3- and 4- positions to generate **2.5**. Nitration of **2.4** was reported by Kreis in 1884 in which nitric acid was added to a solution of **2.5** in sulfuric acid.[44] In 1945 Mozingo modified this method by use of fuming acid and increased control over reaction temperature, giving product in a 30% yield.[45] Further development by Rasmussen and coworkers first increased reaction time to improve yield to 45-50%.[43] This was then further improved by Rasmussen by using

concentrated nitric acid in place of a fuming acid and slowly adding the precursor to fuming sulfuric acid, giving a 90-95% yield.[44]

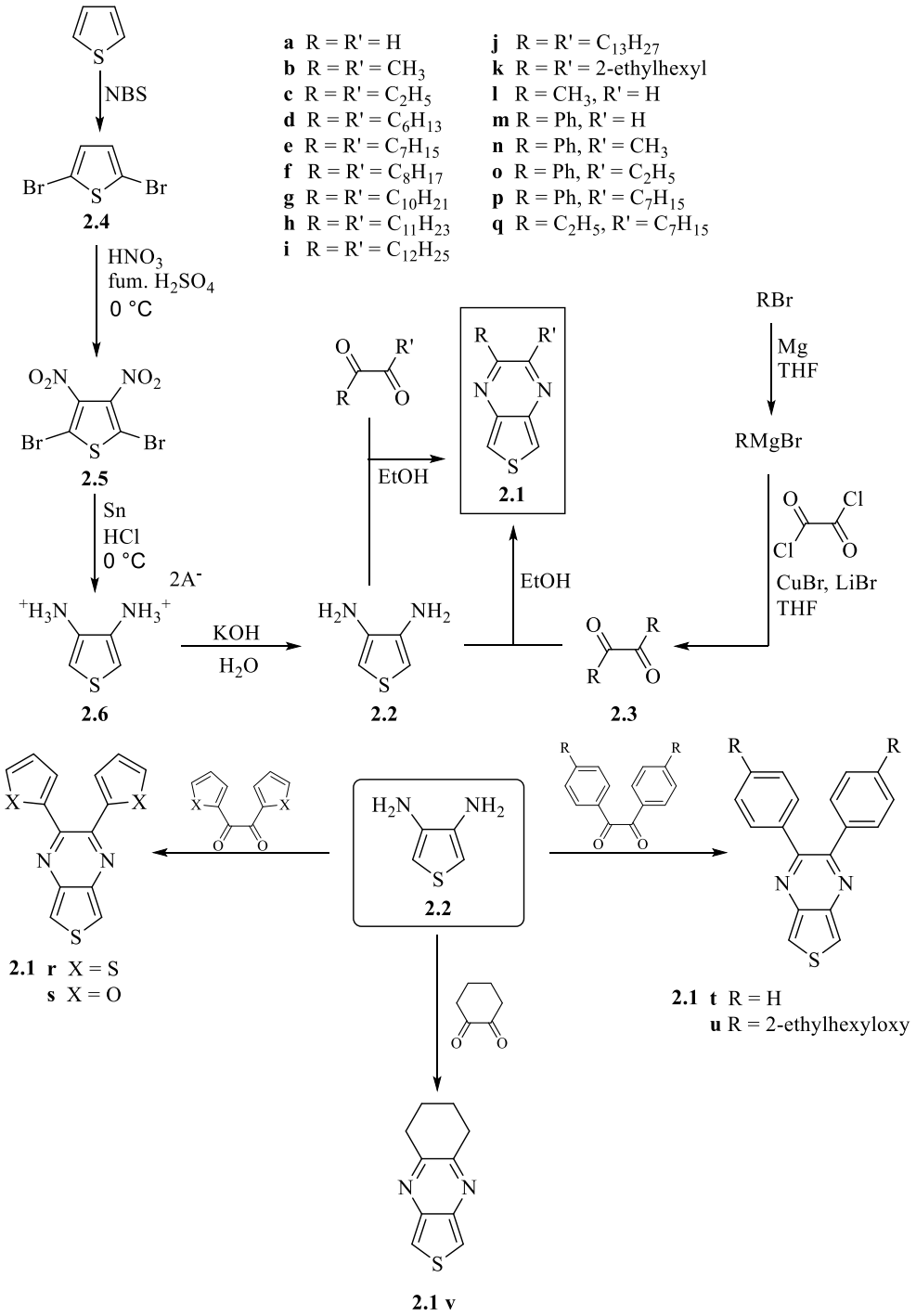

Scheme 2.1. General synthetic scheme for 1st generation TPs.

Reduction of **2.5** to produce the ammonium salt is carried out in HCl with tin power to generate the diammonium salt **2.6**. Initially the counterions in **2.6** were reported by both Imoto and Binder to be **2.6**•2HCl•$SnCl_4$.[46-48] Later Outurquin and Paulmier reported the counter ion to be simple $SnCl_6^{2-}$.[42,50] However, elemental analysis by Rasmussen and coworkers revealed a more complex system with a composition of $[\mathbf{2.6}]_x[SnCl_6^{2-}]_{(x-1/2y)}[Cl^-]_y$.[43] As the exact composition of couterions is variable in each reaction an exact molecular weight cannot be determined. Thus as it is desirable to know molar ratios between **2.6** and the α-dione **2.3** for condensation to generate the monomer, neutralization of **2.6** to form **2.2** is a prerequisite step. This neutralization is accomplished by addition of KOH to the salt in a water solution.[50] Previous methods used NaOH or Na_2CO_3.[43] However, current methods use KOH as it was found to adequately neutralize the salt quickly, without decomposing the material. Condensation with a prepared or commercially available α-dione is then performed, yielding monomer **2.1**.

While this method has proven effective for the generation of TPs, it is limited by the α-diones commercially or synthetically available, primarily including alkyl or aryl groups. To include a wider variety of side chains, including electron withdrawing or donating chains, the Rasmussen group introduced a new method toward the generation of TPs.[50] A TP monomer featuring halides at the 2- and 3- positions would allow simple substitutions to be performed to introduce new electron-donating or withdrawing side chains. The first step in building the target compound was the formation of the basic TP architecture. This was accomplished via condensation of **2.2** with either diethyl oxalate to form **2.7** or 1,4-dibromo-2,3-butanedione to form **2.8**.

From **2.7**, reaction with PBr_5 was performed to generate 2,3-dibromothieno[3,4-*b*]pyrazine **2.9**. This process was modified from previously reported bromination of

quinoxalines.[51,52] The reaction with other systems had previously been performed neat and the process is accomplished by melting the materials, allowing them to react. Thiophene-based materials, however, feature increased sensitivity to oxidizing agents and will readily polymerize. Thus, several changes were made from the quinoxaline method, the foremost of which was the addition of a solvent. Non-coordinating solvents, such as benzene and CCl_4, have been shown to yield the molecular form of PBr_5. Xylenes, which has similar properties to benzene, features a higher boiling point and was thus chosen as the solvent for the reaction. Although favoring the molecular form in non-coordinating solvents, the molecular form is in equilibrium with PBr_3 and Br_2 as shown in Scheme 2.2. The equilibrium is temperature dependent and when heated the equilibrium shifts toward molecular PBr_5, allowing for conversion of the starting material to generate **2.9**. Alternatively, using monomer **2.8**, simple substitution may be performed to generate similar functionalities featuring a methylene spacer.

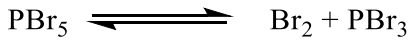

Scheme 2.2. Disassociation of PBr_5 to PBr_3 and Br_2.

From this new set of monomers, in Scheme 2.3, it was shown that control over electronic and optical properties could be accomplished by careful selection of the side chains. As expected electron-donating systems such as alkyloxy and amine groups acted to destabilize energy levels whereas the electron-withdrawing cyano group acted to stabilize HOMO/LUMO levels as seen in Figure 2.1. It was also noted that while HOMO levels were certainly affected by the electronics of the side chain, the LUMO was affected to a far greater extent. This results in an increased HOMO-LUMO gap for donating groups and a decreased HOMO-LUMO gap for

withdrawing groups, which is reflected in the absorption profile. An example of this MO tuning may be observed by comparing the electron-rich alkyloxy substituted TP and electron-poor cyano substituted TP. Those TPs featuring alkyloxy side chain feature a HOMO destabilized by 1.55 eV, LUMO by 2.26 eV and a reduction in HOMO/LUMO gap by 0.71 eV in comparison to the cyano substituted TP analogue.[50] Thus changing the electronic nature of the TP side chain increased control over the material properties is possible.

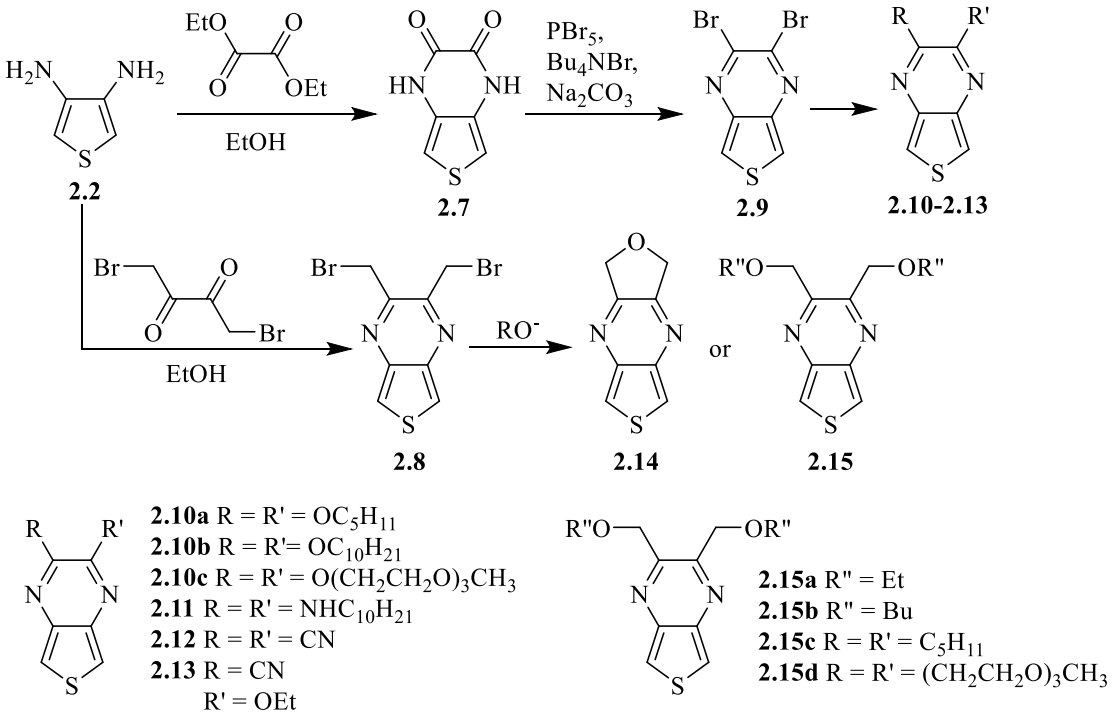

Scheme 2.3. Synthetic outline of new TP monomers.[50]

Although electron-donating groups are well represented in this group of monomers, electron-withdrawing side chains are only represented by halogen and cyano groups. The halide-functionalized TPs feature low solubility and may readily undergo chemical reactions and decomposition and thus are not good candidates for further use. Monomer **2.12** also has several disadvantages including low yield (at ~15 %) and, similar to the halide TPs, low solubility. The

low yield in generating **2.12** is due in large part to the low solubility of the salt (KCN or NaCN) used in the reaction (Scheme 2.4) with aprotic solvents. It was discovered that use of an non-nucleophilic solvent is required for this reaction as nucleophilic solvents, such as alcohols, will add to the monomer in place of the desired CN. The low solubility is also a substantial issue as the generated materials require solution processing. However, it may be overcome by copolymerization with units featuring large solubilizing chains and thus investigation into this monomer unit is of interest due to its strong electron-withdrawing nature. In this chapter will be discussed attempted alternate synthetic paths using metal-catalyzed methods toward generation of **2.12** in an effort to increase yield.

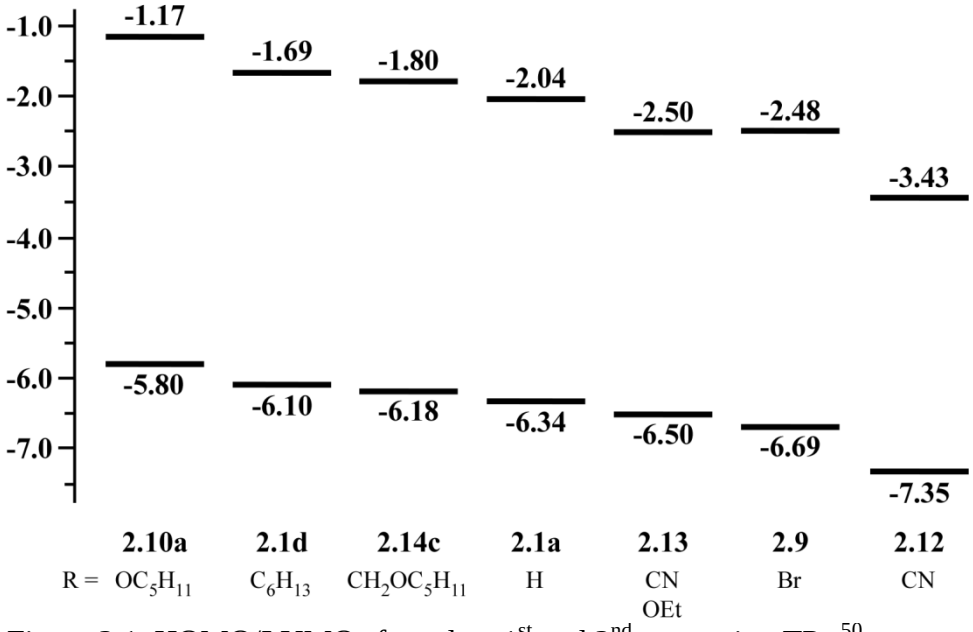

Figure 2.1. HOMO/LUMOs for select 1st and 2nd generation TPs.[50]

While –CN groups provide good electron-withdrawing proficiency, they provide no solubilizing capability which is important for further use in generating polymeric systems. Thus the need for electron-withdrawing side chains featuring some long alkyl functionality is highly

desirable. Later in the chapter will be presented attempts to generate new 2nd generation TPs with ketone and amide side chains, both electron-withdrawing systems featuring the desired solubilizing alkyl chain. An improved synthesis of electron-donating alkyloxy TPs will be presented, generating previously unprepared ethyloxy and hexyloxy analogues. Finally, spectroscopic and electrochemical data of each generated monomer will be presented.

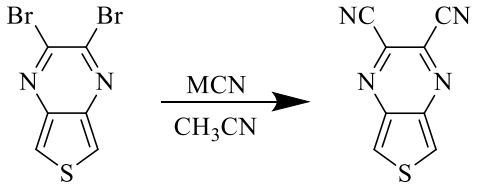

2.9 **2.12**

M = Na or K

Scheme 2.4. Synthesis of CNTP.

2.2. Results and Discussion

2.2.1. *Synthesis*

2,3-Dicyanothieno[3,4-b]pyrazine. Current methods toward generation of 2,3-dicyanothieno[3,4-*b*]pyrazine (CNTP) use CN salt, KCN or NaCN, in MeCN to generate the dicyanoTP. However, as previously mentioned, yields are very low (~15%) due to salt solubility. To increase yield several alternate synthetic methods, shown in Scheme 2.5, were attempted.

The first such method was attempted using a palladium-catalyzed cyanation with $Zn(CN)_2$ as the CN source, following a literature procedure.[53] Previous trials by the authors had been done with phenyl, naphthyl, and pyridine systems and thus a pyrazine should be similar. However, completion of the reaction showed three major products, the monosubstituted TP (~50%), unstubstituted TP (~40%), with only a small 10% yield of disubstituted product. Further substitution of the monocyanoTP was attempted with the idea that more product may be formed

with one position already converted, production of dicyanoTP might be more favorable. However, yields were again low at 10%.

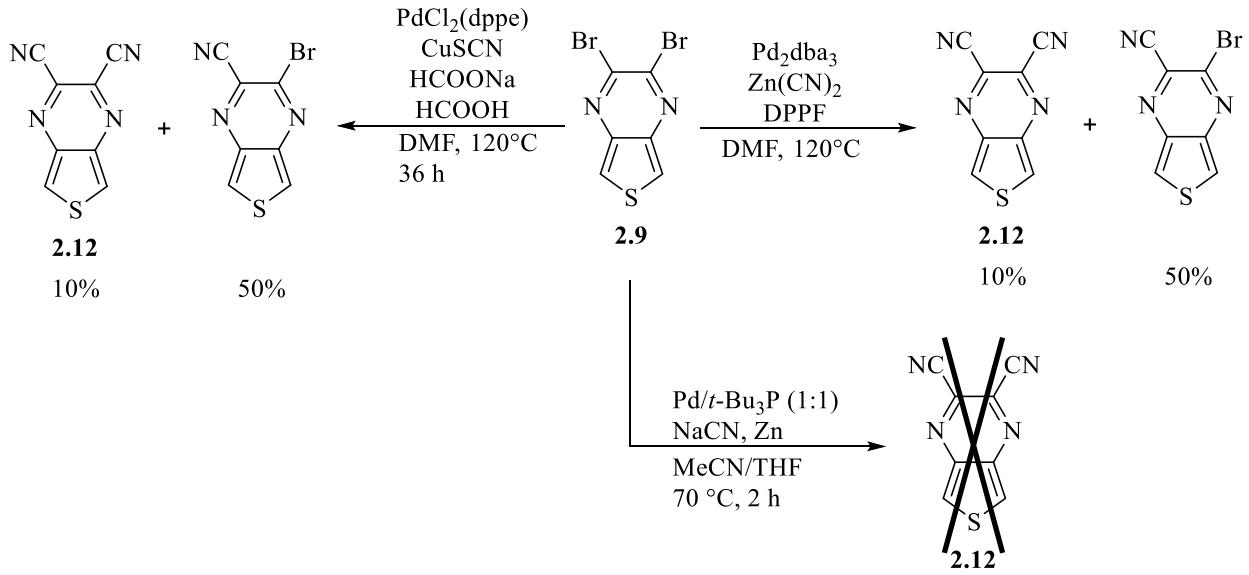

Scheme 2.5. Alternate synthetic routes for the generation of CNTP.

A second reaction using Pd/t-Bu_3P catalyst system and simple a NaCN salt for the CN source was attempted using chemistry developed by Grushin and coworkers; a proposed mechanism for this reaction is found in Scheme 2.6.[54] The catalyst system was prepared a day prior to the reaction. This was then added to the reaction via syringe. Despite reported high yields with monosubstitutions of benezene-based systems, this reaction formed no product from **2.9**. However, it was noted by the authors that excess amounts of CN^- or water will cause catalyst poisoning. In their study the authors did not attempt double cyanation. They also noted that the reaction did not work well with bromopyradines due to N-binding. It is possible that the increased amount of CN^- involved in generating the dicyanated species may cause catalyst poisoning; however, the stoichiometric amount of catalyst was doubled as well. Additionally, as two nitrogens exist on the pyrazine ring, such N-binding is also a potential complication.

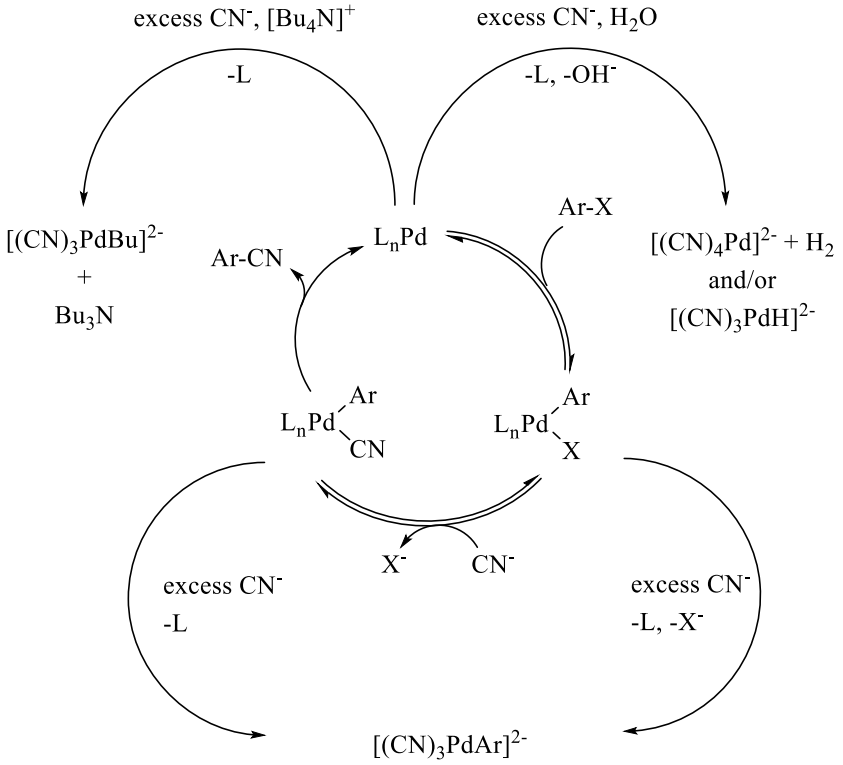

Scheme 2.6. Proposed mechanism of cyanation via methods 1 and 2.[56]

A third method utilized CuSCN for the CN source and a $PdCl_2$(dppe) catalyst.[55] The proposed mechanism for this reaction is found in Scheme 2.7. Sodium formate was used as a base to coordinate to the metal center and formic acid was an additive believed to accelerate the reaction rate. The formic acid appears, as shown in the below mechanism, to play a role in both forming the product and catalyst recovery. However, again, the systems generated by the authors were phenyl-based with no thiophene-based system trials. The reaction with **2.9** behaved similarly to previous efforts, giving product in ~10% yield, with the rest being starting material or monosubstituted TP.

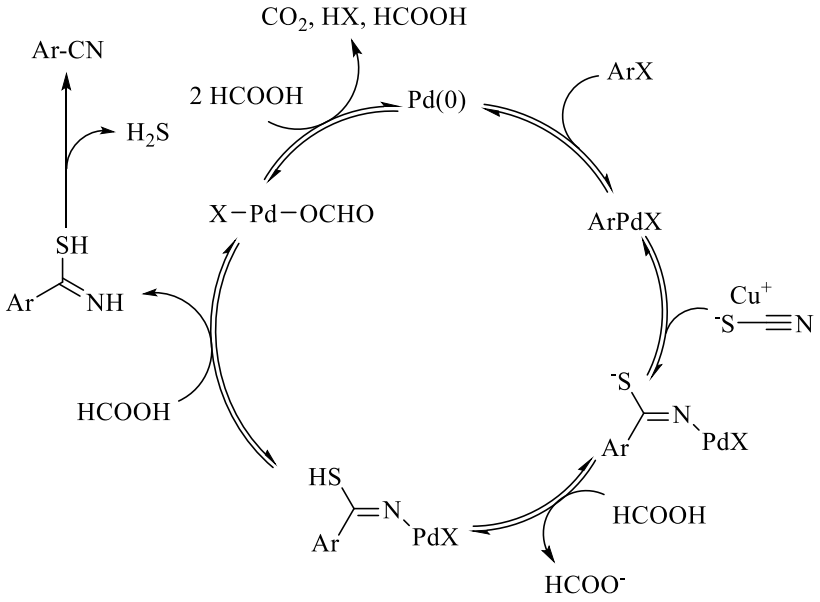

Scheme 2.7. Proposed mechanism for cyanation via method 2.

In reactions using either CuSCN or $Zn(CN)_2$, the monosubstituted TP is generated as the major product with about 10% of the disubstituted product formed. This indicates that each catalytic cycle for disubstitution can occur. The monosubstituted product also is generated in reasonable yield. However, in both cases where the single substitution occurs, the bromide remains, as indicated by the proton NMR, suggesting no oxidative addition to the metal catalyst. It is possible that catalyst poisoning is occurring due to an excess of CN^-, as indicated by Grushin in his account.[54] This would account for inhibition of oxidative addition, which should otherwise be enhanced by the electron deficiency of the ring.

2,3-Di(octanamide)thieno[3,4-b]pyrazine. Attempts were made toward generating a TP with an amide side chain **2.15** (Scheme 2.8). This would not only introduce an electron-withdrawing chain, but also allow for a solubilizing alkyl group. Previous reports from Buchwald and coworkers illustrated a copper-catalyzed amidation using a bidentate amine

ligand.[56,57] This method had been additionally adapted to use in the generation 2nd generation N-acyldithieno[3,2-*b*:2′,3′-*d*]pyrroles.[58]

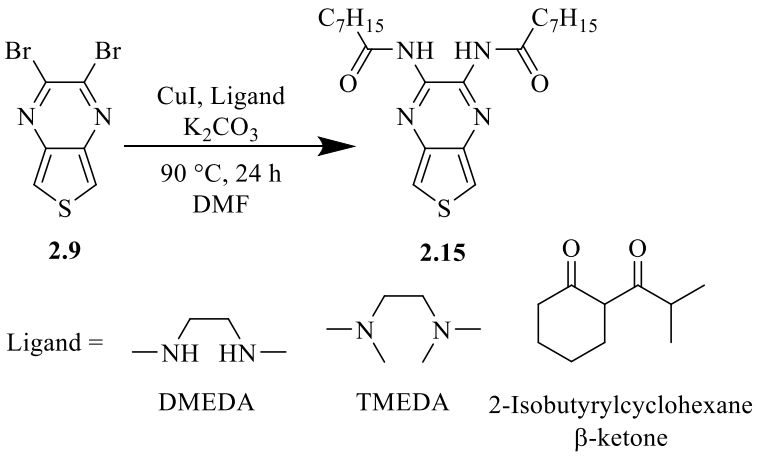

Scheme 2.8. Synthesis of diamide TP.

Upon completion of the reaction NMR data suggested the product had formed, however, evidence of additional peaks was seen. These peaks correlated well with the ligand, N,N'-dimethylethylenediamine (DMEDA), and thus it was thought some remained in the product, even after purification via column chromatography. However, even after placing the sample under vacuum for 12 h DMEDA peaks showed in NMR spectra and it was thought that the DMEDA ligand might be binding to the TP. There are several possible ways this binding might occur; two such are shown in Chart 2.1. The crude yield was found to be 20-25%.

Attempts were made to purify the product further and remove the ligand via a wash with acidified $CHCl_3$. Thus HCl was added to $CHCl_3$ and this solution was used to dissolve the product. A solid precipitated out and the resulting solution was washed with copious amounts of H_2O. This solid dissolved into the organic layer after the addition of water and further $CHCl_3$. After this wash, NMR data showed removal of the DMEDA peaks and thus purified material.

However, yield was brought down to 5%. A reaction was attempted without ligand to determine if it was needed. This resulted in no amidation.

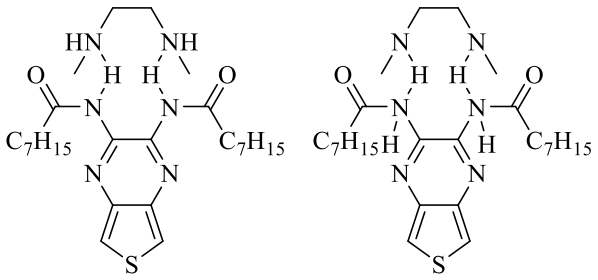

Chart 2.1. Two proposed products of the amideTP reaction with DMEDA.

A second reaction was attempted with *N,N,N',N'*-tetramethylethylenediamine (TMEDA). The logic behind this was that the increased bulk of the ligand might prevent such interactions from occurring while still allowing progression of the reaction. However, minimal product was formed and this was primarily the monofunctionalized species. The problem with this ligand was due to a slower rate of producing the copper complex. Thus the reaction time of ligand with copper was increased from 30 mins to 1 h, resulting in a blue colored solution and production of the product. This reaction was further optimized by increasing the reaction time upon addition of TP. The overall yield with this new method was 45-50%, a substantial increase over the 5% isolated from use of DMEDA as a ligand. It was attempted to determine if, when using DMEDA, the ligand could be removed simply by bromination in the slightly acidic conditions of NBS. However, while full bromination did occur, the resulting material still showed DMEDA peaks in the NMR spectrum. A summary of all conditions attempted in generating **2.15** are shown in Table 2.1.

Table 2.1. Attempted synthetic conditions for production of **2.15**.

Entry	Ligand	Stirring time with ligand	Reaction time	Isolated yield (%)
1	DMEDA	0.5 h	24 h	5%
2	-	-	24 h	0%
3	β-diketone	0.5 h	24 h	0%
4	TMEDA	0.5 h	24 h	0%
5	TMEDA	1 h	24 h	20-25%
6	TMEDA	1 h	48 h	45-50%
7	TMEDA	1 h	72 h	50%

2,3-Dioctanoylthieno[3,4-b]pyrazine. Addition of a third electron-withdrawing, octanoyl side chain, was attempted to generate **2.16**. This acylation was attempted in modulation of a Heck reaction by palladium-catalysis reported by Xiao and coworkers.[60] This work had previously been used primarily on benzene and thiophene derivatives, supporting electron-donating and –withdrawing functionalities, but had thus far not been tested on any nitrogen containing heterocycles. The reaction, shown in Scheme 2.9, used $Pd_2(dba)_3$ for the catalyst, the ligand 1,3-(diphenylphosphino)propane (dppp), and a pyrrolidine additive. Although several trials were performed with this system, every case yielded the monosubstituted TP. Addition of a second ketone group was attempted from the isolated monosubstituted product, however, production of the disubstitutedTP was not observed. Although, this procedure was tried several

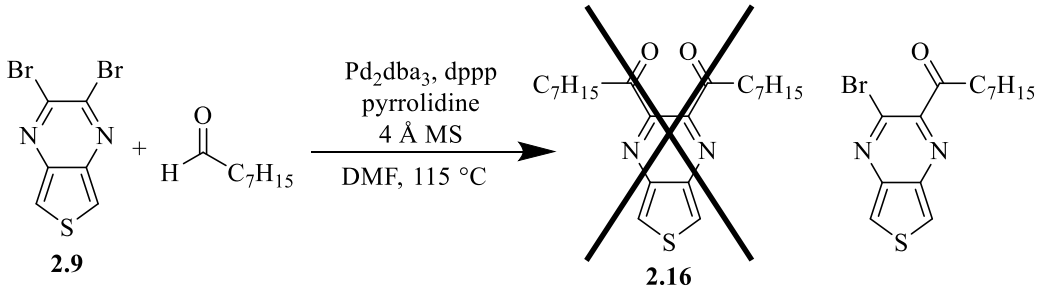

Scheme 2.9. Attempted synthesis of **2.16**.

times, no alteration of conditions was attempted and thus further investigation into the generation of **2.16** is needed.

2.3-Dialkyloxythieno[3,4-b]pyrazines. Synthesis of the alkyloxyTP analogues have previously been performed, yielding product between 70-80 %.[50] It was found that addition of a small excess of NaH and alcohol increased yield. It is thought that in previous attempts, remaining H_2O in the solvent reacted with the base, thus reducing the stoichiometric amount available to deprotonate the alcohol. Adding an excess of base allows for reaction with any H_2O present while the remaining base is still present to fully deprotonate all the alcohol. The excess of base does not appear to have any negative side effect on the formation of product. This is in contrast to the bis(alkoxymethyl)thieno[3,4-*b*]pyrazine analogues which feature substitution at the methylene spacer. With this method, **2.10d** and **2.10e** were generated in yields of >95%, shown in Scheme 2.10. Removal of any remaining alcohol was accomplished by column chromatography using hexanes.

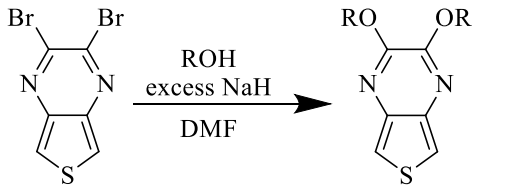

2.9 **2.10 d** R = C_2H_5
e R = C_6H_{13}

Scheme 2.10. Synthesis of alkyloxyTPs.

2.2.2. *UV-vis Absorption Spectroscopy*

A representative spectrum of monomers **2.10d**, **e** and **2.15** are represented below in Figure 2.2 with monomer **2.1d** for comparison. Photochemical studies of several of the TP monomers shown here have been previously reported by Rasmussen and coworkers and are

replicated to illustrate the effect of side chains on the absorption profile. Data for all of these is listed in Table 2.2. All monomers have two distinct absorption band areas. The first set of bands, appearing at 200-250 nm, is due to the π-π* transition. Monomers **2.10d**, **e** and **2.1** all have this peak at ~210 nm. This typically shows as a set of two peaks, with the minor peak at ~230 nm. The π-π* band for **2.15** is slightly red shifted, occurring at 217 nm. The minor peak for **2.15** appears at at ~230 nm, as found with the previously discussed monomers.

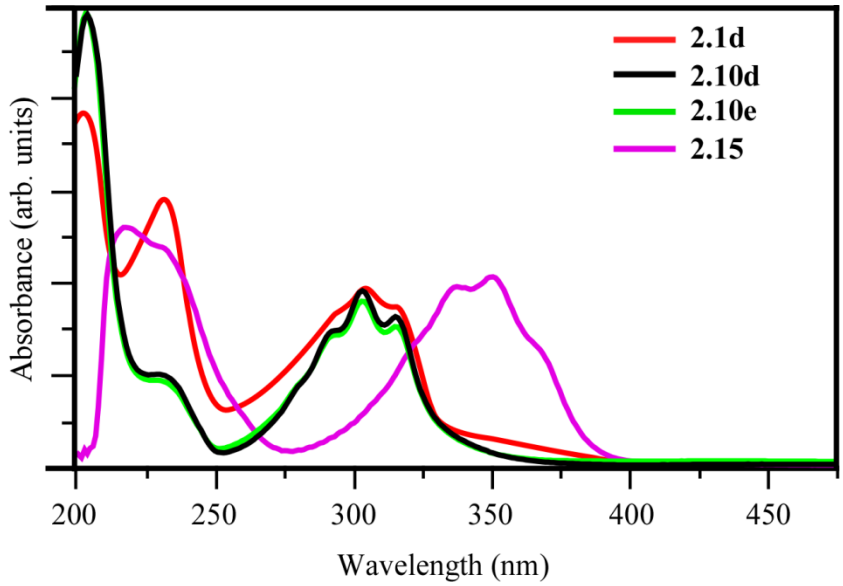

Figure 2.2. Solid-state absorption spectra of 2nd generation TPs with **2.1d**.[50]

The second band is the charge transfer band. This is due to the transfer of electrons from the HOMO, centered about the thiophene ring, to the LUMO, centered about the pyrazine ring. As observed from this figure, the donating or withdrawing nature of the side chain can have an impact on the absorption profile. It is interesting to note that electron-donating systems, such as **2.10d** and **e** do not show significant blue-shift in the CT absorption band, showing a λ_{max} at 305 for both. The electron-withdrawing amide side chain on **2.15** shifts the λ_{max} (363 nm) and onset

(385 nm) further to low energy wavelengths for the CT band. This could be in part due to further electron delocalization through the amide groups.

Table 2.2. Photophysical properties of TP monomers.[a]

Compound	λ_{max} π-π*(nm)[a]	λ_{max} CT (nm)[a]	ε (M^{-1} cm^{-1})	HOMO/LUMO gap (eV)
2.10d	208 (232)	(295) 305 (317)	6500	3.70
2.10e	206 (232)	(293) 305 (315)	20000	3.70
2.15	217 (231)	363 (375)	1300	3.22

[a]In CH_3CN.

2.2.3. *Electrochemistry*

Electrochemical measurements were performed of the three generated TP monomers, shown in Table 2.3 and Figure 2.3. Both alkyloxy TPs featured a onset of oxidation at 1.25 V giving a HOMO of -6.5 eV, consistent with previously reported alkyloxy TPs. These are all more negative than the oxidation potential for alkyl monomer C_6TP, which occurs at 1.35 V, showing destabilization resulting from the electron-donating alkyloxy side chains. This oxidation was coupled with a reduction occurring at 0 V, indicating an irreversible oxidation. No reduction was observed in these experiments. LUMOs for both **2.10d** and **e** were determined by use of the optical HOMO/LUMO gap, yielding -2.8 eV for both.

Table 2.3. Electrochemical properties of TP monomers.

Compound	E_{pa} (V)[a]	E_{pc} (V)[a]	HOMO (ev)	LUMO (eV)	HOMO/LUMO gap (eV)[f]
2.10d	1.38	-	-6.5[b]	-2.8[d]	3.70
2.10e	1.40	-	-6.5[b]	-2.8[d]	3.70
2.15	2.20	-1.71	-6.7[c]	-3.5[e]	3.20

[a] CV experiments performed as solution-state in MeCN. Potentials vs. Ag/Ag^+ in 0.1 M $TBAPF_6$, [b] E_{HOMO} was determined from the onset of oxidation vs ferrocene (5.1 eV vs. vacuum),[60] [c] $E_{HOMO} = E_{LUMO} + E_g$, [d] $E_{LUMO} = E_{HOMO} - E_g$, [e] E_{LUMO} was determined from the reduction onset vs. ferrocene (5.1 eV vs. vacuum).[59] [f] Optical.

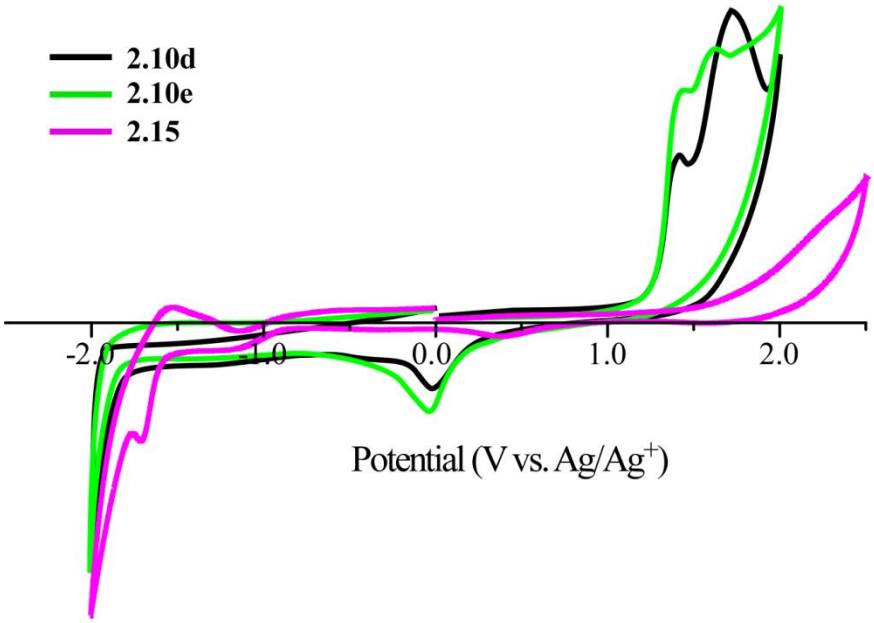

Figure 2.3. Cyclic voltammograms of new monomers in CH_3CN.

Electrochemical studies of **2.15** yielded the opposite trend, where the reduction peak occurred at -1.71 V, yielding a deeper LUMO and a slight oxidation peak was observed at ~2.25 V. The reduction peak also has a small coupled oxidation peak at -1.5 V, indicating quasireversible character. It is likely the small oxidation of **2.15** occurs is only partially seen due to interference of the solvent window. The HOMO for **2.15** was found by taking the onset of oxidation and found to be -6.7 eV. This value agrees with previous trends that a unit featuring electron-withdrawing groups, such as the amide groups here, should have more stabilized frontier orbitals. Thus, although reduction cannot be seen in **2.10d** or **e**, **2.15** shows a strong reduction peak. Similar trends are also apparent in the oxidation of these monomers, with **2.10d** and **e** showing strongly at a lower potential than for **2.15**.

2.3. Conclusion

Although TPs have been shown to rapidly undergo substitution with electron-donating groups in high yield, electron-withdrawing systems are much less successful. Generation of

several electron-withdrawing substituted TPs was attempted, with varying degrees of success. Previous methods toward the generation of CNTP resulted in low 15% yields. Metal-catalyzed substitution reactions were attempted to generate product in higher yields. While disubstituion was still low, an increased amount of monosubstituted CNTP was observed. There is some evidence that the concentration of CN- content may have an effect on the catalyst, with high concentrations acting to poison the catalyst. Additionally, nearly all materials used in these reactions were phenyl-based and the few cases where a nitrogen-containing ring was used there was a noted decrease in yield. Similarly attempts to generate a 2,3-dioctanoylthieno[3,4-*b*]pyrazine analogue resulting in only monosubstituted product. Further attempts to add a second keto side chain resulted only reduction of product. Attempts at generating the diketoTP under Pd-catalyzed conditions also produced monosubstituted product, although in this reaction no disubstituted product was formed.

Slightly more successful was the generation of **2.15**. Similar methods to the previously reported *N*-acylDTP were used to generate **2.15**. The use of the ligand DMEDA resulted in the desired disubstituted product, however, with the ligand bound to the nitrogen-based protons. Attempts to remove ligand from the product resulted in severe reduction of yield. In attempt to eliminate ligand-binding occurring with DMEDA, TMEDA was used. An increased time of stirring prior to addition of starting material and an increased time under reflux conditions resulted in production of clean product in higher yield (50%). Spectroscopy experiments show a significant reduction of HOMO/LUMO gap from other 1st and 2nd generation TPs

Spectroscopic and electrochemical experiments were performed on **2.15**, showing a marked red shift in absorption onset and a stabilization of HOMO and LUMO levels. This is in good agreement with previous trends found for other 2nd generation TPs where EWGs were seen

to both stabilize the frontier orbitals as well as reduce the HOMO/LUMO gap. Monomer **2.15** shows a LUMO at -6.7 eV, similar in energy to **2.9**, and 0.5 eV shifted from **2.1d**.[50]

In this chapter a modified synthesis of dialkyloxythieno[3,4-*b*]pyrazines was used to generate two new systems in near quantitative yields. Chain length was altered from the previously studied pentyloxy **2.10a**, to generate the ethyloxy **2.10d** and hexyloxy **2.10e** systems. Spectral and elecrtrochemical data was collected from these systems, showing similar properties to **2.10a**. These new systems could be useful in further studies of chain length size in polymerized materials.

2.4. Experimental

2.4.1. *General*

Unless noted, all materials were reagent grade and used without further purification. Chromatographic separations were performed using standard column chromatography methods with silica gel (230-400 mesh). Dry DMF was obtained by mixing with $MgSO_4$, followed by flushing through silica gel, storing under molecular sieves, and purging over nitrogen for 1 h. Dry THF and toluene were obtained via distillation over sodium/benzophenone. Dry acetonitrile was obtained via distillation over CaH. All glassware was oven-dried, assembled hot, and cooled under a dry nitrogen stream before use. Transfer of liquids was carried out using standard syringe techniques and all reactions were performed under a dry nitrogen stream. The ^{1}H NMR and ^{13}C NMR were recorded on a 400 MHz spectrometer. All NMR data was referenced to the chloroform signal and peak multiplicity was reported as follows: s = singlet d = double, t = triplet, q = quartet, p = pentet, tt = triplet of triplets, m = multiplet and br = broad. Melting points were determined using a digital thermal couple with a 0.1 °C resolution. The following

compound was synthesized according to previously reported literature procedures: 2,3-dibromothieno[3,4-*b*]pyrazine (**2.9**).[50]

5,7-Diethyloxythieno[3,4-*b*]pyrazine (2.10d). Hexanes (20 mL) was added to a round bottom (RB) flask containing 60% NaH dispersion in mineral oil (0.5 g, 12.5 mmol) and stirred for 20 min. The hexanes was removed via syringe and the material was dried further via evacuation. Dry DMF (40 mL) followed by absolute ethanol (0.35 mL, 6 mmol) were added via syringe and the solution was stirred for 5 min. Monomer **2.9** was added and the reaction stirred for 3 h. Ammonium chloride was added to quench the remaining NaH and DCM was added to extract the product. The organic layer was separated, dried with $MgSO_4$, and solvent was removed via rotary evaporation. Further purification occurred via column chromatography first using hexanes:ethyl acetate (95:5) to generate a white powder (>95% yield). mp 123.1-124 °C. ^{1}H NMR: δ 7.31 (s, 2H), 4.45 (q, *J* = 7.2 Hz, 4), 1.41 (t, *J* = 7.2 Hz, 6H); ^{13}C NMR: δ 150.1, 140.1, 117.3, 65.3, 14.1.

5,7-Dihexyloxythieno[3,4-*b*]pyrazine (2.10e). Monomer **2.10e** was prepared in the same manner as **2.10d**, substituting ethanol with 1-hexanol. The product was purified via column chromatography first using hexanes to remove excess 1-hexanol followed by hexanes:ethyl acetat (95:5) to generate a white powder (>95% yield). mp 69.9-71.1 °C. ^{1}H NMR: δ 7.33 (s, 2H), 4.38 (t, *J* = 6.8 Hz, 4H), 1.81 (p, *J* = 8.8 Hz, 4H), 1.45 (p, *J* = 7.2 Hz, 4H), 1.35-1.30 (m, 8H), 0.85 (t, *J* = 7.4 Hz, 6H); ^{13}C NMR: δ 150.2, 138.3, 112.4, 67.2, 31.6, 28.6, 25.8, 22.7, 14.1.

5,7-Di(octanamide)thieno[3,4-*b*]pyrazine (2.15). To a 3 neck RB flask fitted with a condenser was added K_2CO_3 (0.83 g, 6 mmol) and CuI (0.018 g, 0.09 mmol). The ligand TMEDA (0.03 mL, 0.2 mmol) and toluene (60 mL) were syringed in and the reaction was allowed to stir for 1 h. Monomer **2.9** (0.3 g, 1 mmol) and *N*-octanamide (0.3 g, 2 mmol) were

added and the reaction was heated to reflux for 48 h. The reaction was cooled to RT and H_2O was added. Hexanes was used to extract the product and the organic layer was separated and dried with $MgSO_4$. The product was isolated via rotary evaporation and purified via column chromatography with hexanes:ethyl acetate (50:50) to produce a white solid (50% yield). mp 99.0-99.4 °C. ^{1}H NMR: δ 7.24 (s, 2H), 5.36 (br, 2H), 2.21 (t, *J* = 7.6 Hz, 4H), 1.60 (p, *J* = 6 Hz, 4H), 1.29-1.24 (m, 18H), 0.87 (t, *J* = 4 Hz, 6H); 13C: d 176.05, 144.28, 139.35, 108.83, 47.39, 36.96, 31.87, 29.39, 25.75, 22.80, 14.27.

2.4.2. *Electrochemistry*

All electrochemical techniques were performed on a Bioanalytical Systems BAS 100B/W electrochemical analyzer. Cyclic voltammetry (CV) experiments were performed using a three-electrode cell consisting of a Pt-disc working electrode, Pt coiled wire auxillary electrode, and a Ag/Ag^+ reference electrode. A 0.1 M electrolyte solution was prepared with tetrabutylammonium hexafluorophosphate ($TBAPF_6$) using MeCN distilled over CaH_2 under dry nitrogen. The solutions were deoxygenated with argon for at least 20 min prior to each scan and blanketed with argon during the experiments. Experiments were performed by first performing a background in electrolyte solution followed by addition of product. The product was solubilized in the solution via stirring. Enough product was added until peaks of sufficient magnitude were observed. CV experiments were performed in the above described cell at a sweep rate of 100 mV/s. E_{HOMO} values were determined in a reference to ferrocene (5.1 V vs. vacuum)[59] and the E_{LUMO} was determined from the following equation: $E_{LUMO} = E_{HOMO}$ – optical band gap.

2.4.3. *UV-vis-NIR Absorption Spectroscopy*

All absorption spectroscopy was performed on a Carry 500 dual-beam UV-vis-NIR spectrophotometer. Solution-state spectra were analyzed in chloroform were analyzed with the

polymer spin coated on a glass plate. The optical band gaps were determined from the onset of the lowest energy absorption by extrapolation of the steepest slope to the intersection with the wavelength axis.

2.5. References

(1) Rasmussen S. C.; Ogawa, K.; Rothstein, S. D. In *Handbook of Organic Electronics and Photonics: Electronic Materials and Devices*; Nalwa, H. S. Ed.; American Scientific Publishers; Stevenson Ranch, CA, 2008; Vol. 1, pp 1-50.

(2) Brédas, J. L. *J. Chem. Phys*. **1985**, 82, 3808-3811.

(3) Brédas, J. L. In *Electronic Properties of Polymers and Related Compounds*; Kuzmany, H., Mehring, M., S. Roth, S. Eds.; Springer-Verlang: Berlin, 1985 .

(4) Roncali, J. *Chem. Rev.* **1997**, *97*, 173-205.

(5) Roncali, J. *J. Mater. Chem.* **1999**, *9*, 1875-1893.

(6) Rasmussen, S. C.; Pomerantz, M. In *Handbook of Conducting Polymers*, 3rd Ed.; Skotheim, T. A., Reynolds, J. R., Eds.; CRC Press: Boca Raton, FL, 2007; Vol. 1, Chapter 12.

(7) Rasmussen, S. C.; Ogawa, K.; Rothstein, S. D. In *Handbook of Organic Electronics and Photonics*; Nalwa, H. S., Eds.; American Scientific Publishers: Stevenson Ranch, CA, 2007; Vol. 1, Chapter 1.

(8) Pomerantz, M.; Chaloner-Gill, B.; Harding, L. O.; Tseng, J. J.; Pomerantz, W. J. *J. Chem. Soc., Chem. Commun.* **1992**, 1672-1673.

(9) Pomerantz, M.; Chaloner-Gill, B.; Harding, L. O.; Tseng, J. J.; Pomerantz, W. J. *J. Synth. Met.* **1993**, *55*, 960-965.

(10) Kastner, J.; Kuzmany, H.; Vegh, D.; Landl, M.; Cuff, L.; Kertesz, M. *Synth. Met.* **1995**, *69*, 593-594.

(11) Kastner, J.; Kuzmany, H.; Vegh, D.; Landl, M.; Cuff, L.; Kertesz, M. *Macromolecules* **1995**, *28*, 2922-2929.

(12) van Asselt, R.; Hoogmartens, I.; Vanderzande, D.; Gelan, J.; Froehling, P. E.; Aussems, M.; Aagaard, O.; Schellekens, R. *Synth. Met.* **1995**, *74*, 65-70.

(13) Huskic, M.; Vanderzande, D.; Gelan, J. *Synth. Met.* **1999**, *99*, 143-147.

(14) Hagan, A. J.; Moratti, S. C.; Sage, I. C. *Synth. Met.* **2001**, *119*, 147-148.

(15) Kenning, D. D.; Rasmussen, S. C. *Macromolecules* **2003**, *36*, 6298-6299.

(16) Wen, L..; Duck, B. C.; Dastoor, P. C.; Rasmussen, S. C. *Macromolecules* **2008**, *41*, 4576-4577.

(17) Nietfeld, J. P.; Heth, C. L.; Rasmussen, S. C. *Chem. Commun.* **2008**, *8*, 981-983.

(18) Mulholland, M. E.; Schwiderski, R. L.; Rasmussen, S. C. *Polym. Bull.* **2012**, *69*, 291-301.

(19) Sista, P. Kularatne, R. S. Mulholland, M. E.; Wilson, M.; Holmes, N.; Zhou, X.; Dastoor, P. C.; Belcher, W.; Rasmussen, S. C.; Biewer, M. C.; Stefan, M. C. *J. Polym. Sci., Part A: Polym. Chem.* **2013**, *51*, 2622-2630.

(20) Kitamura, C.; Tanaka, S.; Yamashita, Y. *J. Chem. Soc., Chem. Commun.* **1994**, 1585-1586.

(21) Tanaka, S.; Yamashita, Y. *Synth. Met.* **1995**, *69*, 599-600.

(22) Yamamoto, T.; Yamada, W.; Takagi, M.; Kizu, K.; Maruyama, T. *Macromolecules* **1994**, *27*, 6620-6626.

(23) Kitamura, C.; Tanaka, S.; Yamashita, Y. *Chem. Mater.* **1996**, *8*, 570-578.

(24) Yamamoto, T.; Muramatsu, Y.; Shimizu, T.; Yamada, W. *Macromol. Rapid Commun.* **1998**, *19*, 263-266.

(25) Zhang, Q. T.; Tour, J. M. *J. Am. Chem. Soc.* **1997**, *119*, 5065-5066.

(26) Al-Taweel, S. A.; Al-Saraierh, H. F. *Phosphorus, Sulfur Silicon Relat. Elem.* **1999**, *155*, 47-57.

(27) Sonmez, G.; Shen, C. K. F.; Rubin, Y.; Wudl, F. *Angew. Chem. Int. Ed.* **2004**, *43*, 1498-1502.

(28) Sonmez, G.; Sonmez, H. B.; Shen, C. K. F.; Jost, R. W.; Rubin, Y.; Wudl, F. *Macromolecules* **2005**, *38*, 669-675.

(29) Sonmez, G.; Sonmez, H. B.; Shen, C. K. F.; Wudl, F. *Adv. Mater.* **2004**, *16*, 1905-1908.

(30) Sonmez, G.; Shen, C. K. F.; Rubin, Y.; Wudl, F. *Adv. Mater.* **2005**, *17*, 897-900.

(31) Berlin, A.; Zotti, G.; Zecchin, S.; Schiavon, G.; Vercelli, B.; Zanelli. A. *Chem. Mater.* **2004**, *16*, 3667-3676.

(32) Akoudad, S.; Roncali, J. *Chem. Commun.* **1998**, 2081-2082.

(33) Akoudad, S.; Roncali, J. *Synth. Met.* **1999**, *101*, 149.

(34) Perepichka, I. F.; Levillain, E.; Roncali, J. *J. Mater. Chem.* **2004**, *14*, 1679-1681.

(35) Xia, Y.; Luo, J.; Deng, X.; Li, X.; Li, D.; Zhu, X.; Yang, W.; Cao, Y. *Macromol. Chem. Phys.* **2006**, *207*, 511-520.

(36) Barlow, S.; Zhang, Q.; Kaafarani, B. R.; Risko, C.; Fabrice, A.; Chan, C. K.; Domercq, B.; Starikova, Z. A.; Antipin, M. Y.; Timofeeva,T. V.; Kippelen, B.; Brédas, J.; Khan, A.; Marder, S. R. *Chem. Eur. J.* **2007**, *13*, 3537-3547.

(37) Bundgaard, E.; Krebs, F. C.; *Sol. Energy Mater. Sol. Cells* **2007**, *91*, 954-985.

(38) Petersen, M. H.; Hagemann, O.; Nielsen, K. T.; Jørgensen, M.; Krebs, F. C. *Sol. Energy Mater. Sol. Cells* **2007**, *91*, 996-1009.

(39) Mammo, W.; Admassiea, S.; Gadisab, A.; Zangb, F.; Inganäs, O.; Andersson, M. R. *Sol. Energy. Mater. Sol. Cells* **2007**, *91*, 1010-1018.

(40) Zhang, F.; Perzon, E.; Wang, X.; Mammo, W.; Andersson, M. R.; Inganäs, O. *Adv. Funct. Mater.* **2005**, *15*, 745-750.

(41) Rasmussen, S. C.; Schwiderski, R. L.; Mulholland M. E. *Chem. Commun.* **2011**, *47*, 11394-11410.

(42) Outurquin, F.; Paulmier, C. *Bull. Soc. Chim. Fr. II* **1983**, *5-6*, 159-163.

(43) Kenning, D. D.; Mitchell, K. A.; Calhoun, T. F.; Funfar, M. R.; Sattler, D. J.; Rasmussen, S. C. *J. Org. Chem.* **2002**, *67*, 9073-9076.

(44) Wen, L.; Rasmussen, S. C. *J. Chem. Crystallogr.* **2007**, *37*, 387-398.

(45) Mozingo, R.; Harris, S. A.; Wolf, D. E.; Hoffhine, C. E.; Easton, N. R.; Folkers, K. *J. Am. Chem. Soc.* **1945**, *67*, 2092-2095.

(46) Motoyama, R.; Sato, D.; Imoto, E. *Nippon Kagaku Zasshi*, **1981**, *78*, 793.

(47) Motoyama, R.; Sato, D.; Imoto, E. *Chem. Abstr.* **1960**, *54*, 22560e.

(48) Binder, D.; Noe, C. R.; Geisler, F.; Hillebrand, F. *Arch. Pharm.* **1981**, *314*, 564.

(49) Outurquin, F.; Paulmier,C. *Bull. Soc. Chim. Fr. II*, **1983**, 153.

(50) Wen, L.; Nietfeld, J. P.; Amb, C. M.; Rasmussen, S. C. *J. Org. Chem.* **2008**, *73*, 8529-8536.

(51) Usherwood, E. H.; Whiteley, M. A. *J. Chem. Soc.* **1923**, 1069.

(52) Li, J. J.; Yue, W. S. *Tetrahedron Lett.* **1999**, *40*, 4507-4510.

(53) Maligres, P. E.; Waters, M. S.; Fleitz, F.; Askin, D. *Tetrahedron Lett.* **1999**, 8193-8195.

(54) Ushkov, A. V.; Grushin, V. V. *J. Am. Chem. Soc.* **2011**, *133*, 10999-11005.

(55) Zhang, G.-Y.; Yu, J.-T.; Hu, M.-L.; Cheng, J. *J. Org. Chem.* **2013**, *78*, 2710-2714.

(56) Klapers, A.; Huang, X.; Buchwald, S. L. *J. Am. Chem. Soc.* **2002**, *124*, 7421-7428.

(57) Martin, R.; Lersen, C. H.; Cuenca, A.; Buchwald, S. L. *Org. Lett.* **2007**, *9*, 3379-3382.

(58) Evenson, S. J.; Rasmussen, S. C. *Org. Lett.* **2010**, *18*, 4049-4057.

(59) Ruan, J.; Saidi, O.; Iggo, J. A.; Xiao, J. *J. Am. Chem. Soc.* **2008**, *130*, 10510-10511.

CHAPTER 3. SYNTHESIS AND CHARACTERIZATION OF THIENO[3,4-*b*]PYRAZINE HOMOPOLYMERS VIA GRIGNARD METATHESIS (GRIM)

3.1. Introduction

Conjugated polymers (CPs) are a growing class of materials made for industrial application due to their attractive electronic and optical properties in conjunction with the mechanical flexibility and processability of organic plastics.[1-8] These materials have been applied to electronic devices such as organic light-emitting diodes (OLEDs),[9-13] organic photovoltaics (OPVs),[14-16] field-effect transistors (FETs),[17-19] electrochromics devices,[2,20-23] and sensors[24-29] in an effort to optimize efficiency while reducing cost and environmental impact. One of the key advantages to these materials is the ability to tune the electronic, optical, and mechanical properties on the molecular level, allowing for specific tuning of properties via simple alteration of either the side chain or the polymer backbone.[3,30-33]

As discussed in Chapter 1, introduction of fused-ring systems has been shown to reduce band gap by induction of the high energy quinoidal state in the polymer backbone.[34-36] This approach has been utilized in the generation of several low band gap polymers. The first of these was poly(isothianaphthene) (PITN) with an E_g of 1.0 eV.[34] This material, however, exhibits rotation of the backbone due to steric hindrance from the phenyl-based protons. A related material, thieno[3,4-*b*]pyrazine, was introduced as a theoretical construct featuring a calculated E_g of 0.7 eV,[37] a band gap even lower than that of the PITN system and less than half that of polythiophene (2.0 eV).

The electronic and optical properties of conjugated polymers (CPs) are largely dependent on the band gap (E_g), which is a significant factor in the material's efficiency in applied devices, and thus tuning of this property is of great interest. There are several factors which play a role in

determining a material's E_g; however, the most significant is the extent of conjugation. As the extent of conjugation increases, E_g decreases and so by extending the path of conjugation via polymerization or limiting steric interactions which may hinder intra- or intermolecular interactions the E_g may be minimized.

A second factor significant to the polymer's performance in a device is the energies of the HOMO and LUMO levels. This is often done by selection of materials used in the polymer backbone and can in some cases be more selectively tuned by changing the functionalities attached to these materials. A third critical factor for these materials is the capacity to be soluble in common organic solvents, allowing the materials to be processed via solution. When unfunctionalized with side chains, polymers will often be completely insoluble in most solvents. In order to increase the solubility of these polymers in organic solvents, alkyl chains are commonly attached to the base monomer units. However, these functionalities, while being necessary to allow processing, also increase steric interactions, and reduce backbone planarity. The primary interactions which cause these deviations from planarity are chain-chain interactions and interactions between the polymer backbone and the α-methylene unit.

A class of materials utilizing the fused ring structure that have shown great promise for low band gap materials is that of thieno[3,4-*b*]pyrazines (TPs).[38,39] As discussed in Chapter 2, the HOMO and LUMO of TP monomers may be effectively tuned by selection of the side chain. Introduction of an electron-donating system caused both an increase in HOMO/LUMO gap as well as an overall destabilization of the HOMO and LUMO energies. In contrast, electron-withdrawing systems were shown to reduce HOMO/LUMO gap and stabilize the HOMO and LUMO energies. These electronic effects on TP by side chain selection were further shown in

electropolymerized films of the $–OC_5H_{11}$ and $–NHC_{10}H_{21}$ difunctionalized analogues, showing destabilization with electron-donating groups.[40]

Techniques toward polymerization of TP-based systems have evolved greatly over time in an effort to increase M_n while maintaining solubility. The first TP polymer generated was poly(2,3-dihexylthieno[3,4-*b*]pyrazine) in 1990 by Pomerantz using $FeCl_3$ as a chemical oxidant (Scheme 3.1).[41] The resulting material featured a band gap of 0.95 eV. Pomerantz also noted that the resulting polymer featured paramagnetic properties even after extended attempts to dedope the material. Rasmussen and coworkers later repeated these experiments and determined the unusual properties were due to chelation of Fe^{3+} by the polymer backbone.[42] It was determined the iron in the sample was approximately 4.4 ppm, roughly one iron per 30 repeat units. Dedoping methods were attempted to remove the Fe impurities, however, were unsuccessful.

Other oxidative coupling polymerizations techniques follow the same base mechanism as seen in Scheme 3.1. This includes electropolymerization techniques discussed later in this

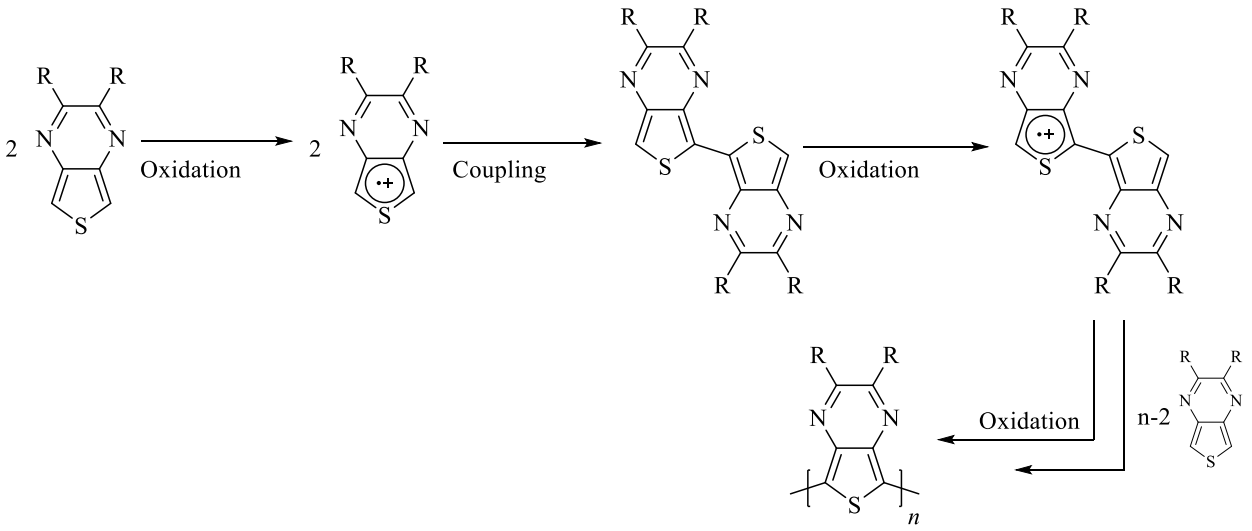

Scheme 3.1. Mechanism for oxidative polymerization of polythieno[3,4-*b*]pyrazines based on the mechanism for analogous thiophene systems.

chapter. First either chemical or electrochemical oxidation occurs in the thiophene unit by removal of an electron from the thiophene-based π-system to generate the radical cation. This state has several resonance forms, but favors the lone electron on the α-position. Coupling of the lone electrons on two such oxidized units and subsequent removal of $2H^+$ generates the dimer species. Further oxidation and coupling follows as described generating the desired polymer until the reaction is terminated.[43]

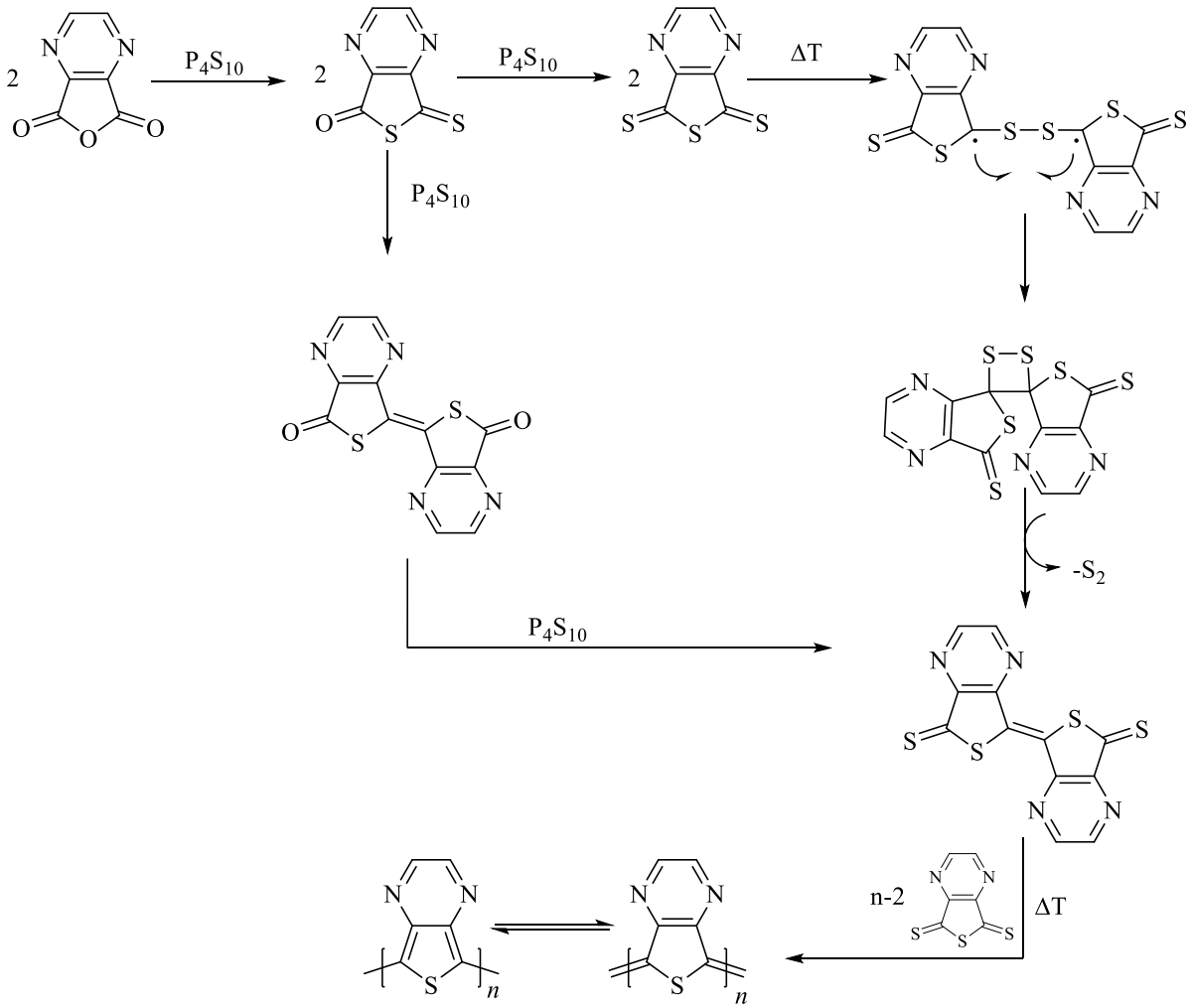

Scheme 3.2. Proposed mechanism for polymerization of TP via polycondensation.[45]

In 1995, Asselt and coworkers reported an alternate polymerization technique of TPs via P_4S_{10} and pyrazinedicarboxylic anhydride.[44] This polycondensation, as shown in Scheme 3.2, begins with pyrazinedicarboxylic anhydride and through thionation of one carbonyl generates 3-thioxothiophenone[*b*]pyrazine.[45] Coupling under thermal conditions then generates the polymer via condensation and expulsion of S_2. The polymer generated via this technique contained significant sulfur and phosphorus impurities and was additionally insoluble. This work was later repeated by Hagan and coworkers, generating a polymer featuring an Eg of 1.0 eV.[46]

In 2002 Rasmussen and coworkers prepared pTP via electropolymerization techniques.[47] Previous attempts at generating a 2,3-methylTP were unsuccessful due to overoxidation, leading to the destruction of electroactivity. In the case of TP, overoxidation can occur with potentials lower than 1.0 V.[48] However, successful polymer films were generated under lower potentials (ca. 1.35 V vs. 1.55 V for parent) (vs. Ag/Ag^+) on both indium tin oxide (ITO) and Pt plates. The mechanism for this technique is the same as shown in Scheme 3.1. However, in this case electrons are removed by induction of a potential to form the radical cation. These polymers exhibited band gaps significantly smaller than those generated via other oxidative coupling. The generated polymers exhibited bang gaps of 0.66-0.79 eV with the highest E_g corresponding to the dodecyl analogue and the lowest corresponding to the methyl analogue. These band gaps were in good agreement with the theoretical E_g of 0.7 eV for pTPs.[39] A fused ring poly(acenaphtho[1,2-*b*]thieno[3,4-*e*]pyrazine) (PATP) was generated via electropolymerization. This material featured a band gap of 0.5 eV, the lowest band gap for TP homopolymers. However, the generated films of all polymers were also completely insoluble.[49] In 2008 Rasmussen and coworkers introduced new TP monomers with electron-donating and withdrawing groups.[50] These monomers were then used to generate polymers via electropolymerization. It was observed through CV that

polymers with electron-donating groups, -OC_5H_{11} and –$NHC_{10}H_{21}$ acted to destabilize the HOMO and LUMO whereas electron-withdrawing CN group acted to stabilize the polymer.[51]

Described above are three techniques, shown in Scheme 3.3, toward generating pTPs. However, in the case of polymers produced via oxidative coupling with $FeCl_3$, low molecular weight and poor film formation limit these for application. Polymers produced via polycondensation were insoluble and featured low conductivity (10^{-5} S cm^{-1}).[44] Electropolymerized materials, although featuring the highest M_n and optical onset, were largely insoluble. Other techniques have also been utilized to produce pTPs. However, these often involved more difficult and rigorous synthetic steps and featured large band gaps.[52-59]

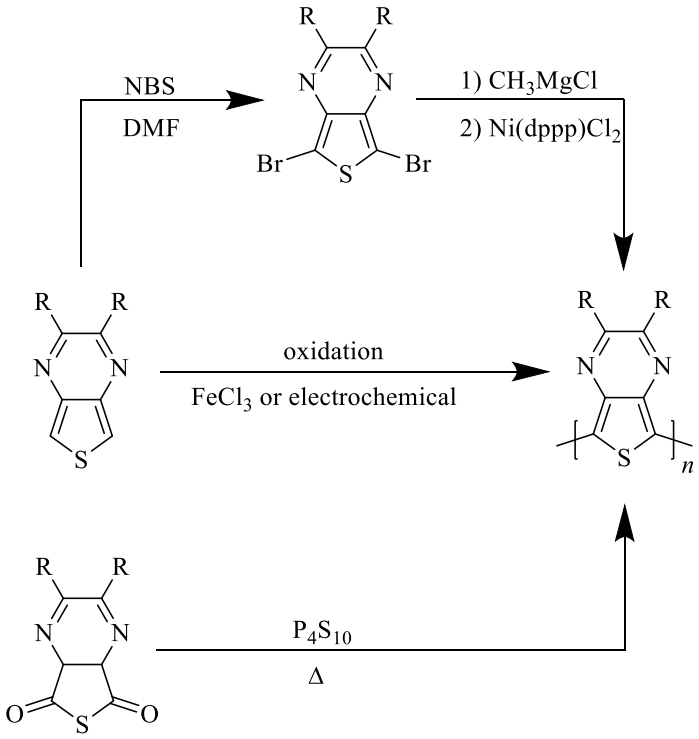

Scheme 3.3. Synthetic routes toward the production of polytheino[3,4-*b*]pyrazine.

In an attempt to generate TP polymers of higher processability, solubility, and purity Rasmussen and workers searched for alternate methods. The McCullough group had previously introduced a Grignard methathesis (GRIM) polymerization (Scheme 3.4) for the generation of regioregular poly(3-alkylthiophenes).[60-62] This method has been used since to generate numerous

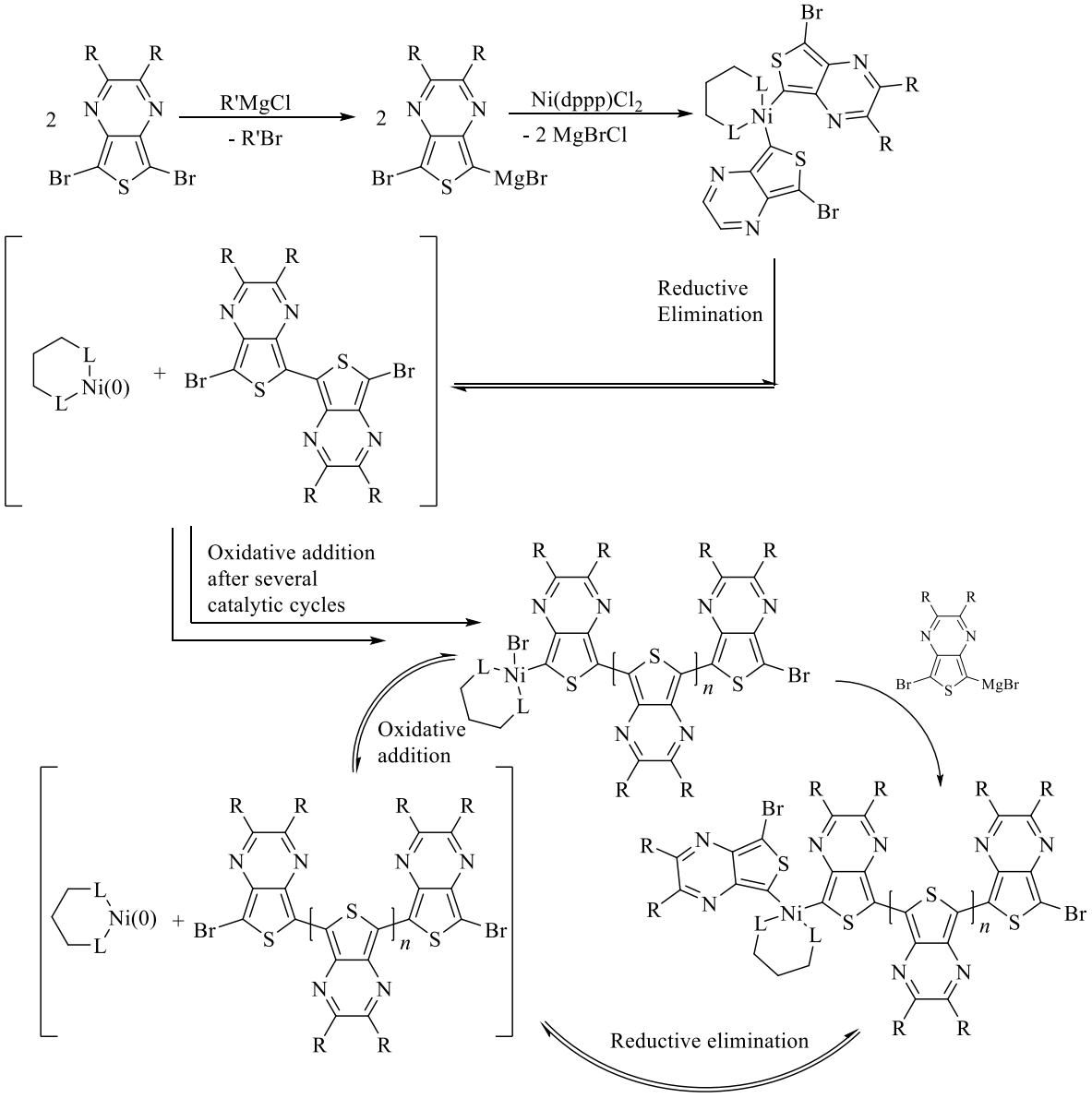

Scheme 3.4. Proposed mechanism for GRIM polymerization to generate pTP based on the mechanism for thiophene systems.[61]

polymeric materials.[63] This method is a quasi-"living" chain-growth polymerization which has been shown to not only increased the regioregular nature of generated polymers, but also yielded materials of high molecular weight.[60] The mechanism for this method begins with the oxidative addition of the nickel catalyst to two equivalents of the Grignard intermidiates. This is then reductively eliminated to form the dimer species. However, as indicated in Scheme 3.4, the nickel catalyst is still bound to the growing polymer in an as of yet unknown manner. This cycle continues with addition of more monomers to the growing polymer chain and may continue as long as more monomer is present.

Poly(3-alkylthiophene) (P3HT) materials generated via this technique gave band gaps of ~2 eV.[64] In 2008 Rasmussen and coworkers applied this technique toward the generation of poly(2,3-dihexylthieno[3,4-*b*]pyrazine.[65] The polymers generated of a purer nature than those generated via polycondensation or oxidative coupling with $FeCl_3$, with yields around 50-55 % of soluble material. Observation of the optical properties (Figure 3.1) additionally shows a slight red shift going from the $FeCl_3$ produced polymer to the GRIM produced polymer. Additionally

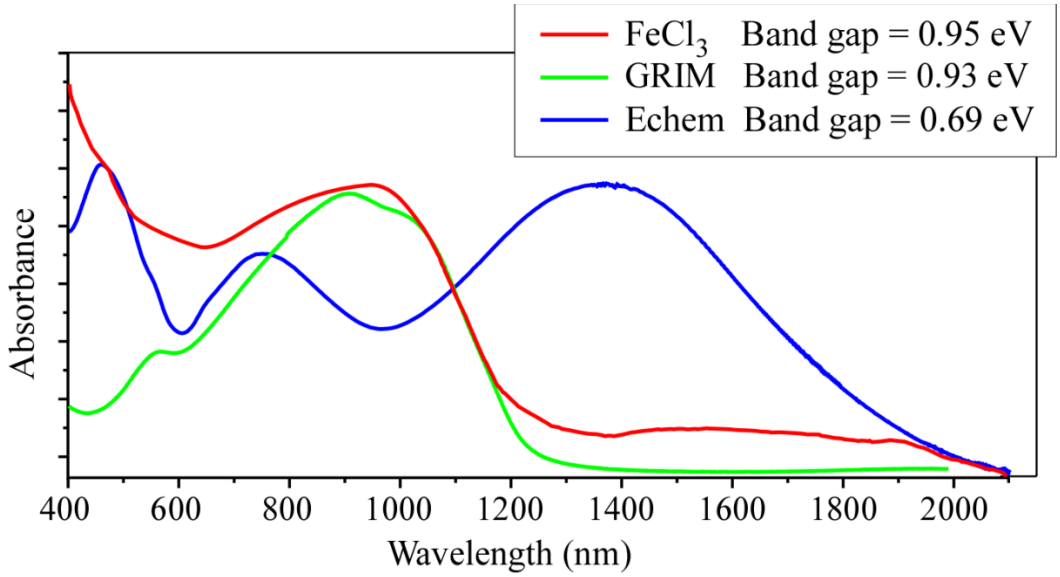

Figure 3.1. Solid-state absorption spectrum of pTP via various techniques.

molecular weights for GRIM polymerized pTPs (M_n = 4800-4900, PDI = 1.48) were improved from those using $FeCl_3$ methods (M_n = 4300, PDI = 2.14). Band gaps for pTPs generated via GRIM (0.93 eV) were lower than those of either condensation or $FeCl_3$ methods, although higher than those generated via electropolymerization.[65]

The work presented in this chapter, shown in Scheme 3.5, will focus on expanding the scope of pTPs generated through GRIM polymerization. This expansion includes increasing the alkyl side chain length, in an effort to determine how side chain size affects both solubility and M_n. Additionally, polymerization of 2nd generation TPs, such as the alkyloxy analogues will be explored. As discussed in Chapter 2, the use of side chains to modify the electronic properties of TP monomers has led to the ability to not only tune the HOMO/LUMO gap, but also to stabilize or destabilize the HOMO and LUMO levels based on the electronic donating or withdrawing nature of the side chain.[49] Thus an effort to polymerize these monomers is of interest in generating materials whose properties may be easily modified. The electronic and optical properties of all generated materials have been characterized and will be discussed.

3.2. Results and Discussion

3.2.1. *Synthesis*

The synthesis of TP homopolymers was performed as followed, shown in Scheme 3.5. The dibromoTPs **3.2a-d** were prepared via standard conditions using *N*-bromosuccinimide (NBS) in *N*,*N*-dimethylformamide (DMF) to produce a yellow solid from the respective monomers. The GRIM polymerization with **3.2a** and **3.2b** was carried out to generate **3.3a** and **3.3b** under previously reported conditions.[62] Yields for these polymers were 55 and 56%, comparable to that of the hexyl analogue. The major focus of this study was to determine the

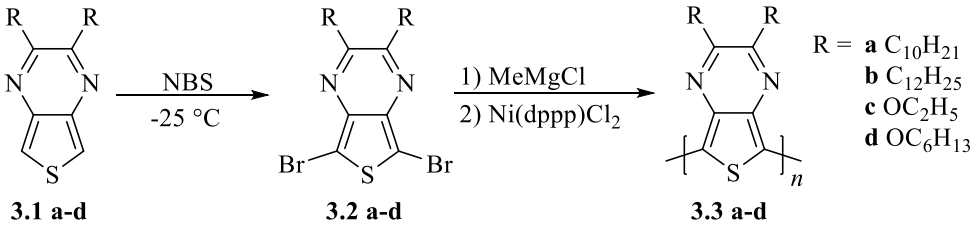

3.1 a-d **3.2 a-d** **3.3 a-d**

Scheme 3.5. Polymerization of TPs via GRIM method.

effect of increasing the size of the side chain on molecular weight, with the idea that increased side chain length might improve the solubility of the material undergoing polymerization. This would allow pTPs of higher molecular weight to be generated, improving film forming properties. However, M_n is significantly reduced for both **3.3a** and **3.3b** analogues. This is believed to be due to side chain crystallization, where side chains pack tightly together.[66,67] This reduces solubility of the material undergoing polymerization, thus causing it to precipitate out of solution at lower molecular weights.

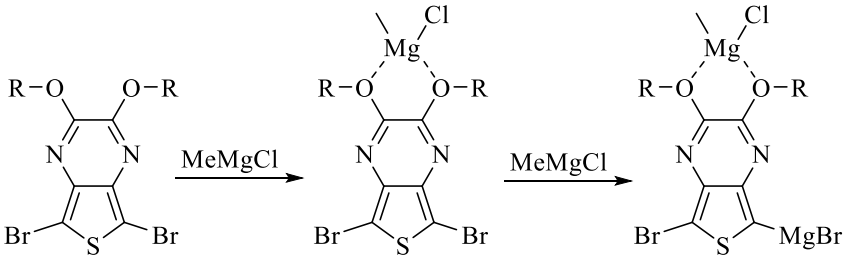

Scheme 3.6. Coordination of MeMgCl with alkyloxy TP followed by generation of the Grignard intermediate with a second equivlaent of MeMgCl.

Upon attempting to generate the Grignard intermediates, it was noted via thin layer chromatography (TLC) that with the addition of one eq. of MeMgCl, some starting material remained. An additional 0.5 eq. of Grignard was added, converting the remaining material to the

mono Grignard, which then underwent polymerization upon addition of the Ni catalyst. It is believed that while most of the Mg is used in the generation of the mono Grignard some portion of the Mg chelates to the oxygens of the alkyloxy side chains as seen in Scheme 3.6. Upon addition of an additional 0.5 eq of MeMgCl, the remaining starting material was converted to the Grignard intermediate. Yields for these polymers were slightly higher than those of the alkyl analogues with 61 % for **3.3c** and 62 % for the **3.3d**. The molecular weight for the hexyloxy analogue is comparable to that of the pC_6TP and the DP for both is similar. This is a marked drop in both M_n and DP for **3.3c**. This is likely due to low solubility of the polymer, causing it to become insoluble in the reaction at an earlier stage of chain growth.

Table 3.1. Yield and molecular weights for generated pTPs with pC_6TP for comparison.

Entry	M_n[a]	PDI[a]	DP	Yield
pC_6TP[65]	4800	1.7	16	50-55 %
3.3a	2500	1.4	6	55 %
3.3b	3300	1.6	7	56 %
3.3c	920	1.3	4	61 %
3.3d	4100	1.2	12	62 %

[a] Determined via gel permeation chromatography.

3.2.2. *UV-vis-NIR Absorption Spectroscopy*

Solution data in $CHCl_3$ and thin films of pTPs made via spin coating were analyzed via UV-vis-NIR spectroscopy; the representative absorption spectra are shown in Figure 3.2 and corresponding absorption data for the pTPs may be found in Table 3.2 with poly(2,3-dihexylthieno[3,4-*b*]pyrazine) data to compare. As seen in Figure 3.3 all TP polymers in both solution and solid state feature two absorption bands. The first absorption peak at ~300 nm corresponds to the high energy π-π^* transition, which does not shift considerably with changing functional groups, however, the alkyloxy pTPs have a larger shoulder ~400 nm.

Table 3.2. Absorbance data of pTPs.

Entry	Solution λ_{max} [b] (nm)	Solid λ_{max} [c] (nm)	Band gap (eV)[d]
pC_6TP[65]	(885), 970	890, (1050)	0.93
3.3a	850, (1008)	(966), 1027	1.03
3.3b	(676),755	(952), 1025	1.03
3.3c	824	880	1.05
3.3d	899	925	1.13

[a] In CH_3CN, [b] In CH_3Cl, [c] Film formed via spin coating on glass plate. [d] Optical.

The second, low energy absorption band is a charge transfer transition and responsible for the optical band gap. Both alkyl analogues, as well as pC_6TP, feature charge transfer bands with an onset roughly ~1200 nm. Comparison between solution and solid state for alkyl polymers reveals a red shift of about 100 nm, indicating strong packing interactions in the solid state. The alkyloxy polymers, in comparison to the alkyl analogues, feature an optical onset which is blue-shifted. This is in good agreement with the molecular orbital data from Chapter 2, in which the alkyloxy monomer experienced a slight HOMO/LUMO gap increase. This would be expected to be compounded in the polymer, giving the expected blue shift in onset of absorption. However, it should be noted **3.3c** is slightly red-shifted from **3.3d** by 80 nm. As **3.3c** has a lower DP compared to **3.3d** it should be expected **3.3d** to be more red shifted. This inconsistancy could be due to the presence of closely packed oligomers or, due to the decreased stability from the alkyloxy side chains, oxidation, causing a red shift in absorption. These theories are supported by the broad shoulder found on the UV-vis spectrum of **3.3c**. Alkyl polymers also feature a shoulder around 900 nm. Polymer **3.3d** shows no analogous shoulder, however, **3.3c**, while not having a distinct shoulder, features the broadened slope at ~1050 nm as previously described.

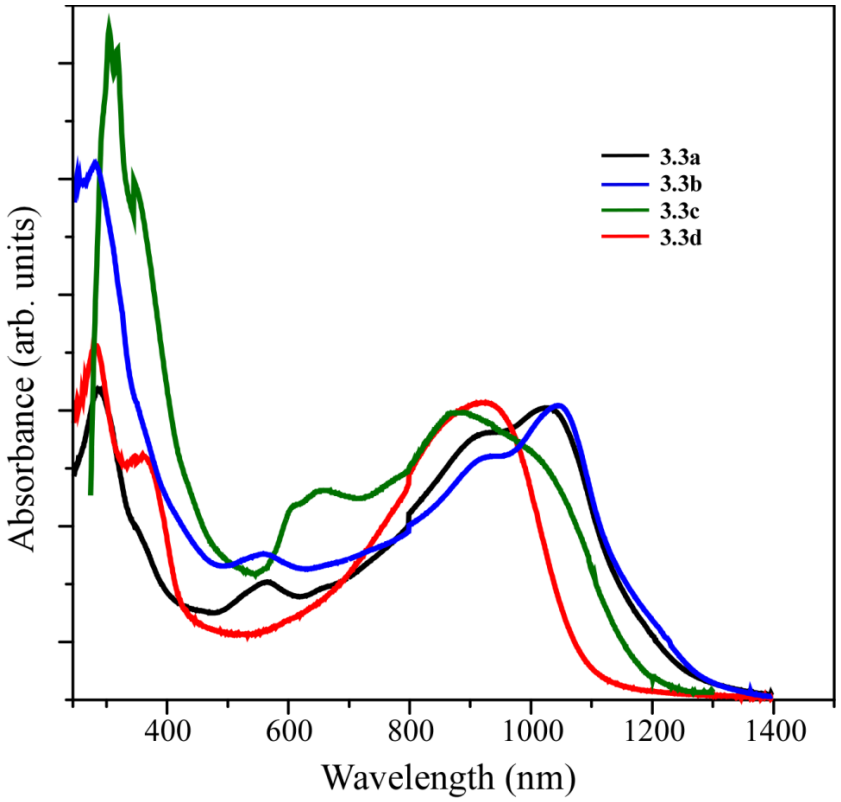

Figure 3.2. Solid-state absorption spectra of pTPs.

3.2.3. *Electrochemistry*

Cyclic voltammetry (CV) experiments were performed on all GRIM prepared polymers. The representative data for all polymers is displayed on Table 3.3 and the corresponding CVs are shown in Figure 3.3. As shown from Figure 3.4, a shift of ~0.30 V to the positive potential is seen going from **3.3d** to the alkyl pTPs. This is in good agreement with the monomer data in which the frontier molecular orbitals (MOs) were destabilized with electron-donating side chains. All polymers feature similar broad oxidation peaks. However, more fine features are found on the alkyl analogues. Interestingly the alkyl oxidation onset potentials all have a slight shift corresponding to a more positive potential from **3.3a** to **3.3b** despite a larger M_n for **3.3b**. This could, however, be due more to solid state packing effects with the larger side chain on **3.3b**. Interestingly, **3.3c** has a unusually high E_{pa} at 1.51 eV and onset of oxidation, even though

it should electronically be destabilized, similar to **3.3d**. However, low molecular weight is likely the cause of this shift to a more positive potential. As the optical and electrochemical data seem inconsistent, more investigation is needed to determine the reason behind the observed behavior.

Table 3.3. Electrochemical properties of pTPs.

Entry	Polymer (**3.3**)			
	Band Gap (eV)[a]	E_{pa} (V)[b]	HOMO (eV)[c]	LUMO(eV)[d]
pC_6TP[65]	0.93	0.65	-5.2	-4.2
a	1.03	0.91	-5.4	-4.4
b	1.03	1.17	-5.5	-4.5
c	1.05	1.51	-5.9	-4.8
d	1.13	0.61	-5.1	-4.0

[a] Optical [b] Film formed by drop casting from $CHCl_3$ solution on Pt disc working electrode. Potentials vs Ag/Ag^+ in 0.1 M $TBAPF_6$ in MeCN. [c] E_{HOMO} was determined from the onset of oxidation vs ferrocene (5.1 eV vs vacuum).[68] [d] $E_{LUMO} = E_{HOMO} - E_g$.

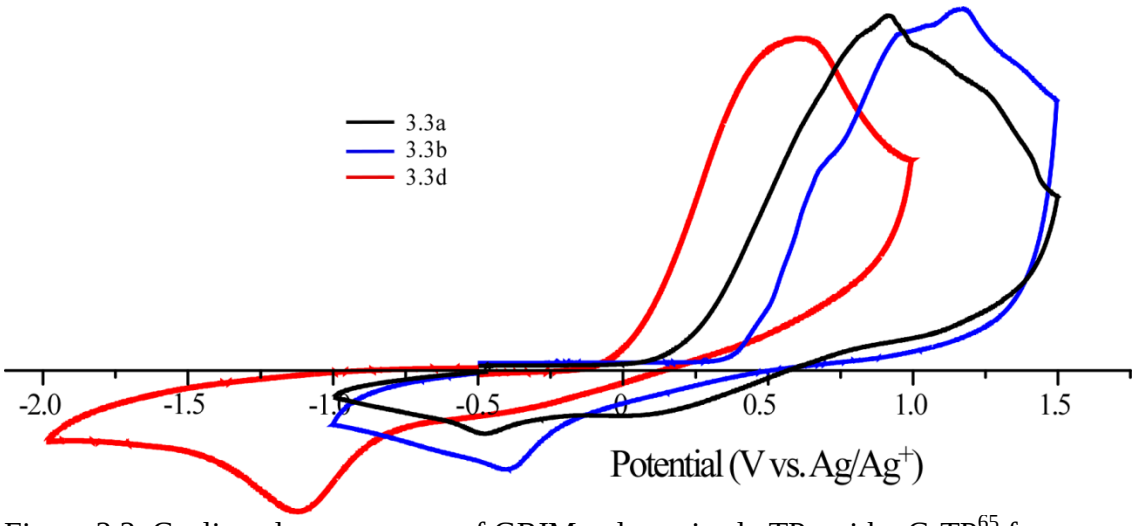

Figure 3.3. Cyclic voltammograms of GRIM polymerized pTPs with pC_6TP[65] for comparison.

It should be noted that all CV curves feature a reduction at -0.45 V, -0.32 V, -0.42 V and -1.10 V for **3.3a**, **3.3b**, **3.3c**, and **3.3d** respectively; however, it is thought these are not due to

reduction of the polymers to the -1 state. The energetic difference between these peaks and the onset of oxidation is substantially lower than the optical E_g and thus these peaks are not likely to correspond to the reduction potential. Instead, it is likely these peaks correspond to the coupled reduction of the oxidation peak and that pTPs are electrochemically irreversible.

3.3. Conclusion

GRIM polymerization techniques were used to generate TP homopolymers featuring side chains of differing length and electronic properties. Polymers **3.3a** and **b** were generated under standard GRIM conditions. These polymers have molecular weights significantly lower than that of pC_6TP. This is likely due to side chain crystallization, making the polymer chains less soluble. This would cause the growing chains to precipitate out of solution earlier terminating the chain growth. The long chain polymers showed absorption profiles similar to that of the previously generated pC_6TP. The alkyloxy polymers **3.3c** and **3.3d** used modified GRIM conditions, by adding an extra 0.5 eq. of MeMgCl to produce the Grignard intermediate, followed by standard procedure. Polymer **3.3c** featured molecular weights similar to that of pC_6TP, likely due to analogous side chain length.

Absorption data was taken for all four polymers. The alkyl analogues **3.3a** and **b** had the largest optical onset thus leading to band gaps of 1.03 eV for both. Polymers **3.3c** and **d** had blue shifted onsets from **3.3a** and **b**, in good agreement with monomeric data, leading to larger band gaps of 1.05 eV and 1.13 eV. However, CV experiments showed unexpected behavior. While **3.3d** featured an oxidation onset shifted to a negative potential, as expected, **3.3c** was shifted to a positive potential. Additionally in the alkyl analogues polymer **3.3b**, with a larger M_n, showed a more stabilized oxidation onset, although this might of be more a factor of packing.

3.4. Experimental

3.4.1. *General*

Unless noted, all materials were reagent grade and used without further purification. Chromatographic separations were performed using standard column chromatography methods with silica gel (230-400 mesh). Dry DMF was obtained by mixing with $MgSO_4$, followed by flushing through silica gel, storing under molecular sieves, and purging over nitrogen for 1 h. Dry THF was obtained via distillation over sodium/benzophenone. All glassware was oven-dried, assembled hot, and cooled under a dry nitrogen stream before use. Transfer of liquids was carried out using standard syringe techniques and all reactions were performed under a dry nitrogen stream. The ^{1}H NMR and ^{13}C NMR were completed on a 400 MHz spectrometer. All NMR data was referenced to the chloroform signal and peak multiplicity was reported as follows: s = singlet d = double, t = triplet, q = quartet, p = pentet, tt = triplet of triplets, m = multiplet and br = broad. Melting points were determined using a digital thermal couple with a 0.1 °C resolution. The following compounds were synthesized according to previously reported literature procedures: 2,3-didecylthieno[3,4-*b*]pyrazine (**3.1a**),[69] 2,3-didodecylthieno[3,4-*b*]pyrazine (**3.1b**).[69]

5.7-Dibromo-2,3-didecylthieno[3,4-*b*]pyrazine (3.2a). To a 100 mL RB flask was added **3.1a** (2.07, 5 mmol), which was then evacuated and placed under a dry nitrogen stream. To this, dry DMF (50 mL) was added via syringe and the solution was cooled to -78 °C (dry ice/acetone). A solution of NBS (2.22 g, 12.5 mmol) in DMF (10 mL) was added dropwise, after which the solution was warmed to -15 °C (ice/salt bath) and stirred for 3 h. The solution was then poured into 100 mL of ice and stirred for 10 min. The resulting precipitate was then filtered, solubilized in diethyl ether, and washed with NH_4Cl, H_2O, and brine. The organic layer was then

dried with $MgSO_4$ and product was concentrated via rotary evaporation. Purification was done by silica gel chromatography in hexanes/Et_2O (3 %) to give a yellow solid product (52 – 63% yield). mp 45.0-46.2 °C; ^{1}H NMR: δ 2.89 (t, *J* = 7.6 Hz, 4H), 1.79 (p, *J* = 8.0 Hz, 4H), 1.46-1.19 (m, 31H), 0.87 (q, J = 6.8 Hz, 6H). ^{13}C NMR: δ 158.4, 139.9, 103.5, 35.6, 32.1, 29.8, 29.8, 29.7, 29.5, 29.3, 28.2, 22.9, 14.3.

5.7-Dibromo-2,3-didodecylthieno[3,4-*b*]pyrazine (3.2b). Monomer **3.2b** was produced as a yellow solid in the same manner as **3.2a** substituting **3.1a** with **3.1b** (50 - 67% yield). mp 45.2 – 46.4 °C; ^{1}H NMR: δ 2.29 (t, *J* = 7.6 Hz, 2H), 1.77 (p, *J* = 7.6 Hz, 2H), 1.34 (m, 18H), 0.87 (t, *J* = 6.8 Hz 6H). ^{13}C NMR: δ 156.6, 141.9, 116.0, 35.9, 32.1, 31.1, 30.0, 29.8, 29.7, 21.6, 29.5, 29.2, 28.5, 22.9, 14.3.

5.7-Dibromo-2,3-ethyloxythieno[3,4-*b*]pyrazine (3.2c). Monomer **3.2c** was produced as a yellow solid in the same manner as **3.2a** substituting **3.1a** with **3.1c** (65% yield). mp 61.2-62.0; ^{1}H NMR: δ 4.64 (q, *J* = 6.8, 4H), 1.47 (t, *J* = 7.2, 6H). ^{13}C NMR: δ 184.8, 153.9, 142.7, 65.6, 14.2.

5.7-Dibromo-2,3-hexyloxythieno[3,4-*b*]pyrazine (3.2d). Monomer **3.2d** was produced as a yellow solid in the same manner as **3.2a** substituting **3.1a** with **3.1d** (67% yield). mp 45.2 - 46.4 °C; ^{1}H NMR: δ 4.48 (t, J = 6.8 Hz, 4H), 1.86 (t, J = 6.8 Hz, 4H), 1.38 (m, 14H), 0.89 (t, J = 2.4 Hz, 6H); ^{13}C NMR: δ 151.1, 136.3, 98.8, 67.9, 31.6, 28.5, 25.8, 22.7, 14.1.

Poly(2,3-didecylthieno[3,4-*b*]pyrazine) (3.3a). Polymerization via GRIM coupling was accomplished using previously reported methods.[63] To a 25 mL RB flask was added, 3.2a,b (1 mmol) which was then evacuated and placed under a dry N_2 stream. THF (10 mL) was then added via syringe and MeMgCl (1.0 mmol, 0.33 mL) was also added via syringe. The solution was heated to reflux for 1 h and Ni(dppp)Cl_2 (0.003 g, 3.90 x 10^{-6} mmol) was added. The

reaction was then heated for another hour, after which was then poured into 100 mL of methanol and stirred for 2 h. The precipitate was then filtered and collected. Soxhlet extraction was performed with methanol, acetone, and hexanes and the solid was then collected in $CHCl_3$. The polymer was concentrated via rotary evaporation giving a purple-black solid (55% yield). ^{1}H NMR: δ 2.90, 2.12, 1.26, 0.89 GPC: M_w = 3500, M_n = 2500, PDI = 1.4.

Poly(2,3-didodecylthieno[3,4-*b*]pyrazine) (3.3b). Polymer **3.3b** was produced in the same manner as **3.3a** substituting **3.2a** with **3.2b**. The polymer was concentrated via rotary evaporation to yield a purple-black solid (56% yield). ^{1}H NMR: δ 1.54, 1.41, 0.84. GPC: M_w = 5300, M_n = 3300, PDI = 1.6.

Poly(2,3-diethyloxythieno[3,4-*b*]pyrazine) (3.3c). To a 25 mL RB flask was added **3.2c** (0.35 g, 1 mmol) which was then evacuated and placed under a dry N_2 stream. THF (10mL) was then added via syringe and MeMgCl (1.5 mmol, 0.45 mL) was also added via syringe. The solution was heated to reflux for 1 h and Ni(dppp)Cl_2 (0.003 g, 3.90 x 10^{-6} mmol) was added. The reaction was then heated for another hour, after which was then poured into 100 mL of methanol and stirred for 2 h. The precipitate was then filtered and collected. Soxhlet extraction was performed with methanol, acetone, and hexanes and the solid was then collected in $CHCl_3$ to give a blue-black solid (61% yield). ^{1}H NMR: δ 4.71, 1.48. GPC: M_w = 1200, M_n = 920, PDI = 1.3.

Poly(2,3-dihexyloxythieno[3,4-*b*]pyrazine) (3.3b). Polymer **3.3d** was produced in the same manner as **3.3c** substituting **3.2c** with **3.2d**. The polymer was concentrated via rotary evaporation to yield a blue-black solid (62% yield). ^{1}H NMR: δ 4.70, 1.89, 1.45, 0.89. GPC: M_w = 4900, M_n = 4100, PDI = 1.2.

3.4.2. *Electrochemistry*

All electrochemical techniques were performed on a Bioanalytical Systems BAS 100B/W electrochemical analyzer. Cyclic voltammetry (CV) experiments were performed using a three-electrode cell consisting of a Pt-disc working electrode, Pt coil wire auxillary electrode, and an Ag/Ag^+ reference electrode. A 0.1 M electrolyte solution was prepared with tetrabutylammonium hexafluorophosphate ($TBAPF_6$) using MeCN distilled over CaH_2 under dry nitrogen. The solutions were deoxygenated with argon for at least 20 min prior to each scan and blanketed with argon during the experiments. Solutions of polymers in $CHCl_3$ were drop cast on the working electrode and dried to form a solid film. CV experiments were performed in the above described cell at a sweep rate of 100 mV/s. E_{HOMO} values were determined in a reference to ferrocene (5.1 V vs. vacuum)[68] and the E_{LUMO} was determined from the following equation: $E_{LUMO} = E_{HOMO}$ – optical band gap.

3.4.3. *UV-vis-NIR Absorption Spectroscopy*

All absorption spectroscopy was performed on a Carry 500 dual-beam UV-vis-NIR spectrophotometer. Solution-state spectra were analyzed in chloroform and solid-state spectra were analyzed with the polymer spin coated on a glass plate. The optical band gaps were determined from the onset of the lowest energy absorption by extrapolation of the steepest slope to the intersection with the wavelength axis.

3.5. References

(1) Barford, W. *Electronic and Optical Properties of Conjugated Polymers*, International Series of Monographs on Physics ed.; Clarendon Press: Oxford, 2005; Vol. 129.

(2) Scrosati, B. In *Applications of Electroactive Polymers*; Scrosati, B., Ed.; Chapman and Hall: London, 1993; pp 250-282.

(3) Rasmussen, S. C.; Ogawa, K.; Rothstein, S. D. In *Handbook of Organic Electronics and Photonics*; Nalwa, H. S., Ed.; American Scientific Publishers: Stevenson Ranch, CA, 2008; Vol. 1, Chapter 1.

(4) Heeger, A. J. *Angew. Chem., Int. Ed. Engl.* **2001**, *40*, 2591-2611.

(5) MacDiarmid, A. G. *Angew. Chem., Int. Ed. Engl.* **2001**, *40*, 2581-2590.

(6) Shirakawa, H. *Angew. Chem., Int. Ed. Engl.* **2001**, *40*, 2575-2580.

(7) Garnier, F. *Acc. Chem. Res.* **1999**, *32*, 209-215.

(8) Yu, G.; Heeger, A. J. *Synth. Met.* **1997**, *85*, 1183-1186.

(9) Antohe, S. In *Handbook of Organic Electronics and Photonics: Electronic Materials and Devices*; Halwa, H. S., Ed..; American Scientific: Stevenson Ranch, CA, 2008; Vol. 1, pp 406-446.

(10) Christian-Pandya, H.; Vaidyanathan, S.; Galvin, M. In *Handbook of Conducting Polymers: Processing and Applications*; Skotheim, T. A., Reynolds, J. R., Eds.; CRC Press: Boca Raton, Fl, 2007; Chapter 5.

(11) Grimsdale, A. C.; Chan, K. L.; Martin, R. E.; Jokisz, P. G.; Holmes, A. B. *Chem. Rev.* **2009**, *109*, 897-1091.

(12) Epstein, A. C.; Chan, K. L.; Martin, E.; Kokisz, P. G.; Holmes, A. B. In *Semiconducting Polymers: Applications, Processing, and Synthesis*; Hsieh, B. R., Wei, Y., Eds.; ACS Symposium Series 735; American Chemical Society: Washington, DC, 1999; pp 119-133.

(13) Chen, S. –A.; Chang, E. –C. In *Semiconducting Polymers: Applications, Processing, and Synthesis*; Hsieh, B. R., Wei, Y., Eds.; ACS Symposium Series 735; American Chemical Society: Washington, DC, 1999; pp 163-172.

(14) Brabec, C. J.; Sariciftci, N. S. In *Semiconducting Polymers;* Hadziioannou, G., van Hutten, P. F., Eds.; Wiley-VCH: Weinheim, Germany, 2000; pp 515-560.

(15) Mozer, A. J.; Sariciftci, N. S. In *Handbook of Conducting Polymers: Processing and Applications,* 3rd ed.; Skotheim, T. A., Reynolds, J. R., Eds.; CRC Press: Boca Raton, FL, 2007; Chapter 10.

(16) Liang, Z.; Wang, Q. In *Handbook of Organic Electronics and Photonics: Electronic Materials and Devices;* Halwa, H. S., Ed.; American Scientific: Stevenson Ranch, CA, 2008; Vol. 1, pp 177-223.

(17) Bao, Z. In *Semiconducting Polymers: Applications, Processing, and Synthesis;* Hsieh, B. R., Wei, Y., Eds.; ACS Symposium Series 735; American Chemical Society: Washington, DC, 1999; pp 244-257.

(18) Facchetti, A. In *Handbook of Thiophene-based Materials: Applications in Organic Electronics and Photonics;* Perepichka, I. F., Perepichka, D. F., Eds.; Wiley: Chinchester: West Sessex, U.K., 2009; pp 595-646.

(19) McCullouch, I.; Heeney, M. In *Handbook of Thiophene-based Materials: Applications in Organic Electronics and Photonics;* Perepichka, I. F., Perepichka, D. F., Eds.; Wiley: Chinchester: West Sussex, U.K., 2009; pp 647-672.

(20) Dyer, A. L.; Reynolds, J. R. In *Handbook of Conducting Polymers: Theory of Conjugated Polymers;* Skotheim, T. A., Reynolds, J. R., Eds.; CRC Press: Boca Raton, FL, 2007; Chapter 20.

(21) Mastragostino, M. In *Applications of Electroactive Polymers;* Scrosati, B., Ed.; Chapman & Hall: London, 1993; pp 223-249.

(22) Invernale, M. A.; Acik, M.; Sotzing, G. A. In *Handbook of Thiophene-based Materials: Applications in Organic Electronics and Photonics;* Perepichka, D. F., Perepichka, I. F., Eds.; West Sussex, U.K., 2009; pp 757-782.

(23) Beaujuge, P.; Reynolds, J. R. *Chem. Rev* **2010**, *110*, 268-320.

(24) McQuade, D. T.; Pullen, A. E.; Swager, T. M. *Chem. Rev.* **2000**, *100*, 2537-2574.

(25) Thomas, S. W.; Guy, J. D.; Swager, T. M. *Chem. Rev.* **2007**, *107*, 1339-1386.

(26) Grigory, Z. V.; Manuel, P. A.; Pavel, A. J. *Org. Lett.* **2008**, *10*, 3681-3684.

(27) Toal, S. J.; Trogler, W. C. *J. Mater. Chem.* **2006**, *16*, 2871-2883.

(28) Amara, J. P.; Swager, T. M. *Macromolecules* **2005**, *38*, 9091-9094.

(29) Yang, J. S.; Swager, T. M. *J. Am. Chem. Soc.* **1998**, *46*, 11864-11873.

(30) Roncali, J. *Chem. Rev.* **1992**, *92*, 711-738.

(31) Roncali, J. *Chem. Rev.* **1997**, *97*, 173-205.

(32) Roncali, J. Advances in the Molecular Design of Functional Conjugated Polymers. In *Handbook of Conducting Polymers*, 2nd ed.; Skotheim, T. A., Elsenbaumer, R. L., Reynolds, J. R., Eds.; Marcel Dekker, Inc.: New York, 1998; pp 311-341.

(33) Ramussen, S. C.; Straw, B. D.; Hutchinson, J. E. In *Semiconducting Polymers: Applications, Synthesis, and Properties;* Hsieh, B. R., Wei, W., Galvin, M., Eds.; ACS Symposium Series 735, American Chemical Society: Washington, DC, 1999; pp 347-366.

(34) Rasmussen, S. C.; Ogawa, K.; Rothstein, S. D. In *Handbook of Organic Electronics and Photonics: Electronic Materials and Devices;* Nalwa, H. S., Ed.; American Scientific Publishers: Stevenson Ranch, CA, 2008; Vol. 1, pp 1-50.

(35) Bredas, J. L. *J. Chem. Phys.* **1985**, *82*, 3808-3811.

(36) Dkhissi, A.; Louwet, F.; Groenendaal, L.; Beljonne, D.; Lazzaroni, R.; Bredas, J. L. *Chem. Phys. Lett.* **2002**, *359*, 466-472.

(37) Xu, B.; Holdcroft, S. *Macromolecules* **1993**, *26*, 4457-4460.

(38) Nayak, K.; Marynick, D. S. *Macromolecules* **1990**, *23*, 2237-2245.

(39) Otto, P.; Ladik, J. *Synth. Met.* **1990**, *36*, 327-335.

(40) Wen, L.; Nietfeld, J. P.; Amb, C. M.; Rasmussen, S. C. *Synth. Met.* **2009**, *159*, 2299-2301.

(41) Pomerantz, M.; Chaloner-Gill, B.; Hardin, L. O.; Tseng, J. J.; Pomerantz, W. J. *J. Chem. Soc., Chem. Commun.* **1992**, 1672.

(42) Kenning, D. D.; Mitchell, K. A.; Funfar, M. R.; Rasmussen, S. C. *Polym. Prepr*. **2001**, *42*, 665.

(43) Heth, C. L.; Tallman, D. E.; Rasmussen, S. E. *J. Phys. Chem. B* **2010**, *114*, 5275–5282.

(44) Hagan, A. J.; Moratti, S. C.; Sage, I. C. *Synth. Met.* **2001**, *119*, 147-148.

(45) Van Asselt, R.; Hoogmartens, I.; Vanderzande, D.; Gelan, J.; Froehling, P. E.; Aussems, M.; Aagaard, O.; Schellekens, R. *Synth. Met.* **1995**, *74*, 65-70.

(46) Paulussen, H.; Haitjemi, H.; van Asselt, R.; Mylle, P.; Adriaensens, P.; Gelan, J.; Vanderzande, D. *Polymer* **2000**, *41*, 3121-3127.

(47) Kenning, D. D.; Ramussen, S. C. *Macromolecules* **2003**, *36*, 6298-6299.

(48) Krische, B.; Zagorska, M. *Synth. Met.* **1989**, *28*, 257-265.

(49) Nietfeld, J. P.; 4, C. L.; Rasmussen, S. C. *Chem. Commun*. **2008**, 981-983.

(50) Wen, L.; Nietfeld, J. P.; Amb, C. M.; Rasmussen, S. C. *J. Org. Chem.* **2008**, *73*, 8529-8536.

(51) Wen, L.; Nietfeld, J. P.; Amb, C. M.; Rasmussen, S. C. *Synth. Met.* **2009**, *159*, 2299-2301.

(52) Kitamura, C.; Tanaka, S.; Yamashita, Y. *J. Chem. Soc., Chem Commun.* **1994**, 1585-1586.

(53) Kitamura, c.; Tanaka, S.; Yamashita, Y. *Chem. Mater.* **1996**, *8*, 570-578.

(54) Sonmez, G.; Shen, C. K. F.; Rubin, Y.; Wudl, F. *Angew. Chem. Int. Ed.* **2004**, *43*, 1498-1502.

(55) Sonmez, G.; Sonmez, H. B.; Shen, C. K. F.; Jost, R. W.; Rubin, Y.; Wudl, F. *Macromolecules* **2005**, *38*, 669-675.

(56) Sonmez, G.; Sonmez, H. B.; Schen, C. K. F.; Wudl, F. *Adv. Mater.* **2004**, *16*, 1905-1908.

(57) Sonmez, G.; Shen, C. K. F.; Rubin, Y.; Wudl, F. *Adv. Mater.* **2005**, *17*, 897-900.

(58) Berlin, A.; Zotti, G.; Zecchin, S.; Schiavon, G.; Vercelli, B.; Zanelli, A. *Chem. Mater.* **2004**, *16*, 3667-3676.

(59) Wienk, M. M.; Turbiez, M. G. R.; Struijk, M. P.; Fonrodona, M.; Janssen, R. A. J. *Appl. Phys. Lett.* **2006**, *88*, 153511-153513.

(60) Lowe, R. S.; Ewbank, P. C.; Liu, J.; Zhai, L.; McCullough, R. D. *Macromolecules*, **2001**, *34*, 4324-4333.

(61) Zhai, L.; Pilston, R. L.; Zaiger, K. L.; Stokes, K. K.; McCullough, R. D. *Macromolecules*, **2003**, *36*, 61-64.

(62) Iovu, M. C.; Sheina, E. E.; Gil, R. R.; McCullough, R. D. *Macromolecules* **2005**, *38*, 8649-8656.

(63) Stefan, M. C.; Bhatt, M. P.; Sista, P.; Magurudeniya, H. D.; *Polym. Chem.* **2012**, *3*, 1693-1701.

(64) Dou, L.; You, J.; Yang, J.; Chen, C.-C.; He, Y.; Murase, S.; Moriarty, T.; Emery, K.; Li, G.; Yang, Y. *Nature Photon.* **2012**, *6*, 180-185.

(65) Wen, L.; Duck, B. C.; Dastoor, P. C.; Rasmussen, S. C. *Macromolecules.* **2008**, *41*, 4576-4578.

(66) Prosa, T. J.; Winokur, M. J.; Moulton, J.; Smith, P.; Heeger, A. J. *Macromolecules* **1992**, *25*, 4364-4372.

(67) Park, K. C.; Levon, K. *Macromolecules* **1997**, *30*, 3175-3183.

(68) Cardona, C. M.; Li, W.; Kaifer, A. E.; Stockdale, D.; Bazan, G. C. *Adv. Mater.* **2011**, *23*, 2367-2371.

(69) Kenning, D. D.; Mitchell, K. A.; Calhoun, T. R.; Funfar, M. R.; Sattler, D. J.; Rasmussen, S. C. *J. Org. Chem.* **2002**, *67*, 9073-9076.

CHAPTER 4. SYNTHESIS AND CHARACTERIZATION OF THIENO[3,4-*b*]PYRAZINE-BASED COPOLYMERS WITH THIOPHENE COMONOMERS.

4.1. Introduction

Over the course of the past decade, the donor-acceptor (DA) approach toward the generation of low band gap (E_g) polymers has become increasingly popular. As previously discussed in Chapter 1, this approach combines an electron-rich donor material with an electron-poor acceptor material in the generation of an alternating copolymer. The HOMO of the resulting polymer is largely modulated by the donor material while the LUMO is largely modulated by the acceptor.[1] The generated DA copolymer then has an E_g lower than that of the homopolymers of either donor or acceptor units. This approach has many advantages, such as the ability to tune the electronic, optical, and bulk properties by careful selection of comonomeric units. Although an inorganic n-i-p-i (n = n-type, p = p-type) structure is one cited explanation of the lowed E_g for DA copolymers,[2] recent studies have suggested instead the combination of aromatic and quinoidal units may cause decreased bond length alternation.[3] Additionally, low energy transitions were thought to be due to a charge transfer from donor to acceptor units. However, more recent studies have pointed to a HOMO delocalized along the polymer backbone and a LUMO localized on the acceptor.[4] This explanation has logic in that it allows for a greater delocalization of electrons, and thus destabilization of the HOMO. Although most materials are classically defined as either a donor or an acceptor, several existing monomeric units do not fit into conventional ‘donor’ or ‘acceptor’ roles and thus produce materials of unanticipated electronic properties.

One such class of materials exhibiting such unconventional behavior in DA copolymers are thieno[3,4-*b*]pyrazines (TPs).[5] Monomeric TPs are commonly considered to be an acceptor-

type moeity, thus primarily involved in the formation of the polymer LUMO. However, careful study of TP-based DA copolymers have shown these materials have a more complex role in DA polymers. TP-based copolymers generated with common strong donor units, such units as thiophene,[6,7] 4-di(2-ethylhexyl)cyclopenta[2,1-*b*:3,4-*b*']dithiophene,[8] and 1,4-didecyloxybenzene,[9] yield polymers with band gaps of 1.03 eV, 1.18 eV, and 1.52 eV respectively. As discussed in Chapter 3, homopolymeric poly(2,3-dihexylthieno[3,4-b]pyrazine) (pC_6TP) has a band gap of 0.93 eV, smaller than the previously mentioned DA materials.[10] Examination of the three DA copolymers frontier orbitals shows that TP does act as an acceptor-type unit in the formation of the polymer LUMO, which occurs at energies similar to TP homopolymers. However, as discussed in Chapter 1, TPs actually have a HOMO higher than that of many other common donor materials.

This was further illustrated by Rasmussen and coworkers by generation of oligomers combining TP with donor units 3,4-ethylenedioxythiophene (EDOT) and thiophene. In this study oligomers with higher TP content showed a red shift in absorption and decrease in potential of oxidation.[11,12] In agreement with these results and previously mentioned copolymeric data, HOMOs of TP-based DA copolymers are typically found between the HOMO of the analogous TP homopolymer and that of the donor homopolymer.[6-9,13-37] A representation of molecular orbital (MO) combinations using dimer models of donor-donor TP-TP and donor-TP is shown in Figure 4.1.

The DA approach has become a powerful tool toward design of materials by alteration of electronic and optical properties. Organic photovoltaics (OPVs) are a device application which has become a large focus of material design in the field of conjugated polymers (CPs). The drive in applying organic systems in solar cells stems from the potential of devices which are light

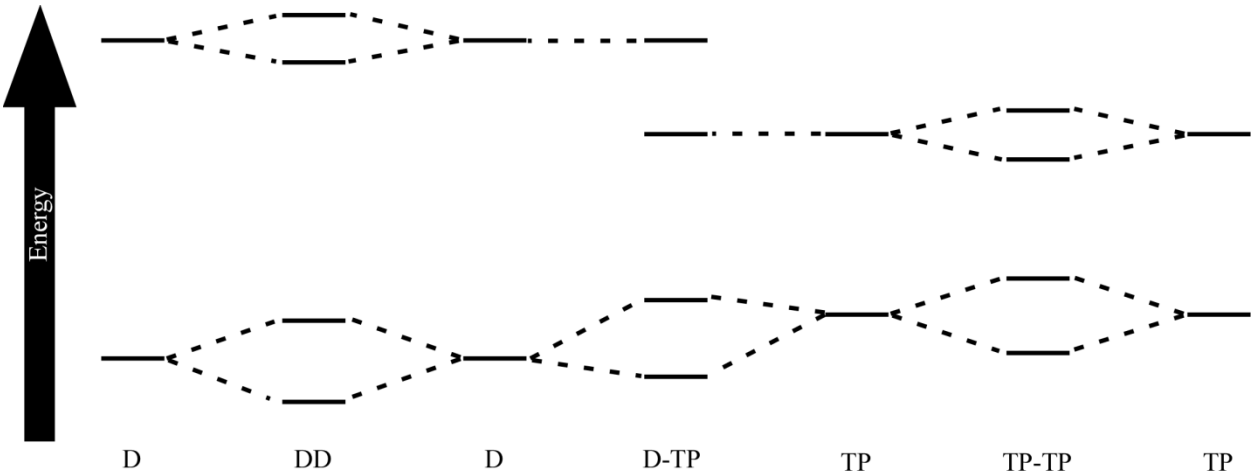

Figure 4.1. Combination of donor-donor, TP-TP, and donor-TP dimers in the ground state to illustrate the effect of electronic tuning of DA copolymers.[38]

weight and solution processable and thus more cost effective.[39-42] In OPVs fabrication the use of a bulk heterojunction active layer has become popular, showing increased efficiency. These architectures use a fullerene acceptor material, with the donor typically being a CP. Thus, while the acceptor material remains largely the same from cell to cell, optimization of the donor component has become a large focus.[43,44] Much of this focus has been aimed at generation of low band gap polymers in order to absorb the majority of the solar flux. However, equally important to the efficiency of the solar cell is the optimization of the V_{oc} which is largely influenced by the offset between the donor HOMO and fullerene LUMO. An example of the structure architecture of an OPV device is shown in Figure 4.2, along with a representation of a bulk heterojunction. Additionally, offset between donor and acceptor material LUMOs must be large enough to drive electrons to the fullerene and eliminate back transfer. Thus, reduction of band gap and optimization of V_{oc} are opposing forces and so fine tuning of electronic properties is of significant interest. A representation of a current vs. potential plot is shown in Figure 4.3 with the calculation of power conversion energy (PCE).

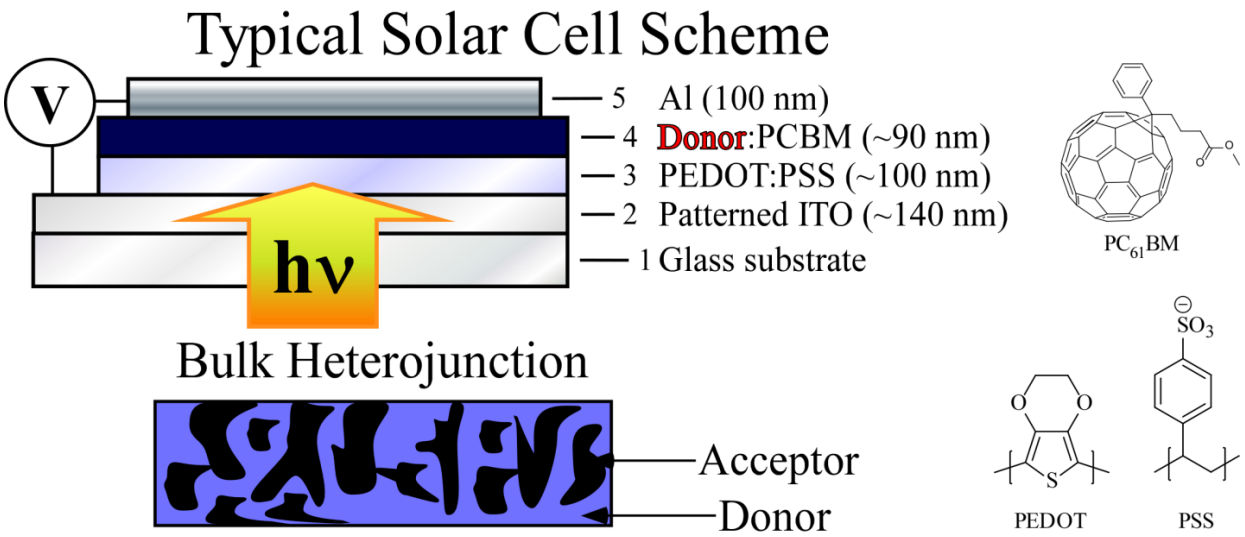

Figure 4.2. Model of a typical BHJ solar cell with the BHJ layer general structure.

Through methods described above, optimization of donor material properties has yielded improved solar cell efficiencies. Previous solar cells using poly(3-hexylthiophene) have reached high efficiencies of 5%.[45-47] However, design of new materials through the DA approach has generated solar cells of efficiencies greater than 9%.[48] To improve this technology to be competitive with silicon solar cells, further optimization of the donor material through careful modification of electronic properties is needed. In an effort to both expand the scope of CP materials and further expand understanding of the structure-function relation of DA polymers, new materials utilizing the previously discussed amibpolar unit, TP, were generated using this approach. Copolymers containing TP were combined with thiophene-based 'donor' materials to examine how electronic and optical properties are changed with altering comonomer and TP-based side chains. Additionally 2nd generation TPs, discussed in Chapter 2, were combined with these donor units to investigate changes in polymer properties by altering the TP-based electronics.

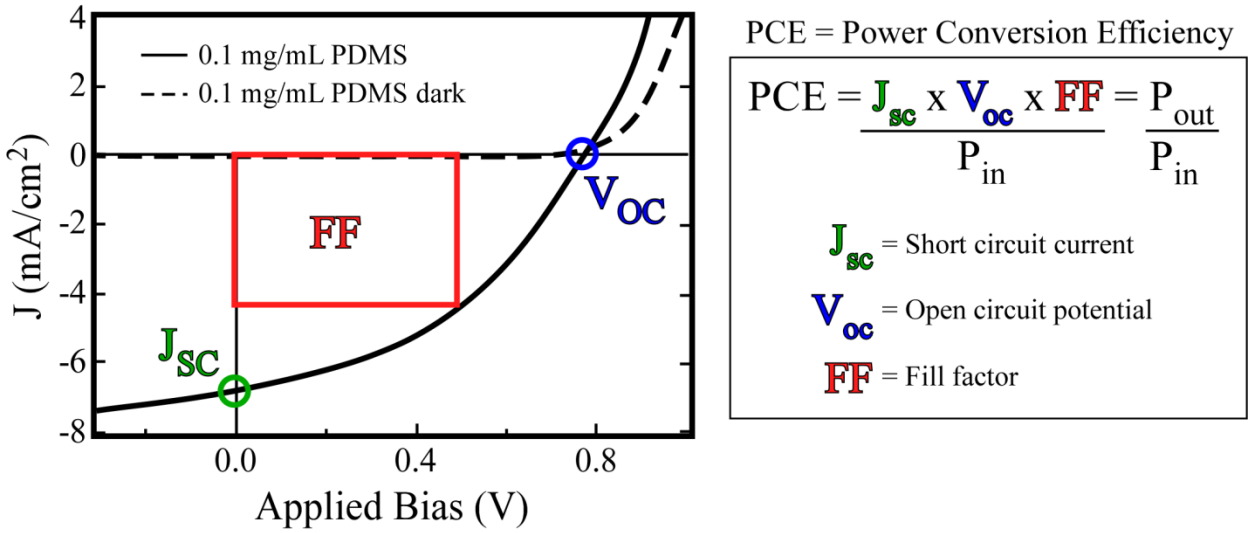

Figure 4.3. Typical current vs. potential plot for an OPV device and calculation of power conversion efficiency (PCE).

N-Octyldithieno[3,2-*b*:2',3'-*d*]pyrroles (DTPs) have been shown to be excellent donor materials with good mobilities. Application of DTPs in DA polymers has successfully generated materials used in devices such as FETs and OPVs.[49-52] In section 4.2, combination of TPs with DTP in the generation of TPDTP copolymers is outlined along with electronic and optical characterization. Also in section 4.2, combination of TP with the donor unit, benzo[1,2-*b*:4,5-*b'*]dithiophene (BDT), is outlined. BDT has previously been shown to generate highly soluble, highly planar materials, which may be easily functionalized.[53-60] Previous application of BDT into copolymers with diketopyrrolopyrrole has generated materials that, when applied into solar cells, have yielded efficiencies greater than 8%.[61] Combination BDT with TPs should allow for further fine tuning of electronic properties by selection of side chain on either unit. Characterization of optical and electronic properties of TPBDT copolymers will also be discussed. These polymers were also applied in conjunction with Paul Dastoor and Mihaela Stefan to BHJ solar cells.[62] The characterization of these devices will be addressed.

4.2. Results and Discussion

4.2.1. *Synthesis*

Synthesis of TPDTP Copolymers.[63] TPDTP copolymers **4.4a-c** featuring varying TP-based side chains were prepared via Stille coupling, as seen in Scheme 4.1. Copolymer **4.4a** was generated by Sean Evenson in a one-pot reaction in which the distannane was produced in situ and immediately reacted with **4.3a** and $Pd(dppe)Cl_2$. Due to inefficient production of the distannane intermediate the resulting polymer was generated in low yields and molecular weight.

Table 4.1. Yields and molecular weight data for TPDTP copolymers.[63]

Entry	M_n[a]	PDI[a]	Yield (%)
4.4a	-	-	79
4.4b	6400	1.8	79-81
4.4c	3600	1.7	75

[a] Determined via gel permeation chromatography (GPC).

In an attempt to generate higher quality polymers, Sean Evenson developed a method of generating and isolating **4.2** in high yield (99%). This was then combined with **4.3b** and **c** via Stille coupling in a 1:1 toluene/THF solution to generate copolymers **4.4b** and **c**. In these reactions the catalyst was changed to Pd_2dba_3 with the ligand P(*o*-tolyl)$_3$ and heated to reflux for four days. Both polymers, **4.4b** and **c**, generated via this method featured higher yields (75-86%). Additionally analysis via gel permeation chromatography (GPC) showed higher molecular weights for these polymers. Copolymer **4.4b** gave a M_n of 11400 with a PDI of 1.8 and **4.4c** gave a M_n of 6100 and PDI of 1.7. The significantly higher M_n of **4.4b** could be due to increased solubility imparted by the extended side chain on the TP unit. Relevant data for all generated polymers can be found on Table 4.1.

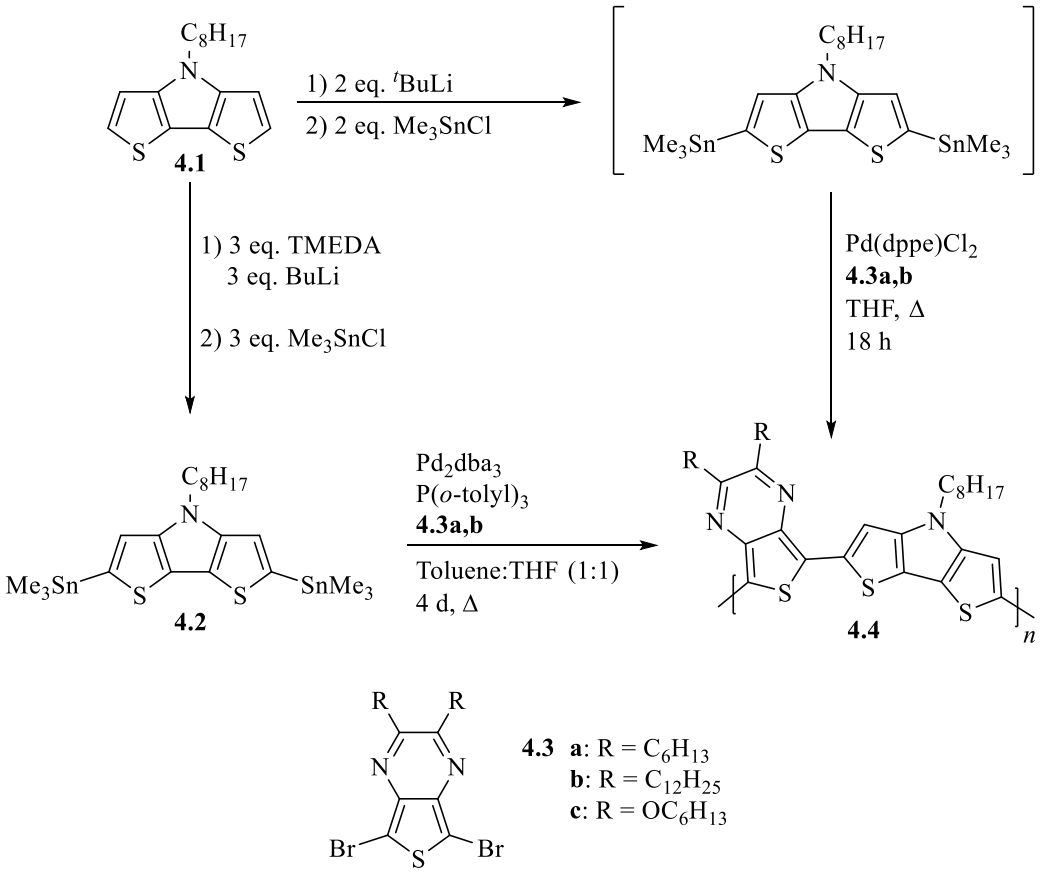

Scheme 4.1. Synthesis of TPDTP copolymers via Stille cross-coupling.

Synthesis of TPBDT Copolymers. TPBDT copolymers **4.6a-c** were generated via Stille polycondensation as shown in Scheme 4.2. The reaction conditions used a catalyst system of Pd_2dba_3/P(*o*-tolyl)$_3$ in toluene for four days yielding chloroform soluble polymer in yields of 67-74%. All three generated polymers are a blue-black solid. Monomer **4.5b**, featuring 2-dodecylthiopene side chains, was generated by Mihaela Stefan and coworkers for use in the production of copolymers **4.6b**[62] and **c**. As shown in Table 4.2 all copolymers were of relatively high yield and molecular weight. There is a noted increase in M_n for copolymer **4.6b**, compared to **a** and **c**. The increase from **4.6a** is likely due to the introduction of the BDT-based side chain.

Copolymer **4.6c** has a shorter alkyloxy side chain, likely contributing to its smaller molecular weight.

Table 4.2. Yields and molecular weight data for TPBDT copolymers.

Entry	M_n[a]	PDI[a]	Yield (%)
4.6a	9700	1.3	67
4.6b[61]	12200	2.5	73
4.6c	27000	2.7	74

[a] Determined by GPC.

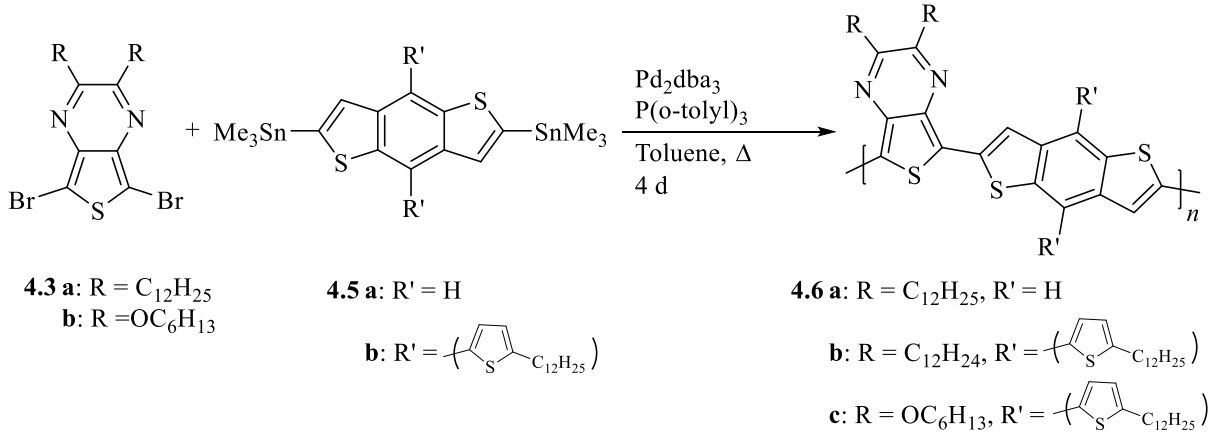

Scheme 4.2. Synthesis of TPBDT copolymers via Stille cross-coupling.

4.2.2. *UV-vis-NIR Absorption Spectroscopy*

Absorption Data for TPDTP Copolymers. Absorption data for TPDTP copolymers **4.4a** and **c** are shown in Figure 4.4. Related absorption data for all TPDTP copolymers can be found in Table 4.3. All three polymers feature three absorption bands in solution (Figure 4.3A). The first two high energy bands at 300-350 nm and 400-450 nm correspond well with π-π* transitions. These transitions closely resemble those often observed with 2,3-disubstitutedTPs.

The third, low energy absorption band is representative of a charge transfer (CT) transition. This transition occurs from the HOMO, located along the polymer backbone, to the

TP pyrazine-based LUMO. The CT band is commonly found in all TP-based materials, including monomers, homopolymers, and other copolymers.[5] As shown in Figure 4.3B, the solid state onset shifts significantly going from **4.3a** to **4.3c**. This is in good agreement with previous TP data in which alkyloxy side chains lead to an increase in band gap.

Table 4.3. Optical data for TPDTP copolymers.[63]

Entry	λ_{max} (solution)[a]	λ_{max} (Solid)[b]	E_g (eV)[c]
4.4a	310, 432, 787	838	0.9
4.4b	301, 431, 805	893	0.8
4.4c	329, 406, 675	675	1.3

[a] In CHCl3, [b] Film formed by spin-coating on glass plate, [c] Optical.

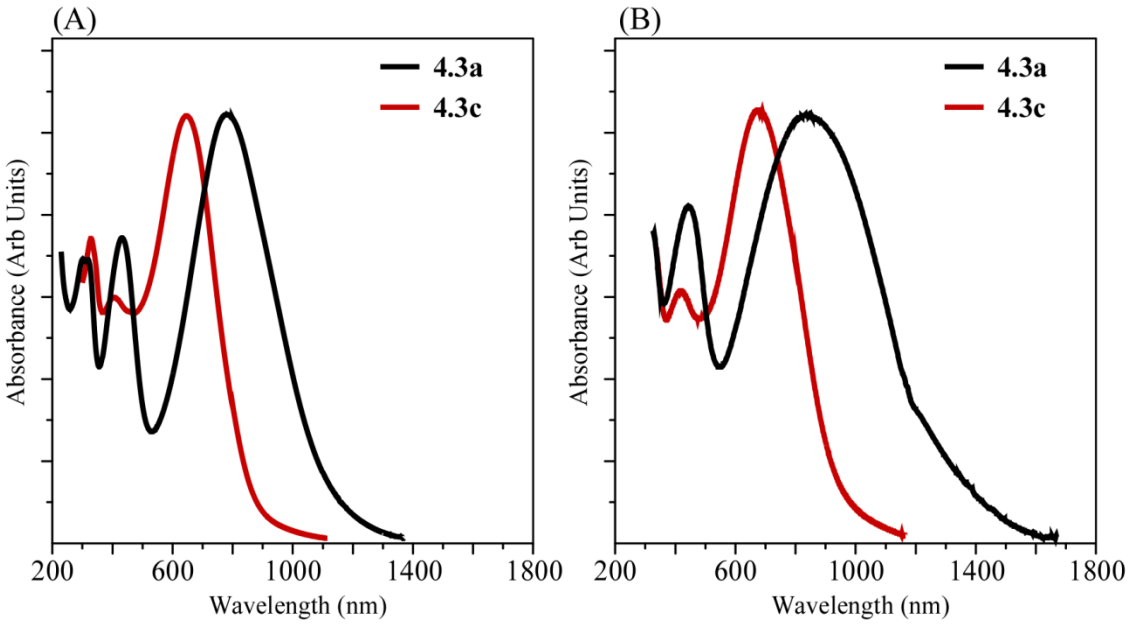

Figure 4.4. (A) Solution (in $CHCl_3$) and (B) solid-state absorption spectra of TPDTP copolymers **4.4a** and **4.4c**.

Absorption Data for TPBDT Copolymers. Absorption data for all three TPBDT copolymers can be found on Table 4.4 and representative spectra in Figure 4.5. As with

previously discussed copolymers, **4.6a-c** all feature two major absorption bands. The first high energy band occurs at 300-500 nm and is the π-π* transition. It is notable that the λ_{max} for **4.6b** and **c** are roughly equivalent at 336 and 349 nm respectively, whereas **4.6c** has a bathochromically shifted λ_{max} at 398 nm. Copolymer **4.6a** lacks the 5-dodecylthiophene side chains found in **4.6b** and **c**, likely accounting for the difference in λ_{max}. Also notable is the small peak at 450 nm only found in the absorption spectra for **4.6b**. In the case of **4.6b** there are TP-based dodecyl side chains vs. TP-based hexyloxy side chains in **4.6c**.

Table 4.4. Optical data for TPBDT copolymers.

Entry	λ_{max} (Solution)[a]	λ_{max} (Solid)[b]	E_g (eV)[c]
4.6a	398, 641	402, 658	1.5
4.6b[62]	336 (450), 696 (760)	342 (450), (688) 760	1.4
4.6c	349, (639) 691	351, (640) 694	1.5

[a] In CH3Cl, [b] Film formed via spin coating on glass plate, [c] Optical.

The second low energy charge transfer (CT) band is a transition from the HOMO, located along the polymer backbone, to the more pyrazine-based LUMO. In solution **4.6a** has the lowest onset and the weakest shoulder; this could be due to a combination of effects including lower molecular weight and removal of the BDT-based 5-dodecylthiophene side chain. In both cases this would result in decreased conjugation and thus a higher E_g. In the solid state there is a ~40 nm red shift, due to packing giving it an onset equal to that of **4.6c**. Copolymer **4.6b** has both the highest λ_{max}, 760 nm for solid-state, and onset of all three polymers. A high molecular weight and extended conjugation through the BDT-based thiophene side-chains are likely the cause of this red shift. Additionally, it is notable that going from solution to solid state spectra for **4.6b**, the λ_{max} shifts from the high energy to low energy peak, indicating increased packing order. The

absorption spectra for **4.6c** changes very little from solution to solid-state. In both cases the onset, low energy λ_{max}, and high energy shoulder remain the same. In solution, **4.6c** has an onset between that of **4.6a** and **c**. However, as previously mentioned, **4.6a** and **b** have a nearly identical onset in solid state. Copolymer **4.6c** has on onset blue-shifted ~35 nm from that of **4.6a**. This is in good agreement with previous polymers featuring TP-based alkyloxy side chains, which all experience a blue-shift in absorption onset due to the electron-donating nature of the functionality.

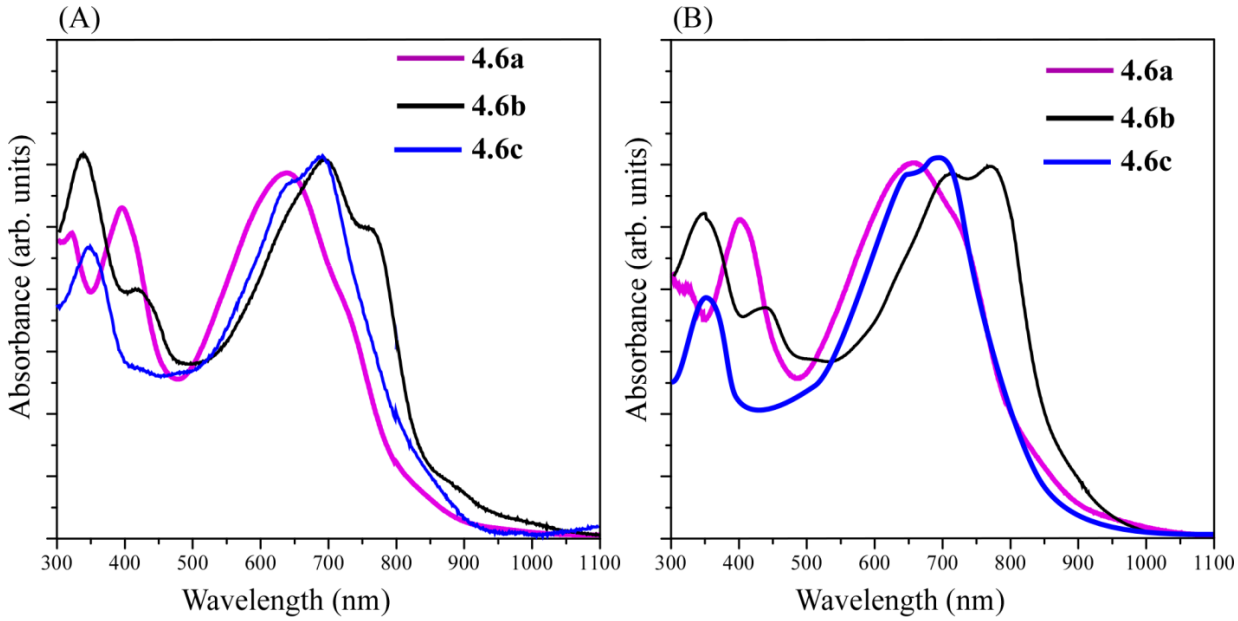

Figure 4.5. (A) Solution (in $CHCl_3$) and (B) solid-state absorption data of TPBDT copolymers.

4.2.3. *Electrochemistry*

Electrochemical Data for TPDTP Copolymers. Electrochemical experiments were performed on generated TPDTP copolymers using cyclic voltammetry (CV), as shown in Figure 4.6. The E_{pa}, along with calculated HOMO and LUMO levels and E_g for each polymer can be found below in Table 4.5. Copolymer **4.4a** shows both a strong oxidation peak at 0.69 V and a

strong reduction peak at -1.70 V. Both appear to be electrochemically reversible. The onset of oxidation for **4.4a** occurs at a much lower potential than the other TPDTP copolymers. Copolymer **4.4b** features a strong oxidation peak at 0.35 V, however, no reduction peak is observed. Based on molecular weight, it would be expected **4.4b** would have an onset of oxidation lower than that of **4.4a** due to increased conjugation. However, it may be the longer side chains on the TP unit cause greater disorder in the polymer film, thus causing the HOMO to be stabilized.

Table 4.5. Electrochemical data for TPDTP copolymers.[63]

Entry	E_{pa} (V)[a]	HOMO (eV)[b]	LUMO (eV)[c]	Eg (eV)[d]
4.4a	0.69	-4.7	-3.8	0.9
4.4b	0.35	-4.8	-4.0	0.8
4.4c	0.65	-5.2	-3.9	1.3

[a] Film formed by drop casting from $CHCl_3$ solution on a Pt disc working electrode. Potentials vs. Ag/Ag^+ in 0.1 M $TBAPF_6$ in MeCN. [b] E_{HOMO} was determined from the onset of oxidation vs. ferrocene (5.1 eV vs. vacuum).[64] [c] $E_{LUMO} = E_{HOMO} - E_g$. [d] Optical.

The lack of a reduction peak is thought to be due to hindrance of the counter ion to enter the site of reduction due to the longer side chains of TP. The potential of oxidation for copolymer **4.4c** occurs at 0 V, yielding a HOMO at 4.1 eV, the same as poly(2,3-dihexyloxythieno[3,4-*b*]pyrazine). This indicates a HOMO largely dominated by the TP unit. Again, no reduction peak is seen, potentially again due to side chain hindrance of the counter ion. Several attempts were made, both with **4.4b** and **c** to produce a reduction peak, however, none were successful.

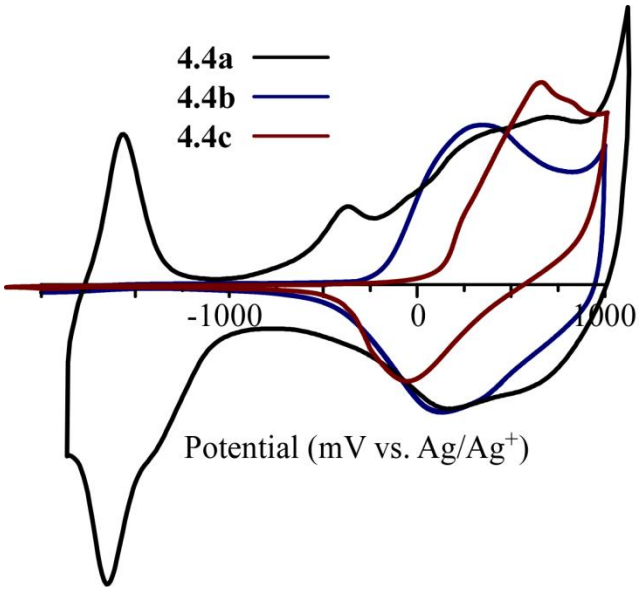

Figure 4.6. Cyclic voltammograms of TPDTP copolymers.

Electrochemical Data for TPBDT Copolymers. Electrochemical studies of TPBDT copolymers were performed via cyclic voltammetry. The data for these polymers is found in Table 4.6 and representative spectra can be found in Figure 4.7. Copolymers **4.6a** and **c** both have an oxidation onset at ~0.55 V, giving a HOMO of -5.6 eV. It would typically be expected from TP-based alkyloxy side chains on **4.6c** to see destabilization of the HOMO compared to the alkyl chains on **4.6a**. However, due to the additional BDT-based thiophene side chains on **4.6c** no direct comparison between the two can be made. No reduction peaks appeared for polymer **4.6a** and so the LUMO was calculated based on the optical E_g; both appear at -4.1 eV. Although a reduction is seen for **4.6c**, this is a coupled reduction to the previously mentioned oxidation peak and not representative of the first polymer reduction. Thus the LUMO for **4.6c** was found in the same manner as **4.6a**. Polymer **4.6b** shows significantly different behavior from the other polymers. The onset of oxidation occurs at ~0.20 V, giving a destabilized HOMO of -5.3 eV.

This increased destabilization of the HOMO is likely due to high molecular weight. This is also the only polymer showing a reduction peak, giving an onset of -1.50 V and LUMO of -3.6 eV.

Table 4.6. Electrochemical data for TPBDT copolymers.

Entry	E_{pa} (V)[a]	HOMO (eV)[b]	LUMO (eV)[c]	Eg (eV)[d]
4.6a	1.05	-5.6	-4.1	1.5
4.6b[62]	1.25	-5.3	-3.6	1.4
4.6c	1.66	-5.6	-4.1	1.5

[a] Film formed by drop casting from a $CHCl_3$ solution on a Pt disc working electrode. Potentials vs. Ag/Ag^+ in 0.1 M $TBAPF_6$ in MeCN. [b] E_{HOMO} was determined from the onset of oxidation vs. ferrocene (5.1 eV vs. vacuum).[64] [c] $E_{LUMO} = E_{HOMO} - E_g$. [d] Optical.

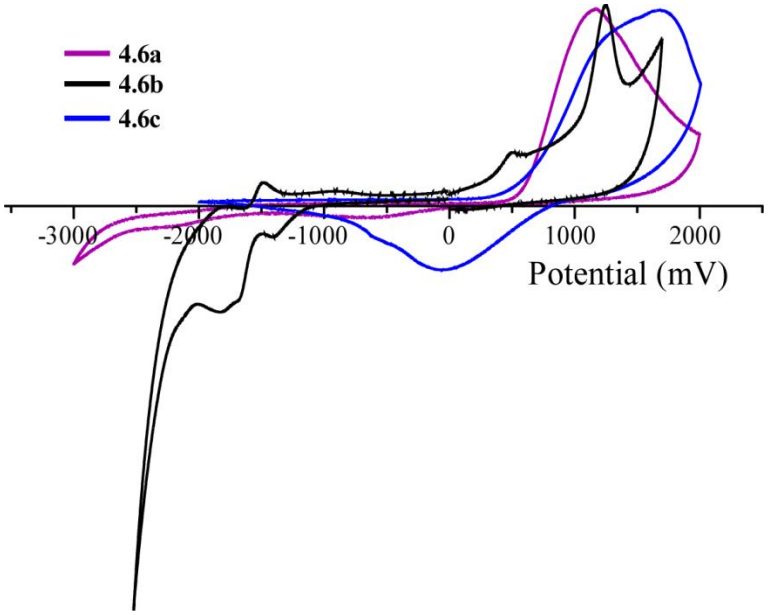

Figure 4.7. Cyclic voltammograms of TPBDT copolymers.

4.2.4. *OPV Device Properties*

Solar Cell Properties of 4.6a. All polymers generated in this chapter were evaluated as an active layer donor material in bulk heterojunction solar cells. Copolymers **4.4a-c**, although showing photo response, yielded no functioning solar cells. Devices featuring copolymers **4.6a-c**, however, did generate functioning solar cells. The data from these devices can be found in

Table 4.7. As shown from the data, as the blend increases in $PC_{61}BM$ content, V_{oc} decreases. However, this is offset by an increasing J_{sc} and FF, yielding an overall increase in efficiency as the $PC_{61}BM$ content increases. The maximum efficiency is found with the 1:4 polymer:$PC_{61}BM$ blend with an efficiency of 0.42%. The IV (current vs. voltage) curve from this device can be found in Figure 4.8.

Table 4.7. OPV device data for copolymer **4.6a**.

4.6a:$PC_{61}BM$	V_{oc} (V)	I_{sc} (mA)	FF (%)	η (%)
1:1[a]	0.44	-0.080	31.3	0.22
1:2[a]	0.44	-0.099	34.7	0.31
1:3[a]	0.42	-0.115	38.7	0.37
1:4[a]	0.39	-0.112	44.0	0.42

[a] Annealed.

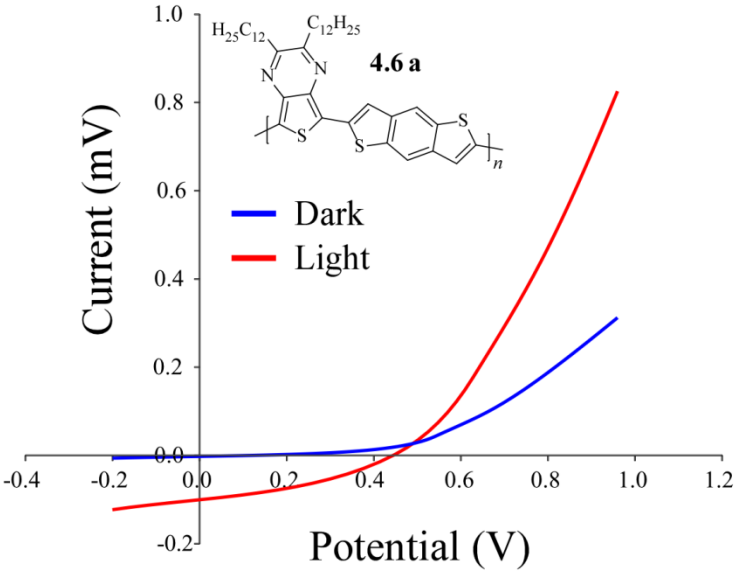

Figure 4.8. IV characteristics for **4.4a** at 1:3 polymer:$PC_{61}BM$ blend.

Solar Cell Properties of 4.6b. Stefan and coworkers generated solar cell devices from copolymer **4.6b** and tested these under various **4.6b**:$PC_{61}BM$ solution ratios.[62] The results of

these tests may be found below in Table 4.8. The device with a blend of **4.6b**:$PC_{61}BM$ (1:3) yielded the highest efficiency. Although devices with a higher $PC_{61}BM$ blend gave a higher V_{oc}, both J_{sc} and FF decreased. The addition of diiodooctane (DIO) as a cosolvent was attempted to improve the efficiency of the 1:3 polymer:$PC_{61}BM$ devices. However, a decrease in efficiency was observed. This is owed mostly to a decrease in fill factor, possibly contributed by poor film formation. These results are not shown.

Table 4.8. OPV device data for copolymer **4.6b**.[62]

4.6b:$PC_{61}BM$	V_{oc} (V)	J_{sc} (mA/cm^2)	FF (%)	η (%)
2:1	0.40	0.83	32	0.10
1:1	0.47	1.35	43	0.27
1:2	0.46	1.53	49	0.34
1:3	0.48	1.71	64	0.52
1:4	0.46	1.67	53	0.40
1:5	0.50	1.69	55	0.47
1:6	0.50	1.70	60	0.51

[a] This data represents the highest measured values.

Solar Cell Properties of 4.6c. Solar cells were made of copolymer **4.6c** by Trent Anderson. The data from these devices can be found in Table 4.9 and the representative data of the light curves for all three ratios can be found in Figure 4.9. This polymer did not produce devices as efficient as the prior two TPBDT copolymers. This is likely due to the difference in electronics from the alkyloxy side chains on TP.

The data shows that both the 1:1 and 1:3 (polymer:$PC_{61}BM$) cells produced the highest efficiencies of 0.19% for these materials. A drop in efficiency is seen going to the 1:2 blend which is mostly attributed to the drop in J_{sc}. All three devices have roughly similar V_{oc} values so this is not greatly affected by changing the active layer blend. Fill factor, however, appears to increase with increasing $PC_{61}BM$ content.

Table 4.9. OPV device data for copolymer **4.6c**.

4.6a:$PC_{61}BM$	V_{oc} (V)	J_{sc} (mA/cm^2)	FF (%)	η (%)
1:1[a]	0.41	1.56	23.4	0.19
1:2[a]	0.42	0.88	31.4	0.12
1:3[a]	0.37	1.41	35.9	0.19

[a] Annealed.

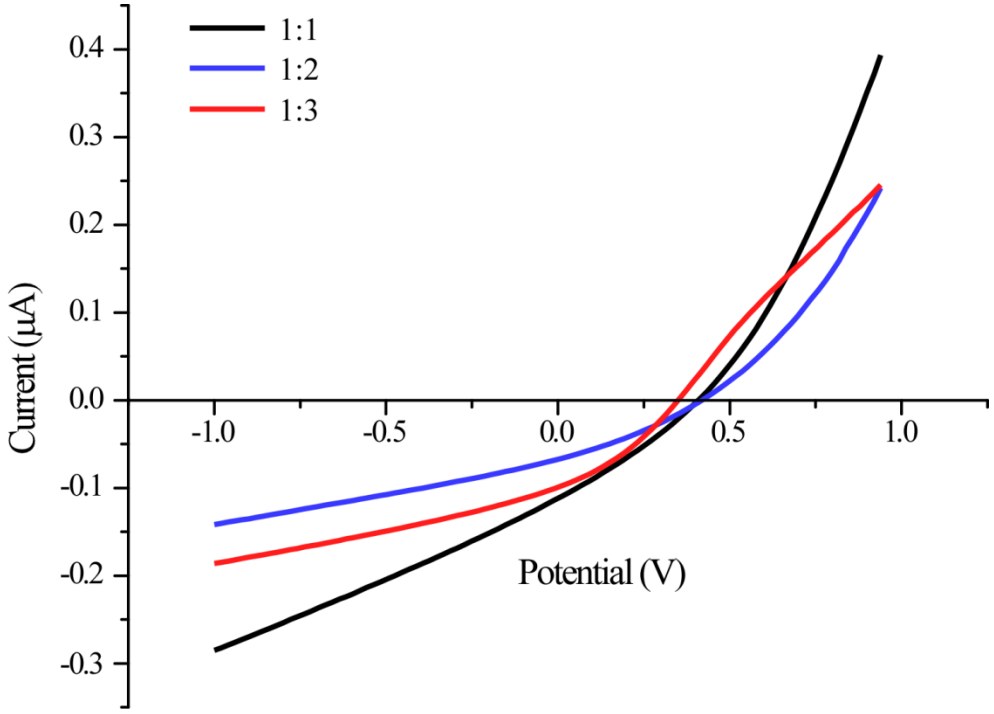

Figure 4.9. IV light characteristics for **5.6c**.

4.3. Conclusion

Two sets of TP-based copolymers were made by Stille polycondensation. The first set of polymers combines the TP and DTP projects. The generated TPDTP copolymers all feature band gaps below 1.5 eV, making them low band gap materials. Copolymer **4.4b**, with the TP-based dodecyl side chain displayed the highest molecular weight, likely due to increased solubility of the growing polymer. Correspondingly, the band gap of **4.4b** is also the lowest. The highest band

gap TPDTP is **4.4c**, which is in good agreement with other polymers featuring alkyloxy-fuctionalized TPs. However, in contradiction to previous alkyloxy TP compounds, **4.4c** features the deepest HOMO of all TPDTP copolymers. Due to the electron donating nature of the alkyloxy side chain destabilization of the HOMO should be expected. This inconsistency could be due to lowered molecular weight of **4.4c**, compared to the other two TPDTP copolymers. Although application of these materials into OPV devices was attempted and showed photo response, no current was generated. This is likely due to the high HOMO observed with these polymers.

The second group of copolymers discussed in this chapter combined TP with two forms of BDT. Copolymer **4.5a** featured protons at the 4- and 8- positions while **b** and **c** have 5-dodecylthiophene side chains. All three polymers were generated in good yield and have high molecular weights. These polymers had slightly larger band gaps, likely due to the introduction of a phenyl unit in BDT, all at around 1.5 eV. Copolymer **4.6c** has a blue shifted onset in comparison to **4.6b**, likely due to the alkyloxy side chains. Polymers **4.6a** and **c** show similar HOMO and LUMO energies, while **4.6b** shows an overall destabilization of MO energies.

The TPBDT copolymers were applied to solar cell devices. Solar cells featuring **4.6a** as the donor in the active layer were made in Newcastle, Australia and yielded a high PCE of 0.42% with the **4.6a**:$PC_{61}BM$ blend of 1:4. Stefan and coworkers produced solar cells containing a **4.6b** donor material. Devices produced with **4.6b** yielded a high PCE of 0.52% with the **4.6b**:$PC_{61}BM$ blend of 1:3. Although attempts were made to further increase efficiency with cosolvent DIO, no increase was observed. Trent Anderson generated solar cells with **4.6c** as the donor material. A high efficiency was observed in the 1:1 and 1:3 polymer:PC61BM devices at 0.19%, considerably lower than previously generated TPBDT copolymers. However, this might

be due to the differing electronics from the TP-based alkyloxy side chains. While V_{oc} did not greatly alter from cell to cell, J_{sc} experienced a strange decrease with the 1:2 blend and Fill Factor increased with increasing $PC_{61}BM$ content, likely due to increased charge separation capabilities.

Although high efficiency cells were not generated from these polymers, a greater understanding of structure-function relation was obtained, which may then be used in future endeavors. Use of electron-withdrawing side chains, either TP-based or DTP-based, would stabilize the polymer HOMO and might lead to working solar cells. Additionally, as introduction of electron-donating TP-based side chains led to reduction in solar cell efficiency for TPBDT polymers, a change to electron-withdrawing TP-based side chains would be worth attempting to further examine structure-function relations in solar cell devices.

4.4. Experimental

4.4.1. *General*

Unless noted, all materials were reagent grade and used without further purification. Chromatographic separations were performed using standard column chromatography methods with silica gel (230-400 mesh). Dry THF and toluene were obtained via distillation over sodium/benzophenone. All glassware was oven-dried, assembled hot, and cooled under a dry nitrogen stream before use. Transfer of liquids was carried out using standard syringe techniques and all reactions were performed under a dry nitrogen stream. The ^{1}H NMR and ^{13}C NMR were completed on a 400 MHz spectrometer. All NMR data was referenced to the chloroform signal and peak multiplicity was reported as follows: s = singlet d = double, t = triplet, q = quartet, p = pentet, tt = triplet of triplets, m = multiplet and br = broad. The following compounds were synthesized according to previously reported literature procedures: *N*-octyldithieno[3,2-*b*:2’,3’-

d]pyrrole (**4.1**),[63] *N*-octyl-2,6-bis(trimethylstannyl)dithieno[3,2-*b*:2',3'-*d*]pyrrole (**4.2**),[63] 5,7-dibromo-2,3-dihexylthieno[3,4-*b*]pyrazine (**4.3a**),[63] poly(2,3-dihexyltheino[3,4-*b*]pyrazine-*co*-*N*-octyldithieno[3,2-*b*:2',3'-*d*]pyrrole) (**4.4a**),[63] poly(2,3-didodecyltheino[3,4-*b*]pyrazine-*co*-*N*-octyldithieno[3,2-*b*:2',3'-*d*]pyrrole) (**4.4b**),[63] poly(2,3-dihexyloxytheino[3,4-*b*]pyrazine-*co*-*N*-octyldithieno[3,2-*b*:2',3'-*d*]pyrrole) (**4.4c**),[63] 2,6-(trimethylstannyl)benzo[1,2-*b*:4,5-*b*']dithiophene (**4.5a**), 2,6-(trimethylstannyl)-4,8-bis(5-dodecylthiophene-2-yl)benzo[1,2-*b*:4,5-*b*']dithiophene (**4.5b**).[62]

Poly(benzo[1,2-*b*:4,5-*b*']dithiophene-*co*-2,3-didodecylthieno[3,4-*b*]pyrazine) (4.6a). To a three-neck round-bottom flask, **4.5b** (0.128 g, 0.128 mmol), **4.3b** (0.081 g, 0.128 mmol), Pd_2dba_3 (0.002 g, 0.002 mmol), and tri(*o*-tolyl)phosphine (0.002 g, 0.007 mmol) were added under a nitrogen atmosphere. Toluene (20 mL) was added to dissolve all reagents and the system was again evacuated and backfilled with nitrogen four times. The solution was heated at reflux for 4 days. The polymerization was stopped by cooling to room temperature and precipitating the polymer in methanol. The polymer was filtered and then purified using Soxhlet extractions with methanol, acetone, hexane, and chloroform. The polymer was obtained from the chloroform fraction upon evaporation of the solvent. The polymer was obtained was a dark bluish/black solid (73% yield). ^{1}H NMR: 7.52, 3.33, 2.61, 1.54, 1.29, 0.89. GPC: Mw = 12600, M_n = 9700, PDI = 1.3.

Poly(4,8-bis(5-dodecythiophene-2-yl)benzo[1,2-*b*:4,5-*b*']dithiophene-*co*-2,3-didodecylthieno[3,4-*b*]pyrazine) (4.6b). Polymer **4.6b** was produced as reported in literature procedures (73% yield).[61] ^{1}H NMR: ($CDCl_3$, 500 MHz), δ 7.70, 7.15, 3.63, 2.64, 1.56, 1.28, 0.89. SEC: Mw = 30000, M_n = 12200, PDI = 2.5.

Poly(4,8-bis(5-dodecythiophene-2-yl)benzo[1,2-*b*:4,5-*b*']dithiophene-*co*-2,3-dihexyloxythieno[3,4-*b*]pyrazine) (4.6c). Polymer **4.6c** was produced in the same manner as **4.6a** substituting **4.3b** with **4.3c**. The polymer was obtained was a dark bluish/black solid (73% yield). ^{1}H NMR: δ 7.70, 7.13, 4.71, 3.17, 1.60, 1.53, 1.26, 0.89. GPC: M_w = 73400, M_n = 27000, PDI = 2.7.

4.4.2. *Electrochemistry*

All electrochemical techniques were performed on a Bioanalytical Systems BAS 100B/W electrochemical analyzer. Cyclic voltammetry (CV) experiments were performed using a three-electrode cell consisting of a Pt-disc working electrode, Pt coil wire auxillary electrode, and an Ag/Ag^+ reference electrode. A 0.1 M electrolyte solution was prepared with tetrabutylammonium hexafluorophosphate ($TBAPF_6$) using MeCN distilled over CaH_2 under dry nitrogen. The solutions were deoxygenated with argon for at least 20 min prior to each scan and blanketed with argon during the experiments. Solutions of polymers in $CHCl_3$ were drop cast on the working electrode and dried to form a solid film. CV experiments were performed in the above described cell at a sweep rate of 100 mV/s. E_{HOMO} values were determined in a reference to ferrocene (5.1 V vs. vacuum)[64] and the E_{LUMO} was determined from the following equation: $E_{LUMO} = E_{HOMO}$ – optical band gap.

4.4.3. *UV-vis-NIR Absorption Spectroscopy*

All absorption spectroscopy was performed on a Carry 500 dual-beam UV-vis-NIR spectrophotometer. Solution-state spectra were analyzed in chloroform and solid-state spectra were analyzed with the polymer spin coated on a glass plate. The optical band gaps were determined from the onset of the lowest energy absorption by extrapolation of the steepest slope to the intersection with the wavelength axis.

4.4.4. *OPV Device Fabrication*

OPV Device Fabrication for 4.6a. Glass substrates coated with patterned indium-tin oxide (ITO) were cleaned prior to use by heating in a bath of detergent at 90 °C followed by 15 min sonication. The detergent was then poured out and the plates were rinsed 3 times with deionized water. The plates were then placed in under sonication in acetone and isopropanol in succession for 15 min each, followed by drying under dry N_2. A 0.5 mm filtered dispersion of PEDOT:PSS in H_2O was spun cast at 5000 rpm for 60 s onto the cleaned ITO plates and then heated to 200 °C for 5 min to yield a film of ~40 nm. A blend of polymer:$PC_{61}BM$ at concentrations of 40 mg/mL were filtered through a 0.45 mm filter and spun cast at 700 rpm for 60 s onto the PEDOT:PSS layer. The substrate was then dried at 60 °C for 10 min. The aluminum cathode was vacuum deposited at a pressure of 1×10^{-7} mbar, giving a thickness of 100 nm. The IV characteristics of the devices were then measured at AM 1.5 simulated light.

OPV Device Fabrication for 4.6b.[61]OLED-grade glass slides were purchased with prepatterned indium tin oxide (ITO) electrodes from Luminescense Technology (Taiwan). The substrates were cleaned with deionized water, acetone, and isopropanol successively by sonication for 20 min each and then the substrates were subjected to UV/ozone treatment for 10 min prior to use. Immediately after ozone treatment, PEDOT:PSS was spin cast (4000 min^{-1}, 1740 min^{-1} s^{-1}, 90 s) onto the substrates, followed by annealing at 120 °C for 20 min under nitrogen, resulting in a film thickness of ~20–25 nm. The PCBM/polymer blend was prepared in chloroform at different weight ratios of polymer and PCBM, but maintaining a total concentration of 15 mg/mL. This blend was then spun cast (2000 min^{-1}, 1740 min^{-1} s^{-1}, 60 s) onto the PEDOT-PSS/substrate. Cathodes consisting of calcium (10 nm) and aluminum (100 nm) were thermally evaporated at a rate of ~2.5 Å/s through a shadow mask to define solar cell active

areas. IV testing was performed under a controlled N_2 atmosphere using a Keithley 236, model 9160 interfaced with LabView software. The solar simulator used was a THERMOORIEL equipped with a 300 W xenon lamp; the intensity of the light was calibrated to 100 mW cm^{-2} with a NREL-certified Hamamatsu silicon photodiode. The active area of the devices was 10.0 mm^2. The active layer film thickness was measured using a Veeco Dektak VIII profilometer.

OPV Device Fabrication for 4.6c. Organic solar cells were fabricated on patterned indium tin oxide (ITO) glasses with a sheet resistance of 20 Ω/sq. The ITO glass was cleaned by sequential ultrasonic treatment in detergent, deionized water, acetone, and isopropanol, and then treated in a bench-top plasma cleaner (PE-50 bench top cleaner, The Plasma Etch, Inc., USA) for 2 min. PEDOT:PSS (Clevious P VP AI 4083 H. C. Stark, Germany) solution was filtered through a 0.45 μm filter and then spin coated at 4000 rpm for 60 s on the ITO electrode. The PEDOT:PSS layer was baked at 100 ºC for 40 min in the air to remove any moisture that might be present in film. The PEDOT:PSS coated substrates were transferred to a N_2 filled glove box. A blend solution of THE POLYMERS(Rieke Metals, Inc., MW = 17kDa) and PCBM (Nano-C) at a concentration of 30-40 mg/mL (at varying ratios w/w) in 0.25 mL of chloroform. The solution was spun on the top of the PEDOT:PSS layer at 800 rpm for 45 seconds. After an hour of aging half of the POLYMER:PCBM blend films were thermally annealed at 105 ºC for 5 minutes. The edges of the solar cell were cleaned using chloroform before being capped with the cathode consisting of LiF (~1 nm) and Al (~100 nm) which were thermally evaporated on the active layer under a shadow mask in a base pressure of $1x10^{-6}$ mbar. The device active area was ~7.9 mm^2 for all the solar cells discussed in this work. The J-V measurement of the devices was conducted on a computer controlled Keithley 2400 source meter. The J-V measurement system

uses a solar simulator with a Class-A match to the AM1.5 Global Reference Spectrum. It is calibrated with KG5-filtered silicon reference cell with calibration traceable to NREL and NIST.

4.5. References

(1) Liang, Y.; Xu, Z.; Xia, J.; Tsai, S.; Wu, Y.; Li, G.; Ray, C.; Yu, L. *Adv. Mater.* **2010**, *22*, 1-4.

(2) van Mullekoma, H. A. M.; Vekemans, J. A. J. M.; Havinga, E. E.; Meijer, E. W. *Mater. Sci. Eng. R* **2001**, *32*, 1-40.

(3) Bundgaard, E.; Krebs, F. C. *Sol. Energy Mater. Sol. Cells* **2007**, *91*, 954-985.

(4) Beajuge, P. M.; Amb, C. M.; Reynolds, J. R. *Acc. Chem. Res.* **2010**, *43*, 1396-1407.

(5) Rasmussen, S. C.; Schwiderski, R. L.; Mulholland, M. E. *Chem. Commun.* **2011**, 11394-11410.

(6) Cheng, K.; Liu, C.; Chen, W. *Polym. Sci., Part A: Polym. Chem.* **2007**, *45*, 5872-5883.

(7) Lee, W.; Cheng, K.; Liu, C.; Lin, S.; Chueh, C.; Tsai, F.; Chen, W. *J. Polym. Res.* **2009**, *16*, 239-244.

(8) Bijleveld, J. C.; Shahid, M.; Gilat, J.; Wienk, M. M.; Janssen, R. A. J. *Adv. Funct. Mater.* **2009**, *19*, 3262-3270.

(9) Renz, J. A.; Ashraf, R. S.; Erb, T.; Shokhovets, S.; Gorbsch, G.; Klemm, E.; Hoppe, H. *Macromol. Chem. Phys.* **2010**, *211*, 1689-1694.

(10) Wen, L.; Duck, B. C.; Dastoor, P. C.; Rasmussen, S. C. *Macromolecules*. **2008**, *41*, 4576-4578.

(11) Wen, L.; Rasmussen, S. C.; *Polym. Prepr.* **2007**, *48*, 132.

(12) Wen, L. *PhD Dissertation*, North Dakota State University, Fargo, ND, 2008.

(13) Kitamura, C.; Tanaka, S.; Yamashita, Y. *J. Chem.* **1994**, 1585-1586.

(14) Kitamura, C.; Tanaka, S.; Yamashita, Y. *Chem. Mater.* **1996**, *8*, 570-578.

(15) Delegado, C. R.; Hernandez, V.; Navarrete, J. T. L.; Tankaka, S.; Yamashita, Y. *J. Phys. Chem. B* **2004**, *108*, 2516-2526.

(16) Zhu, Y.; Champion, R. D.; Jenekhe, S. A. *Macromolecules* **2006**, *39*, 8712-8719.

(17) Wienk, M. M.; Turbiez, G. R.; Struijk, M. P.; Fonrodona, M.; Janssen, R. A. J. *Appl. Phys. Lett.* **2006**, *88*, 153511-153511-3.

(18) Zoombelt, A. P.; Fonrodona, M.; Turbiez, M. G. R.; Wienk, M. M.; Janssen, A. J. *J. Mater. Chem.* **2009**, *19*, 5336-5342.

(19) Zoombelt, A. P.; Leenen, M. A. M.; Fonrodona, M.; Nicholas, Y.; Wienk, M. M.; Janssen, R. A J. *Polymer*, **2009**, *50*, 4564-4570.

(20) Cai, T.; Zhou, Y.; Wang, E.; Hellstorm, S.; Zhang, F.; Xu, S.; Inganas, O.; Andersson, M. R. *Sol. Energy. Mater. Sol. Cells* **2010**, *94*, 1275-1281.

(21) Sonmez, G.; Shen, C. K. F.; Rubin, Y.; Wudl, F. *Angew. Chem., Int. Ed.* **2004**, *43*, 1498-1502.

(22) Sonmez, G.; Sonmez, H. B.; Shen, C. K. F.; Wudl, F. *Adv. Mater.* **2004**, *16*, 1905-1908.

(23) Sonmez, G.; Sonmez, H. B.; Shen, C. K. F.; Jost, R. W.; Rubin, Y.; Wudl, F. *Macromolecules* **2005**, *38*, 669-675.

(24) Tarkuc, S.; Unver, E. K.; Udum, Y. A.; Tanyeli, C.; Toppare, L. *Electrochim. Acta.* **2010**, *55*, 7254-7258.

(25) Berlin, A.; Zotti, G.; Zecchin, S.; Schiavon, G.; Vercelli, B.; Zanelli, A. *Chem. Mater.* **2004**, *16*, 3667-3676.

(26) Casado, J.; Ortiz, R. P.; Delgado, M. C. R.; Hernandez, V.; Navarrete, J. T. L.; Raimundo, J.; Blanchard, P.; Allain, M.; Roncali, J. *J. Phys. Chem. B.* **2005**, *109*, 16616-16627.

(27) Wu, W.; Liu, C.; Chen, W.; *Polymer*, **2006**, *47*, 527-538.

(28) Chueh, C.; Lai, M.; Tsai, J.; Wang, C.; Chen, W. *J. Polym. Sci., Part A: Polym. Chem.* **2010**, *48*, 74-81

(29) Lai, M.; Tsai, J.; Chueh, C.; Wang, C.; Chen, W. *Macromol. Chem. Phys.* **2010**, *211*, 2017-2025.

(30) Li, J.; Seo, S.; Beak, M.; Lee, S.; Lee, Y. *Macromol. Res.* **2010**, *18*, 304307.

(31) Li, J.; Hwang, M.; Lee, E.; Lee, S.; Yu, S.; Lee, Y. *Bull. Korean Chem. Soc.* **2010**, *31*, 2073-2076.

(32) Nietfeld, J. P.; Evenson, S. J.; Wen, L.; Rasmussen, S. C. *Polym. Prepr.* **2009**, *50*, 503.

(33) Bijleveld, J. C.; Shahid, M.; Gilat, J.; Wienk, M. M.; Janssen, R. A. J. *Adv. Funct. Mater.* **2009**, *19*, 3262-3270.

(34) Hou, J.; Park, M.; Zhang, S.; Yao, Y.; Chen, L.; Li, J.; Yang, Y. *Macromolecules* **2008**, *41*, 6012-6018.

(35) Yuan, M.; Rice, A. H.; Luscombe, C. K. *J. Polym. Sci., Part A: Polym. Chem.* **2011**, *49*, 701-711.

(36) Ashraf, R. S.; Hoppe, H.; Shahid, M.; Gobsch, G.; Sensfuss, S.; Klemm, E. *J. Polym. Sci., Part A: Polym. Chem.* **2006**, *44*, 6952-6961.

(37) Renz, J. A.; Ashraf, R. S.; Erb, T.; Shokhovets, S.; Gorbsch, G.; Klemm, E.; Hoppe, H. *Macromol. Chem. Phys.* **2010**, *211*, 1689-1694.

(38) Rasmussen, S. C.; Low Bandgap Polymers. In *The Encyclopedia of Polymeric Nanomaterials*, Muellen, K.; Kobayashi, S., Eds.; Springer: Heidelberg, 2013; Chapter 57.

(39) Dennler, G.; Sharber, M. C.; Brabec, C. J. *Adv. Mater.* **2009**, *21*, 1323-1338.

(40) Thompson, B. C.; Frechet, J. M. J. *Angew. Chem. Int. Ed.* **2008**, *47*, 58-77.

(41) Blouin, N.; Michaud, A.; Leclerc, M. *Adv. Mater.* **2007**, *19*, 2295-2300.

(42) Gunes, S.; Neugebauer, H.; Sariciftci, N. S. *Chem. Rev.* **2007**, *107*, 1324-1338.

(43) Helgesen, M.; Sondergaard, R.; Krebs, F. C. *J. Mater. Chem.* **2009**, *20*, 36-60.

(44) Piligo, C.; Holocombe, T. W.; Douglas, J. D.; Woo, C. H.; Beaujuge, P. M.; Frechet, J. M. J. *J. Am. Chem. Soc.* **2010**, *132*, 7595-7597.

(45) Dubois, C. J.; Abboud, K. A.; Reynolds, J. R. *Phys. Chem. B* **2004**, *108*, 8550-8557.

(46) Steckler, T. T.; Zhang, X.; Hwang, J.; Honeyager, R.; Ohira, S.; Zhang, X.-H.; Grant, A.; Ellinger, S.; Odom, S. A.; Sweat, D.; Tanner, D. B.; Rinzler, A. G.; Barlow, S.; Brédas, J.-L.; Kippelen, B.; Marder, S. R.; Reynolds, J. R. *J. Am. Chem. Soc.* **2008**, *131*, 2824-2826.

(47) Li, G.; Shrotriya, V.; Huang, J. S.; Yao, Y.; Moriarty, T.; Emery, K.; Yang, Y. *Nat. Mater.* **2005**, *4*, 864-868.

(48) Solar Novus Today. Konarka Power Plastic Solar Cell Certified at 9% :Efficiencyhttp://www.solarnovus.com/index.php?option=com_content&view=article&id=4418:konarka-power-plastic-solar-cell-certified-at-9-efficiency&catid=41:applications-tech-news&Itemid=245 (accessed July 2013).

(49) Liu, J.; Zhang, R.; Sauve, G.; Kowalewski, T.; McCullough, R. D. *J. Am. Chem. Soc.* **2008**, *130*, 13167-13176.

(50) Zhang, W.; Li, J.; Zou, L.; Zhang, B.; Qin, J.; Lu, Z.; Poon, Y. F.; Chan-Park, M. B.; Li, C. M. *Macromolecules* **2004**, *41*, 8953-8955.

(51) Zhou, E.; Nakamura, M.; Nishizawa, T.; Zhang, Y.; Wei, Q.; Tajima, K.; Yang, C..; Hashimoto, K. *Macromolecules* **2008**, *41*, 8302-8305.

(52) Zhang, M.; Fan, H.; Guo, X.; He, Y.; Zhang, Z.; Min, J.; Zhang, J.; Zhao, G.; Zhan, X.; Li, Y. *Macromolecules*, **2010**, *43*, 5707-5712.

(53) Pan, H.; Li, Y.; Wu, Y.; Liu, P.; Ong, B. S.; Zhu, S.; Xu, G.; *Chem. Mater.* **2006**, *18*, 3237-3241.

(54) Hou, J.; Park, M.-H.; Zhang, S.; Yao, Y.; Chen, L.-M.; Lu, J.-H.; Yang, Y.; *Macromolecules* **2008**, *41*, 6012-6018.

(55) Liang, Y.; Feng, D.; Wu, Y.; Tsai, S.-T.; Li, G.; Ray, C.; Yu, L.; *J. Am Chem. Soc.* **2009**, *131*, 7792-7799.

(56) Sista, P.; Bhatt, M. P.; McCary, A. R.; Nguyen, H.; Hao, J.; Biewer, M. C.; Stefan, M. C. *J. Polym. Sci., Part A: Polym. CHem.* **2001**, *49*, 2292-2302.

(57) Sista, P.; Hao, J.; Elkassih, S.; Sheina, E. E.; Biewer, M. C.; Janesko, B. G.; Stefan, M. C. *J. Polym. Sci., Part A: Polym. Chem.* **2011**, *49*, 4172-4179.

(58) Sista, P.; Biewer, M. C.; Stefan, M. C. *Macromol. Rapid Commun.* **2012**, *33*, 9-20.

(59) Hundt, N.; Palaniappan, K.; Servello, J.; Dei, D. K.; Stefan, M. C.; Biewer, M. C. *Org. Lett.* **2009**, *11*, 4422-4425.

(60) He, Y.; Zhou, Y.; Zhao, g.; Min, J.; Guo, X.; Zhang, B.; Zhang, M.; Zhang, J.; Li, Y.; Zhang, F.; Inganaes, O. *J. Polym. Sci., Part A: Polym. Chem.* **2010**, *48*, 1822-1829.

(61) Dou, L.; Gao, J.; Richard, E.; You, J.; Chen, C.-C.; Cha, K. C.; He, Y.; Li, G.; Yang, Y. *J. Am. Chem. Soc.* **2012**, *134*, 10071-10079.

(62) Sista, P.; Kularatne, R. S.; Mulholland, M. E.; Wilson, M.; Holmes, N.; Zhou, X.; Dastoor, P. C.; Belcher, W.; Rasmussen, S. C.; Biewer, M. C.; Stefan, M. C. *J. Polym. Sci. Part A: Polym. Chem.* **2013**, *51*, 2622-2630.

(63) Evenson, S. J. *PhD Dissertation*, North Dakota State University, Fargo, ND, 2008.

(64) Cardona, C. M.; Li, W.; Kaifer, A. E.; Stockdale, D.; Bazan, G. C. *Adv. Mater.* **2011**, *23*, 2367-2371.

CHAPTER 5. SYNTHESIS AND CHARACTERIZATION OF THIENO[3,4-*b*]PYRAZINE-BASED COPOLYMERS WITH PHENYL COMONOMERS.

5.1. Introduction

The field of conjugated polymers (CPs) has grown substantially in the past few decades due to interest in their use in technological applications. Much of this interest is due to their unique combination of inorganic electronic and optical properties with the processability and mechanical flexibility of typical organic polymers.[1-8] Additionally these materials may be tuned on the molecular level by modification of monomer units, addition of side chains, or combination with other units.[1, 9-12]

Thieno[3,4-*b*]pyrazines are a class of materials which have been shown to feature a low band gap, advantageous in absorbing light in the solar spectrum.[13-15] As discussed in Chapter 2, pTPs may be generated easily via Grignard metathesis (GRIM) polymerization.[15] However, a common drawback to these types of materials is a high HOMO which, while increasing solar absorption, reduces open circuit potential in OPV devices. Thus, while TPs are typically designated as an electron accepting group due to their stabilized LUMO, it has been shown that the HOMO has donating capabilities equal to and even exceeding that of 3,4-ethylenedioxythiophene (EDOT).[17,18] Thus one of the goals of this research is to utilize the unique properties of TPs and combining them with methods previously used to generate materials yielding high device efficiency.

As previously discussed, tuning of the band gap as well as frontier molecular orbitals is of particular interest in optimizing materials for use in electronic devices. The approach of combining strong electron-rich units with electron-deficient units to generating donor-acceptor (DA) copolymers has become a popular in tuning electronic properties.[19,20] Materials generated

from this approach have yielded materials with promising electronic and optical properties for device application.[20-26] However, as TPs have been reported to have character of both a strong donor and acceptor,[16] a goal of research in this area was to use TPs as a donor unit and examine the properties when combining them with common aryl-based units. Of particular interest is combining TPs with other typical acceptor units.

In the first section of this chapter various TPs were combined with fluorene (FLO). Fluorene is an aryl-based system, commonly used in the generation of organic light-emitting diodes (OLEDs) due to its high quantum efficiency and charge transport ability.[27,28] Fluorene is classically considered to be a donor system due to its aromatic backbone. As fluorene has been used in numerous DA copolymers, it serves as a good comonomer for comparison of new materials.[29-34] Additionally, combination of TPs with fluorene should stabilize the HOMO, while still maintaining the TP-based LUMO. Several TPFLO copolymers were generated via Suzuki cross-coupling; the synthesis and characterization of TPFLO copolymers are described in Section 5.2. A TP-based terthiophene was also combined with fluorene to examine the nature of flanking thiophene units on the polymer backbone. A solar cell device was also made and characterized from one TPFLO copolymer.

A previously state goal of this research was to combine TPs with typical acceptor units, thus using TP as the donor material. This approach would allow the generation of materials which maintain a low band gap, but have slightly stabilized HOMOs to improve device performance. In an effort to examine the properties of such materials, TP was combined with two materials classified as acceptor materials. The monomer 2,3,1-benzothiadiazole (BTD) is a commonly used system in the generation of DA copolymers as an acceptor material and has yielded materials of high OPV efficiency.[35] Phthalimide (PTH) is another phenyl-based acceptor

unit commonly used in DA copolymers. In 2009 Watson and coworkers generated copolymers with N-alkylphthalimide with field-effect mobilities of 0.28 $cm^2/(V\ s)$ thus making it a promising material for device application.[36] Preparation of copolymers featuring both BTD and PTH combined with TP are described in Section 5.2. These polymers, however, were generated by direct hetero(arylation), an increasingly popular method of cross-coupling.

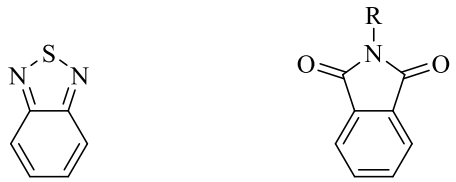

2,3,1-Benzothiadiazole (BTD) Phthalimide (PTH)

Chart 5.1. Acceptor materials combined with TPs in acceptor-acceptor polymers.

Methodologies toward the generation of new carbon-carbon bonds, in an effort to expand the scope of new materials available, for synthesis have been a well research topic. In aromatic systems this typically takes the form of metal-catalyzed cross coupling reactions. Such reactions as Stille, Suzuki, and Kumada cross coupling have successfully been applied in the field of CPs to generate new polymers in good yield and high molecular weight. However, in cases such as Stille or Suzuki coupling, functionalization with an organometallic moiety such as $–SnR_3$ or $–B(OR)_3$, respectively, is required to couple with a leaving group (I, Br, OTf, etc.) prior to polymerization.[37,38] This both increases the number of synthetic steps required and introduces potential synthetic complication such as instability of a polymer precursor. Organostannyls, used in Stille coupling, are highly toxic and thus elimination of their use is highly advantageous.

Thus, a push for use of new synthetic methods toward cross-coupling is of significant interest. In 2006 Fagnou and coworkers introduced a cross-coupling method to combine electron-deficient aromatics using a palladium catalyst and phosphine ligand.[39] This work along with subsequent optimization has yielded the method coined direct(heteroarylation) polycondensation.[40-47] In copolymerizations, this method requires one unit to be a dihalide while the other may remain unfuctionalized, thus removing the required organometallic moiety. Like other cross-coupling methods direct(hetero)arylation uses transition metal catalysts and a base to

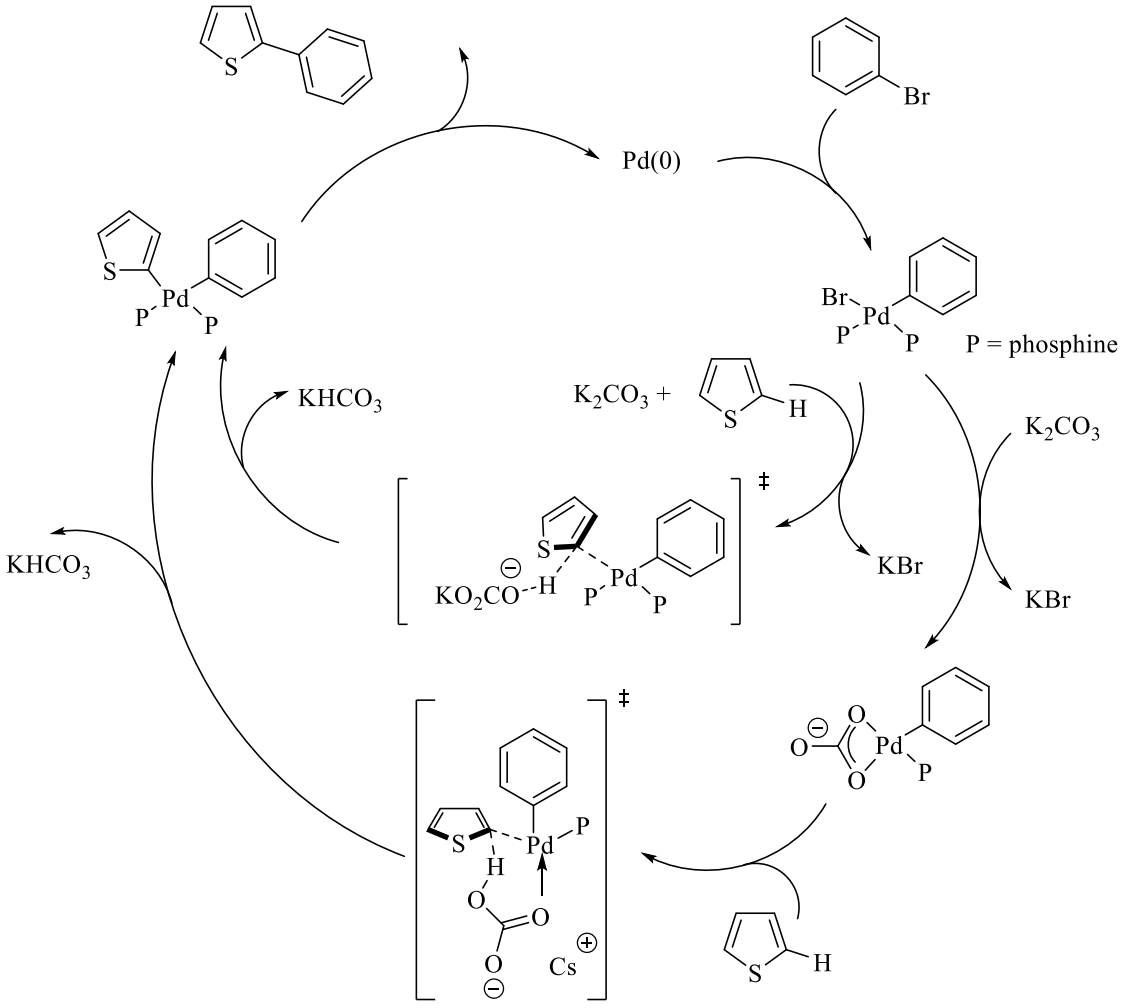

Scheme 5.1. Mechanism for direct (hetero)arylation between thiophene and bromobenzene without a carboxylate additive.[47]

deprotonate. The proposed mechanism without a carboxylic additive, submitted by Leclerc and coworkers, is represented in Scheme 5.1.[47] In this mechanism are common transformations seen in other cross-coupling mechanisms including oxidative addition of the aryl halide and reductive elimination to form the final product. However, this mechanism utilizes C-H activation to add the alternating monomer. This method has been used to generate several polymers in high yield and molecular weight.[40-49] Although highly efficient, selectivity is an issue with this method. As units such as thiophene may contain both α and β protons free for coupling, cross-linking or coupling at the β position occurs as shown in Scheme 5.2.[38] To avoid such issues careful selection of monomeric units is required.

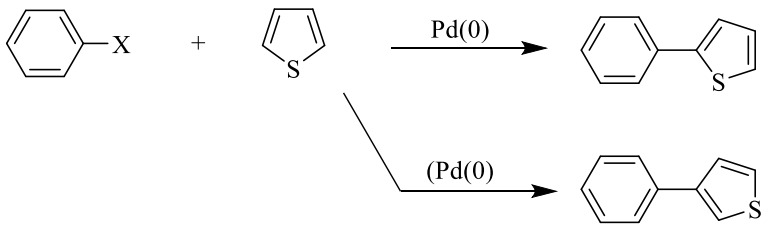

Scheme 5.2. General example of DHAP coupling benzene to a thiophene through the 2- and 3- positions.

5.2. Results and Discussion

5.2.1. *Synthesis*

Synthesis of TPFLO Copolymers. TPFLO copolymers **5.3a,b** were generated via Suzuki polycondensation with the dibromoTP and fluorene-diboronic ester as shown in Scheme 5.3. The reaction was heated to reflux using a $Pd(PPh_3)Cl_2$ in toluene for four days to give **5.3a** and **5.3b** in 43% and 41% respectively. Both reactions began yellow and changed color over time with **5.3a** changing to a bright red and **5.3b** changing to a yellow-brown color, corresponding to the color of emission for each polymer. Both polymers were endcapped with

phenylboronic acid and phenylbromide to remove reactive endgroups which may chemically react and stabilize the polymers. Additionally boronic acids may act to trap electrons, thus lowering the efficiency of any prepared devices, and so removal of these groups should inhibit the capabilities.[50,51]

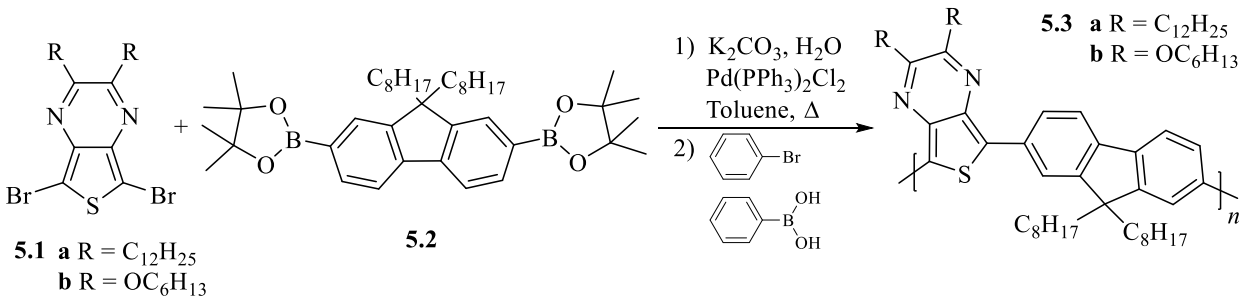

Scheme 5.3. Synthesis of polymers **5.3a,b** via Suzuki polycondensation.

In order to analyze the effect of flanking thiophenes on TPFLO copolymers, a terthienyl analogue of **5.2b** was generated.[52] The synthesis of this polymer is shown in Scheme 5.4. Synthesis of this polymer first required assembly of the terthienylOC_6TP. To generate this, first **5.1a** and 2-tributyltinthiophene were combined to generate **5.4** via Stille coupling. A bromination of **5.4** was then attempted; however, all trials resulted in decomposition of the material. In an effort to continue the project, Stille coupling of the terthienyl and dibromofluorene was attempted. Generation of **5.5** was completed by deprotonation with BuLi and subsequent addition of Me_3SnCl. Purification of **5.5** was accomplished by running it through a Et_3N-treated silica gel plug. This generated the pure **5.5** which was then combined with **5.6** using a Pd_2dba_3 catalyst and P(*o*-tolyl)$_3$ for a ligand in toluene to generate the polymer **5.7** via Stille coupling. The polymer was generated in a 41% yield.

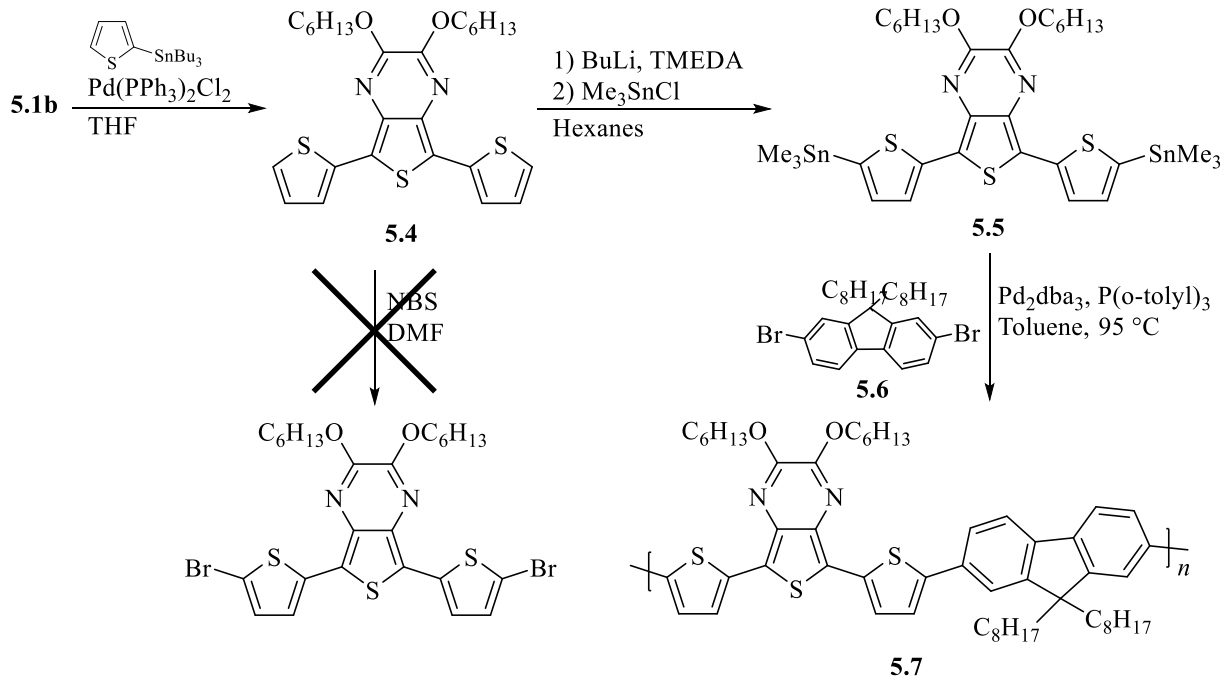

Scheme 5.4. Synthesis of **5.7** via Suzuki polycondensation.

All three polymers have similar yields at 41-43% regardless of polymerization technique used. All the molecular weights, found in Table 5.1, of all three polymers were obtained via GPC with giving an M_n of 4800 for **5.3a** and 2700 for **5.7**. All three M_n values are relatively low, with the lowest being that of the terthienyl polymer. The lower M_n for **5.7** could be due in part to the scale of the reaction, which was at a third the scale of either **5.3a** or **b**. All three polymers were readily soluble in $CHCl_3$ and THF and thus the low molecular weights are not due to the polymer precipitating out of solution.

Table 5.1. Yields and molecular weight data for TPFLO copolymers.

Entry	M_n[a]	PDI[a]	Yield (%)
5.3a	4800	1.3	43
5.3b	-	-	41
5.7[52]	2700	1.5	41

[a] Determined via gel permeation chromatography (GPC).

5.2.2. *UV-vis-NIR Absorption Spectroscopy*

Absorption Data for TPFLO Copolymers. The representative solution and solid state absorption spectra of **5.3a**, **b**, and **5.7** are shown in Figure 5.1; the data from these spectra can be found on Table 5.2. All polymers show the two absorption bands typically seen in TP-based polymers, with the first transitions at 300-400 nm, representative of the polymer backbone π-π* transfer. The low energy transfer bands in **5.3b** and **5.7** are blue shifted from **5.3a**, likely due to molecular weight differences. The low energy band in the solid state for 4.7 appears to largely disappear, blending into one broad peak.

The second low energy bands are representative of the charge transfer from polymer backbone to the TP-based pyrazine. Both **5.3a** and **5.3b** show a slight red shift in absorbance going from solution to solid state, due to polymer packing. Comparison of optical onset for **5.3a** (660 nm) and **5.3b** (620 nm) shows a shift of 40 nm to higher energy in the latter, giving a larger band gap for **5.3b**. This is in good agreement with both the TP monomer and homopolymer data, in which alkyloxy TP analogues show larger HOMO/LUMO gaps than those of the alkyl TPs. Some contribution, however, may be a product of lower molecular weight. Copolymer **5.7** shows little affect from solid state packing, having a similar onset as in the solution spectrum and has the lowest optical onset at 540 nm. Due to the low molecular weight of **5.7** this is not unsurprising.

Table 5.2. Optical properties of TPFLO copolymers.

Entry	Solution λ_{max} [a]	Solid λ_{max} [b]	Band gap (eV) [c]
5.3a	360, 515	365, 558	1.87
5.3b	300, 454	338, 475	2.0
5.7[52]	343, 451	444	2.3

[a] In CH_3Cl, [b] Film formed via spin coating on glass plate. [c] Optical.

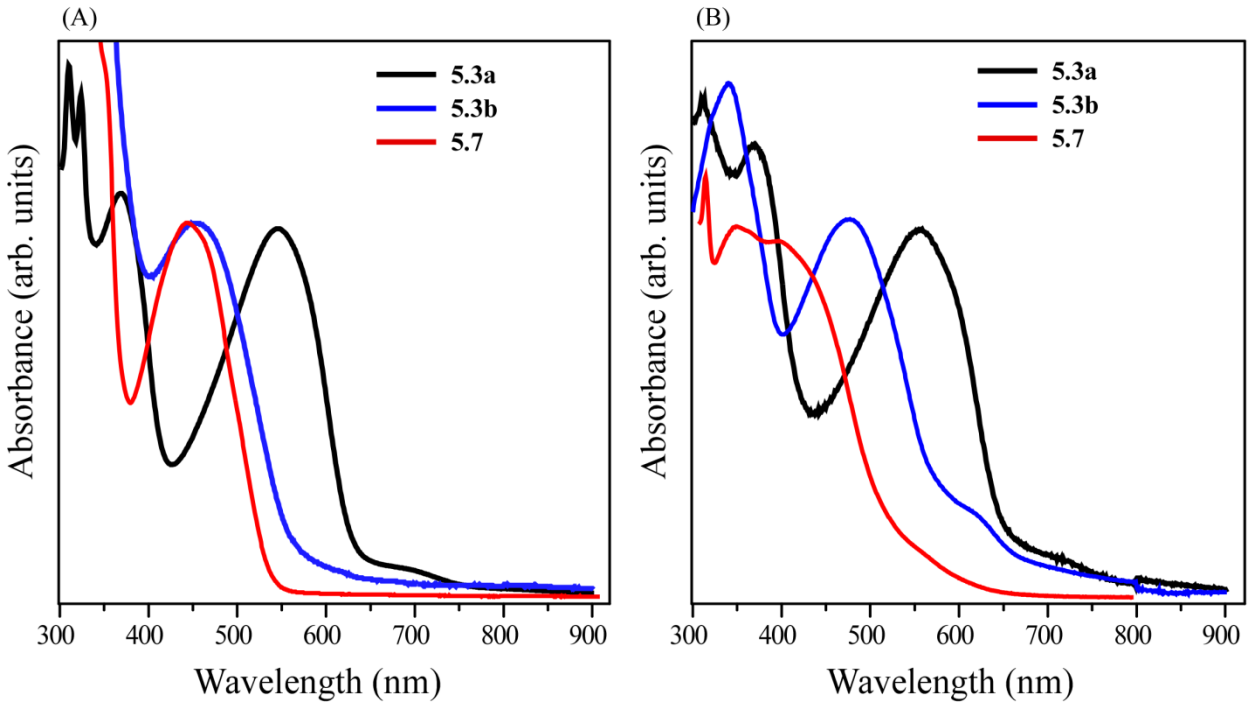

Figure 5.1. (A) Solution (in $CHCl_3$) and (B) solid-state absorption spectra of TPFLO copolymers**.**

5.2.3. *Electrochemistry*

Electrochemistry of TPFLO Copolymers. The CV experiments were performed on TPFLO copolymers with data found on Table 5.3 and representative CVs can be found in Figure 5.2. The TPFLO copolymers **5.3a** and **5.3b** feature oxidation peaks shifted 100 mV to a negative potential going from an alkyl to an alkyloxy side chain. This indicates a destabilization of the HOMO and is in good agreement with monomer and homopolymer data seen previously in Chapters 2 and 3. Copolymer **5.7**, also with an alkyloxy side chain, features an even further negatively shifted oxidation peak, indicating further destabilization of the HOMO. Although a reduction peak is observed in each polymer it is likely, as with the homopolymers, these are due to a coupled reduction of the oxidation peak, indicating these polymers to have electrochemically irreversible oxidation. Based on the optical band gap, reductions of each polymer should be observed at a more negative potential than seen, lending credibility to this assumption.

Table 5.3. Electrochemical properties of TPFLO copolymers.

Entry	E_{pa} (V)[a]	HOMO (eV)[b]	LUMO (eV)[c]	E_g (eV)[d]
5.3a	1.19	-5.8	-3.9	1.9
5.3b	1.09	-5.4	-3.4	2.0
5.7[52]	0.66	-5.4	-3.1	2.3

[a] Film formed by drop casting from a $CHCl_3$ solution on a Pt disc working electrode. Potentials vs Ag/Ag^+ in 0.1 M $TBAPF_6$ in MeCN. [b] EHOMO was determined from the onset of oxidation vs ferrocene (5.1 eV vs vacuum).[53] [c] $E_{LUMO} = E_{HOMO} - E_g$, [d] Optical.

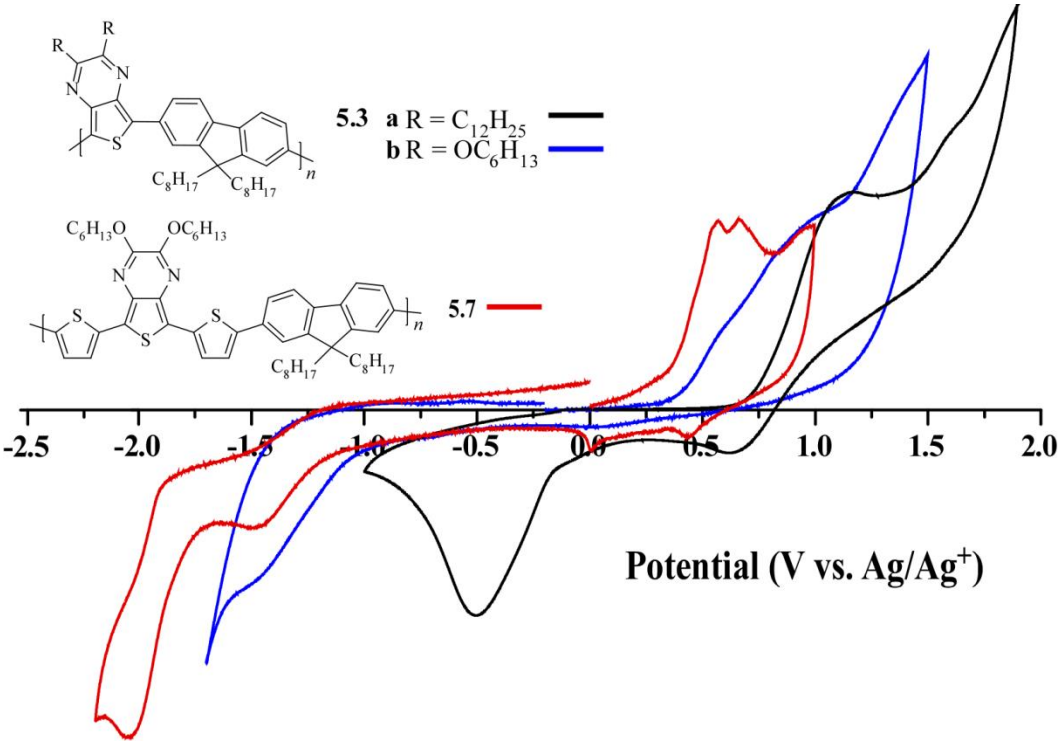

Figure 5.2. Cyclic voltammogram of TPFLO copolymers.

5.2.4. *Synthesis*

Synthesis of Other TP-aryl Copolymers via Direct (Hetero)arylation. The copolymer poly(thieno[3,4-*b*]pyrazine-co-2,3,1-benzothiadiazole) (TPBTD) **5.9** was generated via direct heteroarylation of **5.1a** and **5.8** (prepared by Cole Larsen). The reaction used a $Pd(OAc)_2$ catalyst with K_2CO_3 as a base and a tri(*o*-methoxyphenyl)phosphine ligand, performed in THF at

70 °C for two days generating the polymer **5.9** in 31.3% yield. The reaction color started as yellow. However, after 5 h of heating, the reaction turned black-purple.

A second polymer poly(thieno[3,4-*b*]pyrazine-co-*N*-octylphthalimide) (pTPPTH) **5.11** was prepared in a similar fashion to **5.9**, via combination of **5.1a** and **5.10**. However, the solvent was changed to toluene in order to increase the reaction temperature. This reaction began a yellow solution and turned red in color upon heating to reflux. The synthesis of both polymers is shown in Scheme 5.5 and yields and molecular weight data can be found on Table 5.4.

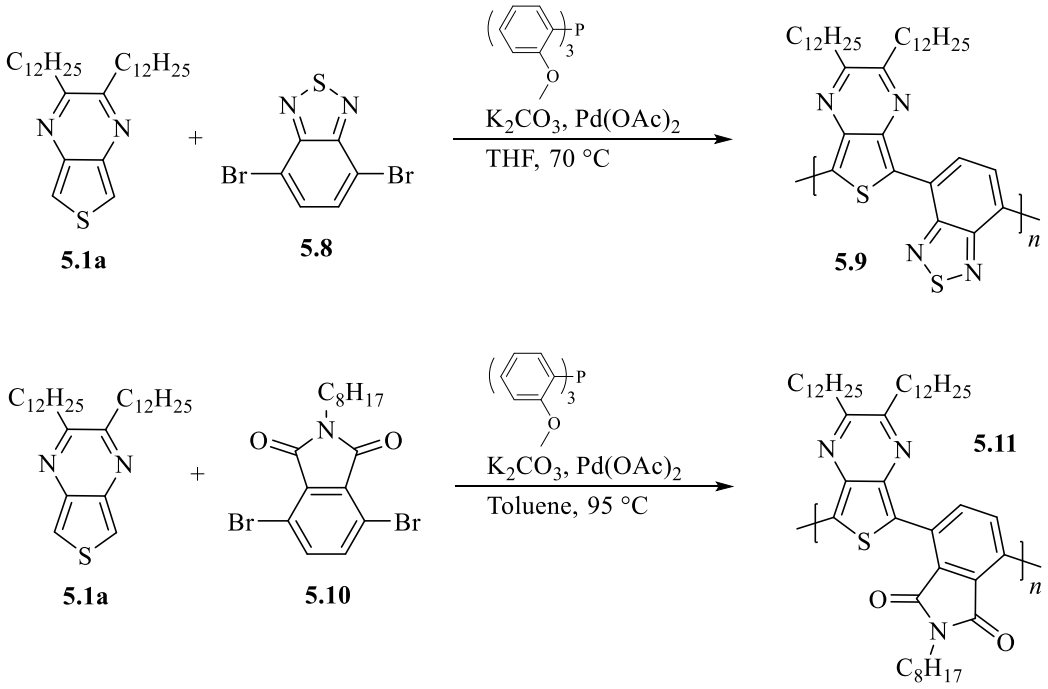

Scheme 5.5. Synthesis of **5.9** and **5.11** via direct (hetero)arylation cross-coupling.

Table 5.4. Yields and molecular weight data for TP-arylene copolymers.

Entry	M_n[a]	PDI[a]	Yield (%)
5.9	1200	1.4	31.3
5.11	3400	1.3	52.8

[a] Determined via gel permeation chromatography (GPC).

5.2.5. *UV-vis-NIR Absorption Spectroscopy*

Absorption Data for TP-arylene Copolymers. The absorption data for **5.9** and **5.11** is found on Table 5.5 and the representative data can be found in Figure 5.3. As with the previous polymers, these have a dual band absorption profile. The first high energy band at ~300 nm, again, is representative of the π-π* transition. Copolymer **5.9** has a low energy band with onset at 900 nm is due to the afore mentioned charge transfer excitation. This band features shoulders,

Table 5.5. Optical properties of TP-arylene copolymers.

Entry	Solution λ_{max} [a]	Solid λ_{max} [b]	Band gap (eV) [c]
5.9	257, 317, 561 (615)	320, 584 (630)	1.3
5.11	321, 462	322, 483	2.0

[a] In CH_3Cl, [b] Film formed via spin coating on glass plate. [c] Optical.

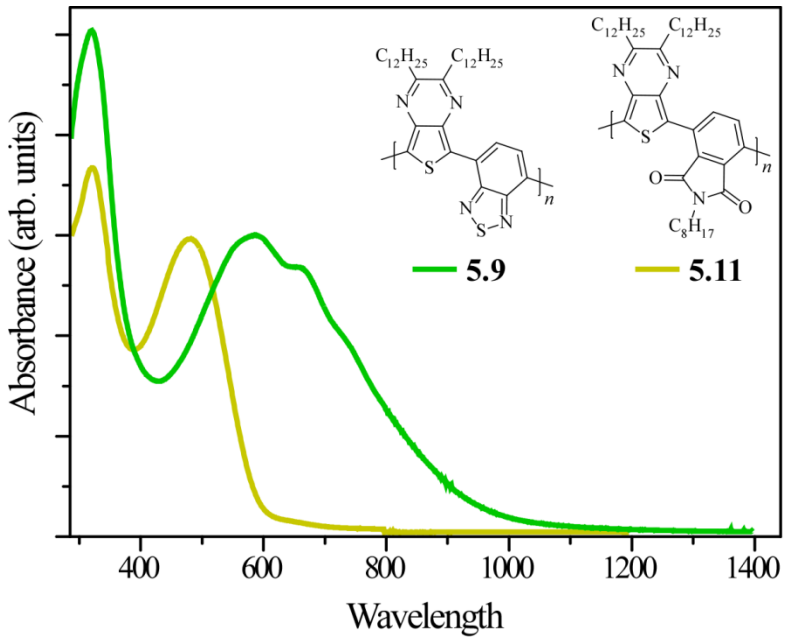

Figure 5.3. Solid-state absorption of TP-arylene copolymers **5.9** and **5.11**.

showing good vibrational activity. There is a slight red shift in all λ_{max} peaks and onset going from solid to solution state, indicative of polymer packing. The polymer has good absorption over the entire visible region, into the infrared and has good potential for solar cell application. Copolymer **5.11** also features two major optical transitions, the first of which is the π-π^* transition seen in TP-based materials, occurring at 322 nm, similar to that seen in **5.9**. However, **5.11** has an onset significantly blue shifted by over 200 nm, despite higher molecular weight. This polymer also has less vibrational structure in the low energy band than **5.9**. Due to similar odd effects in the electrochemistry, discussed later, there is an unknown effect in this polymer affect its properties.

5.2.6. *Electrochemistry*

Electrochemistry of TP-arylene Copolymers. Electrochemical characteristics of **5.9** and **5.11** were performed, yielding the data seen in Table 5.6 from the CV spectrum in Figure 5.4. As observed for **5.9**, a weak oxidation peak occurs at ~1.2 V with a coupled reduction at 0.1 V, indicating the oxidation is electrochemically irreversible. The polymer has a reduction onset occurring at ~0.9 V, yielding an electrochemical E_g of 1.4 eV, in good agreement with the optical E_g.

Elecrochemical experiments were performed on **5.11**, however, no activity was observed. Upon forming a film on the working electrode, thick films caused no electroactivity to occur while thin films yielded normal background electroactivity. Solution-based electrochemistry was attempted in $CHCl_3$, however, again only normal background activity was observed. As a final test, O_2 was blown over the sample in $CHCl_3$, but yielded no color change. Ultimately it was concluded copolymer **5.11** was not electroactive.

Table 5.6. Electrochemical properties of TP-arylene copolymers.

Entry	E_{pa} (V)[a]	HOMO (eV)[b]	LUMO (eV)[c]	E_g (eV)[d]
5.9	1.15	-5.6	-4.2	1.3
5.11	-	-	-	2.0

[a] Film formed by drop casting from a $CHCl_3$ solution on a Pt disc working electrode. Potentials vs. Ag/Ag^+ in 0.1 M $TBAPF_6$ in MeCN. [b] E_{HOMO} was determined from the onset of oxidation vs. ferrocene (5.1 eV vs. vacuum).[53] [c] $E_{LUMO} = E_{HOMO} - E_g$, [d] Optical.

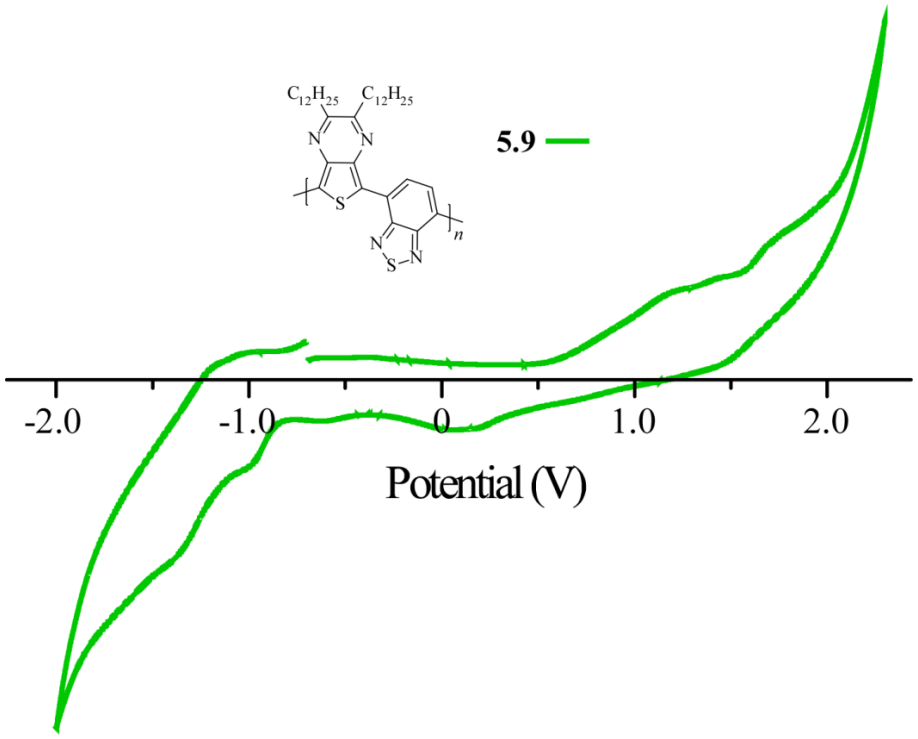

Figure 5.4. Cyclic voltammogram of copolymer **5.9**.

5.2.7. *OPV Device Properties.*

Device Properties for Copolymer 5.3a. Polymer **5.3a** was applied as an active layer donor material in bulk heterojunction solar cells. Only one blend of polymer:$PC_{61}BM$ was attempted due to time constraints using a 1:1 mixture. The IV characteristics can be found on Figure 5.5 and data in Table 5.7. The device produced gave an efficiency of 0.027%. The low PCE seen here could be a contribution of several factors, including low molecular weight and

polymer absorption. Polymers of low M_n will often produce inferior films such as those produced spin coating with **5.3a**:$PC_{61}BM$ blend.

Table 5.7. OPV device data for copolymer **5.3a**.[a]

Polymer	Polymer:$PC_{61}BM$ (w:w)	V_{oc} (V)	J_{sc}(mA/cm^2)	FF(%)	η(%)
5.3a	1:1[a]	0.23	-0.44	0.26	0.027

[a] annealed.

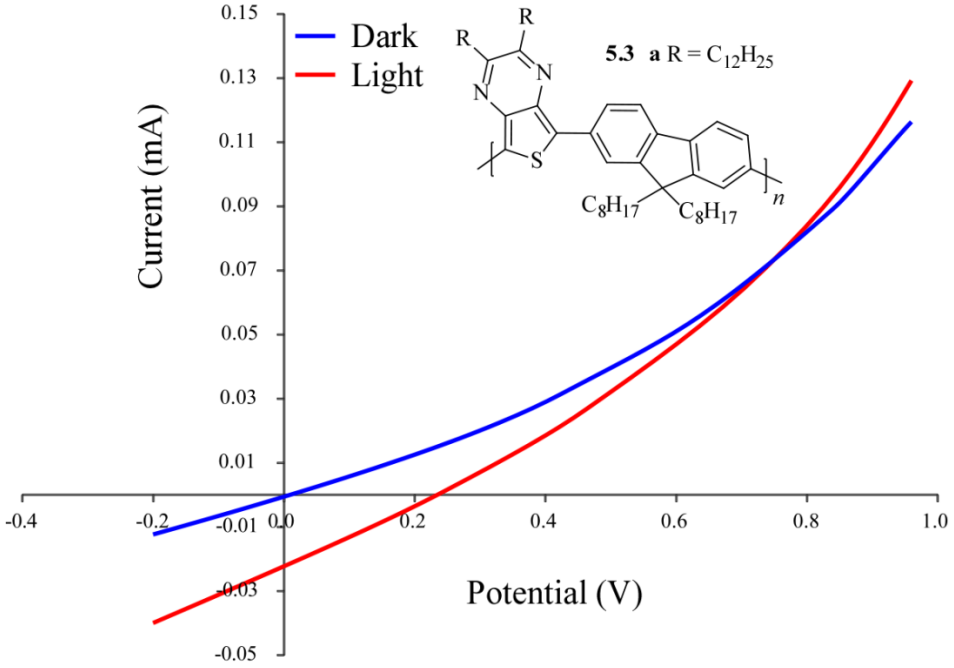

Figure 5.5. IV characteristics for **5.3a** at 1:1 polymer:$PC_{61}BM$ blend.

Device Properties for Copolymer 5.9. Devices were made using copolymer **5.9** as a donor in the active layer by Trent Anderson. Successful devices were made using **5.9**:$PC_{61}BM$ blends of 1:2 and 1:3, although efficiencies were relatively low in both cases. The IV characteristics can be found on Figure 5.6 and data in Table 5.8. Although both V_{oc} and FF were reasonable, J_{sc} for both cells was very low, likely the cause of the low efficiencies observed in both devices. One factor which may have contributed to the low efficiencies of generated devices

is poor film morphology. The films formed via spin coating were both thin and gelatinous. It is notable that going from 1:2 to 1:3 (polymer:$PC_{61}BM$) there is a rough halving of both V_{oc} and J_{sc} and consequently, PCE.

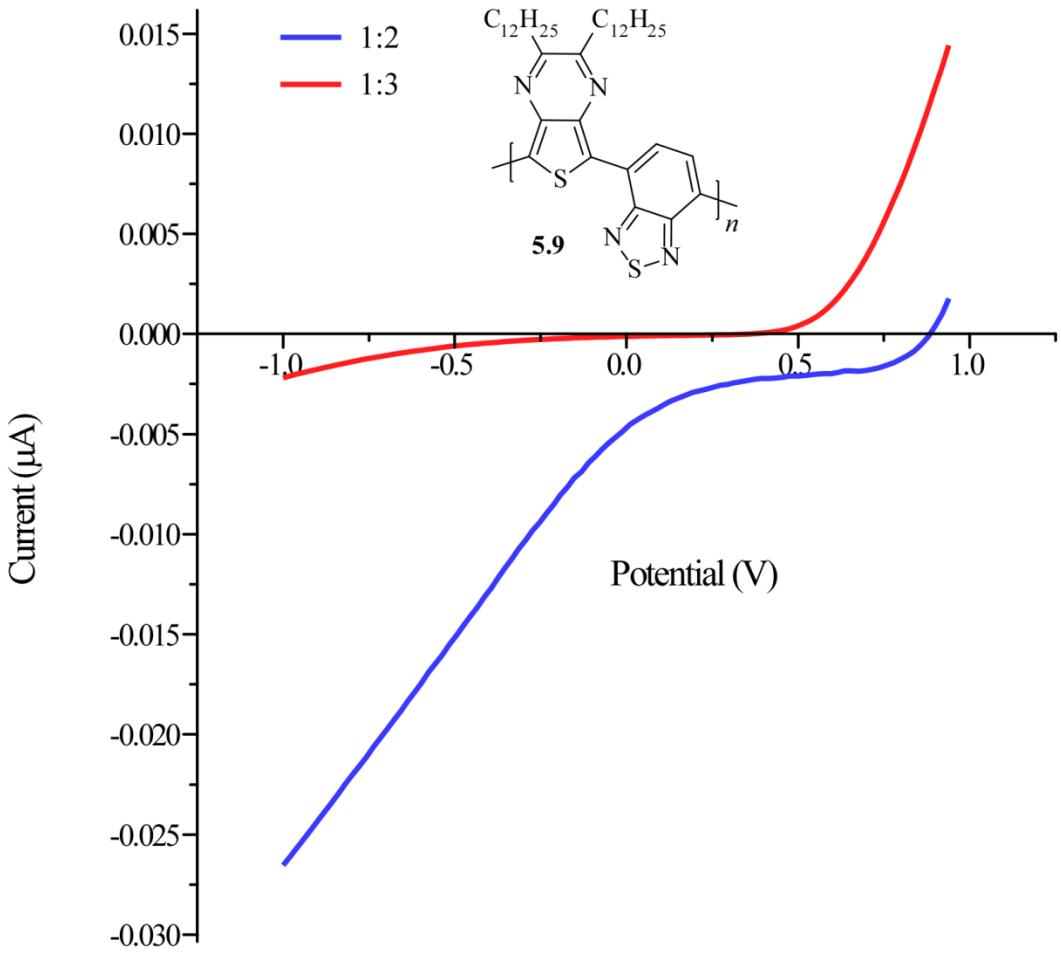

Figure 5.6. IV characteristics for copolymer **5.9** at 1:2 polymer:$PC_{61}BM$ blend.

Table 5.8. OPV device data for copolymer **5.9**.[a]

Polymer:$PC_{61}BM$ (w:w)	V_{oc} (V)	J_{sc}(mA/cm^2)	FF(%)	η(%)
1:2	0.89	0.06	31.2	0.02
1:3	0.49	0.03	44.3	0.01

[a] annealed.

5.3. Conclusion

Two DA copolymers featuring an alternating TP and fluorene units have been generated via Suzuki coupling. A third TP based TP-based terthienyl copolymer with fluorene was generated via Stille coupling. These are representative of more of the traditional DA systems where the fluorene is considered to be a donor material. All three polymers have profiles absorbing in the visible region, with the dodecyl analogue being the furthest red shifted. The copolymer **5.3b** shows an expected blue shift in the low energy onset, showing the capability of tuning the optical properties by altering the TP-based side chains as previously seen in the homopolymeric materials. Although the terthienyl copolymer **5.7** features a further blue-shifted absorption profile, this is likely due to low molecular weight and further optimization of coupling conditions may show a bathochromic shift with higher M_n. Copolymer **5.3a** was applied as a donor material in the active layer of a generated solar cell. Although low efficiency was seen from the device, further optimization of polymer:PCBM blends, along with higher M_n copolymers might improve PCE.

Direct (hetero)arylation polycondensation was used to combine TP with arylene groups benzothiadiazole and *N*-octylphthalimide to generate copolymers pTPBTD **5.9** and pTPPTH **5.11**. These systems are also DA type polymers. However, in the case of these TP is acting as the donor material and is combined with other traditionally classified acceptors. Copolymer **5.9** had an absorption onset blue-shifted >300 nm from that of **5.11**. This was also one of the few copolymers showing both oxidation and reduction peaks in cyclic voltammetry experiments. Copolymer **5.11**, despite showing reasonable spectral absorption showed no electroactivity. It is unknown at this time why this occurred and thus attempts to generate this polymer under varied conditions is of interest to make a more useful polymer. Solar cell devices were made from

copolymer **5.9**. Although these showed both low J_{sc} and PCE, it might be of interest to attempt to generate copolymers with BTD featuring different 2nd generation TP-based side chains to observe the effect these electronic properties have on device performance.

While DHAP showed promise as a method to generate copolymers much work is needed to optimize conditions. The current conditions used to generate TP-based copolymers worked well for **5.9**, however, less success was observed for **5.11**. Upon generation of materials with high molecular weight with both materials, fabrication of new OPV devices will be desired to obtain a more accurate measure of these materials' capabilities in device application. This technique is very attractive allowing previously unavailable avenues in polymerization as well as removing difficult synthetic steps and will likely be a focus in future research for these materials.

5.4. Experimental

5.4.1. *General*

Unless noted, all materials were reagent grade and used without further purification. Chromatographic separations were performed using standard column chromatography methods with silica gel (230-400 mesh). Dry THF and toluene were obtained via distillation over sodium/benzophenone. All glassware was oven-dried, assembled hot, and cooled under a dry nitrogen stream before use. Transfer of liquids was carried out using standard syringe techniques and all reactions were performed under a dry nitrogen stream. The ^{1}H NMR and ^{13}C NMR were completed on a 400 MHz spectrometer. All NMR data was referenced to the chloroform signal and peak multiplicity was reported as follows: s = singlet d = double, t = triplet, q = quartet, p = pentet, tt = triplet of triplets, m = multiplet and br = broad. Melting points were determined using a digital thermal couple with a 0.1 °C resolution. The following compounds were synthesized according to previously reported literature procedures: 9,9-diocyl-2,7-bis(4,4',5,5'-tetramethyl-

1,3,2-dioxaborolan-2-yl)-9H-fluorene (**5.2**),[54] 2,7-dibromo-9,9-dioctyl-9H-fluorene (**5.6**),[55] 4,7-dibromo-2,3,1-benzothiadiazole (**5.8**),[35] N-ocytyl-3,6-dibromophthalimide (**5.10**).[36]

Poly(2,3-didodecyl-thieno[3,4-*b*]pyrazine-*co*-9,9-dioctyl-9*H*-fluorene (5.3a). To a 100 mL flask was added **5.1a** (0.22 g, 0.37 mmol), **5.2** (0.25 g, 0.39 mmol), and $PdCl_2(PPh_3)_2$ (0.013 g, 0.019 mmol). The tube was then evacuated and backfilled with N2 five times. N_2-purged toluene (60 mL) and a solution of N_2-purged K_2CO_3 in H_2O (2 mL, 1.6 M) were then added via syringe and the reaction was heated to 95 °C for 4 days. Bromobenzene (0.003 mL, 0.035 mmol) was added and the solution was stirred for 1 h after which phenylboronic acid (0.004 g, 0.035 mmol) was added and the reaction was stirred at 95 °C for 1 day. The reaction was then cooled to RT and precipitated in MeOH (300 mL). The crude polymer was purified via Soxhlet extraction with MeOH, acetone, and hexanes before being collected in $CHCl_3$. The polymer was then concentrated via rotary evaporation to produce a red solid (43% yield). ^{1}H NMR: δ 7.61, 7.30, 3.20, 2.52, 1.50-0.88. GPC: M_w = 6200, M_n = 4800, PDI = 1.3.

Poly(2,3-dihexyloxy-thieno[3,4-*b*]pyrazine-*co*-9,9-dioctyl-9H-fluorene (5.3b). Polymer **5.3b** was produced in the same manner as **5.3a** substituting **5.1a** with **5.1b**. The polymer was concentrated via rotary evaporation to yield a yellow-brown solid (41% yield). ^{1}H NMR: δ 7.62, 7.31, 4.50, 2.01, 1.59-0.61.

2,3-Dihexyloxy-5,7-bis(2-thienyl)thieno[3,4-*b*]pyrazine (5.4).[52] 2-(Tributylstannyl)thiophene (0.39 g, 1.08 mmol) and **4.1a** (0.21 g, 0.42 mmol) were combined in a 250 mL flask, evacuated, and backfilled with dry N_2. Dry THF (100 mL) was then added via syringe, followed by a second N_2 cycling. $PdCl_2(PPh_3)_2$ (0.015 g , 0.02 mmol) was added, the solution was heated to reflux, and stirred for 16 h. The solution was then allowed to cool to room temperature and the solvent was removed via rotary evaporation. The resulting material was

dissolved in CH_2Cl_2, washed with H_2O, dried with $MgSO_4$, and concentrated via rotary evaporation. Purification was done by silica chromatography in (95:5, hexanes:CH_2Cl_2) yielding an orange solid (48% yield). ^{1}H NMR: δ 7.45 (dd, *J* = 3.0, 1.2 Hz, 2H), 7.31 (dd, *J* = 4.5, 1.2 Hz, 2H), 7.06 (dd, *J* = 3.0, 4.5 Hz, 2H), 4.55 (t, *J* = 7.0 Hz, 2H), 1.93 (t, *J* = 7.0 Hz, 4H), 1.52-1.38 (m, 12H), 0.94 (t, *J* = 6.5 Hz, 6H). ^{13}C NMR: δ 150.16, 135.40, 134.03, 127.47, 123.29, 120.48, 68.08, 31.77, 28.52, 25.95, 22.80, 14.22.

2,3-Dihexyloxy-5,7-bis(5-trimethylstannyl-2-thienyl)thieno[2,4-*b*]pyrazine (5.5).[52] Dry hexanes (60 mL) was added via syringe to a flask containing 4.4 (0.06 g, 0.12 mmol) and the solution was cooled to 0 °C. *N,N,N',N'*-tetramethylethylenediamine (TMEDA) (0.05 mL, 0.35 mmol) was then added followed by BuLi (0.13 mL, 0.33 mmol) and the solution was stirred for 2 h. Me_3SnCl (0.3 mL, 0.33 mmol) was then syringed into the solution and the reaction was allowed to stir overnight. The solution was poured over Et3N-treated silica gel, filtered, and rinsed with 100 mL hexanes. The solution was then concentrated via rotary evaporation to yield a yellow liquid (99%). ^{1}H NMR: δ 7.44 (d, *J* = 3.2 Hz, 2H), 7.10 (d, *J* = 1.6 Hz, 2H), 4.40 (t, *J* = 6.4 Hz, 4H), 1.81 (m, *J* = 6.8 Hz, 4H), 1.53-1.20 (m, 16H), 0.86 (t, *J* = 6.8 Hz, 6H), 0.40 (s, 18H).

Poly(2,3-dihexyloxy-5,7-bis(2-thienyl)thieno[3,4-*b*]pyrazine-*co*-9,9-dioctyl-9*H*-fluorene) (5.7).[52] Fluorene **5.6** (0.06 g, 0.12 mmol), **5.5** (0.10 g, 0.12 mmol), Pd_2dba_3 (0.002 g, 0.002 mmol), and P(*o*-tolyl)$_3$ (0.02 g, 0.08 mmol) were combined in a flask. N_2-purged toluene (15 mL) was then added via syringe and the solution was evacuated and backfilled with N_2 five times. The reaction was then placed in an oil bath, heated to 95 °C, and allowed to stir for 4 days. The reaction was then cooled, poured into 300 mL MeOH, and filtered. The soluble fraction was collected in $CHCl_3$ and isolated via rotary evaporation. Further purification was accomplished

via additional washes with MeOH giving a red solid (75% yield). ^{1}HNMR: δ 7.5, 7.44, 7.30, 4.55 (br), 1.92, 1.6-0.6. GPC: M_w = 4000, M_n = 2700, PDI = 1.48.

Poly(2,3-didodecylthieno[3,4-*b*]pyrazine-*co*-2,3,1-benzothiadiazole (5.5). To a 20 mL Schlenk tube was added **5.1a** (0.1 g, 0.21 mmol), **5.8** (0.06 g, 0.21 mmol), $Pd(OAc)_2$ (20 mg, 0.09 mmol), K_2CO_3 (0.044 g, 0.32 mmol), and tris-(*o*-methoxyphenyl)phosphine (0.022 g, 0.063 mmol) and the vessel was then was evacuated and refilled with N_2 four times. N_2-purged THF was syringed into the solution; the reaction was heated to 70 °C and allowed to stir for 2 days. The reaction was cooled to RT, poured into 300 mL MeOH, and filtered. The soluble fraction was collected in $CHCl_3$ and concentrated via rotary evaporation. Further purification was accomplished via Soxhlet extraction with MeOH, acetone, and hexanes. The polymer was then dissolved in $CHCl_3$ and concentrated via rotary evaporation to give a purple-black solid (31.3% yield). ^{1}H NMR: δ 7.99, 3.02, 1.97, 1.40-1.21, 0.89-0.81. GPC: M_w = 1700, M_n = 1200, PDI = 1.4.

Poly(2,3-didodecylthieno[3,4-*b*]pyrazine-*co*-*N*-octylphthalimide (5.11). Polymer **5.11** was produced in the same manner as **5.9** substituting **5.8** with **5.10**. Solvent was used in this reaction in place of THF and heating was done at 95 °C. The polymer was concentrated via rotary evaporation to yield a yellow-brown solid (52.8% yield). ^{1}H NMR: δ 8.05, 2.92, 2.82, 1.40-1.18, 0.853 GPC: M_w = 4400, M_n = 3400, PDI = 1.3.

5.4.2. *Electrochemistry*

All electrochemical techniques were performed on a Bioanalytical Systems BAS 100B/W electrochemical analyzer. Cyclic voltammetry (CV) experiments were performed using a three-electrode cell consisting of a Pt-disc working electrode, Pt coil wire auxillary electrode, and an Ag/Ag^+ reference electrode. A 0.1 M electrolyte solution was prepared with

tetrabutylammonium hexafluorophosphate ($TBAPF_6$) using MeCN distilled over CaH_2 under dry nitrogen. The solutions were deoxygenated with argon for at least 20 min prior to each scan and blanketed with argon during the experiments. Solutions of polymers in $CHCl_3$ were drop cast on the working electrode and dried to form a solid film. CV experiments were performed in the above described cell at a sweep rate of 100 mV/s. E_{HOMO} values were determined in a reference to ferrocene (5.1 V vs. vacuum)[53] and the E_{LUMO} was determined from the following equation: $E_{LUMO} = E_{HOMO}$ – optical band gap.

5.4.3. *UV-vis-NIR Aborption Spectroscopy*

All absorption spectroscopy was performed on a Carry 500 dual-beam UV-vis-NIR spectrophotometer. Solution-state spectra were analyzed in chloroform and solid-state spectra were analyzed with the polymer spin coated on a glass plate. The optical band gaps were determined from the onset of the lowest energy absorption by extrapolation of the steepest slope to the intersection with the wavelength axis.

5.4.4. *OPV Device Fabrication*

OPV Device Fabrication for Copolymer 5.3a. Glass substrates coated with patterned indium-tin oxide (ITO) were cleaned prior to use by heating in a bath of detergent at 90 °C followed by 15 min sonication. The detergent was then poured out and the plates were rinsed 3 times with deionized water. They were then placed in under sonication in acetone and isopropanol in succession for 15 min each, followed by drying under dry N_2. A 0.5 mm filtered dispersion of PEDOT:PSS in H_2O was spun cast at 5000 rpm for 60 s onto the cleaned ITO plates and then heated to 200 °C for 5 min to yield a film of ~40 nm. A blend of polymer:$PC_{61}BM$ at concentrations of 40 mg/mL were filtered through a 0.45 mm filter and spun cast at 700 rpm for 60 s onto the PEDOT:PSS layer. The substrate was then dried at 60 °C for 10

min. The aluminum cathode was vacuum deposited at a pressure of 1 x 10^{-7} mbar, giving a thickness of 100 nm. The IV characteristics of the devices were then measured at AM 1.5 simulated light.

OPV Device Fabrication for 5.9. Organic solar cells were fabricated on patterned indium tin oxide (ITO) glasses with a sheet resistance of 20 Ω/sq. The ITO glass was cleaned by sequential ultrasonic treatment in detergent, deionized water, acetone, and isopropanol, and then treated in a bench-top plasma cleaner (PE-50 bench top cleaner, The Plasma Etch, Inc., USA) for 2 min. PEDOT:PSS (Clevious P VP AI 4083 H. C. Stark, Germany) solution was filtered through a 0.45 μm filter and then spin coated at 4000 rpm for 60 s on the ITO electrode. Subsequently, the PEDOT:PSS layer was baked at 100 ºC for 40 min in the air to remove any moisture that might be present in film. The PEDOT:PSS coated substrates were transferred to a N_2 filled glove box. A blend solution of **5.9** (Rieke Metals, Inc., MW = 17kDa) and PCBM (Nano-C) at a concentration of 30-40 mg/mL (at varying ratios w/w) in 0.25 mL of chloroform. The solution was spun on the top of the PEDOT:PSS layer at 800 rpm for 45 seconds. After an hour of aging half of the **5.9**:PCBM blend films were thermally annealed at 105 ºC for 5 minutes. The edges of the solar cell were cleaned using chloroform before being capped with the cathode consisting of LiF (~1 nm) and Al (~100 nm) which were thermally evaporated on the active layer under a shadow mask in a base pressure of 1x10^{-6} mbar. The device active area was ~7.9 mm^2 for all the solar cells discussed in this work. The J-V measurement of the devices was conducted on a computer controlled Keithley 2400 source meter. The J-V measurement system uses a solar simulator with a Class-A match to the AM1.5 Global Reference Spectrum. It is calibrated with KG5-filtered silicon reference cell with calibration traceable to NREL and NIST.

5.5. References

(1) Rasmussen, S. C.; Ogawa, K.; Rothstein, S. D. In *Handbook of Organic Electronics and Photonics*; Nalwa, H. S., Ed.; American Scientific Publishers: Stevenson Ranch, CA, 2008; Vol. 1, Chapter 1.

(2) Garnier, F. *Acc. Chem. Res.* **1999**, *32*, 209-215.

(3) Scrosati, B. In *Applications of Electroactive Polymers*; Scrosati, B., Ed.; Chapman and Hall: London, 1993; pp 250-282.

(4) Barford, W. *Electronic and Optical Properties of Conjugated Polymers*, International Series of Monographs on Physics ed.; Clarendon Press: Oxford, 2005; Vol. 129.

(5) Heeger, A. J. *Angew. Chem., Int. Ed. Engl.* **2001**, *40*, 2591-2611.

(6) MacDiarmid, A. G. *Angew. Chem., Int. Ed. Engl.* **2001**, *40*, 2581-2590.

(7) Shirakawa, H. *Angew. Chem., Int. Ed. Engl.* **2001**, *40*, 2575-2580.

(8) Yu, G.; Heeger, A. J. *Synth. Met.* **1997**, *85*, 1183-1186.

(9) Roncali, J. *Chem. Rev.* **1992**, *92*, 711-738.

(10) Roncali, J. *Chem. Rev.* **1997**, *97*, 173-205.

(11) Roncali, J. Advances in the Molecular Design of Functional Conjugated Polymers. In *Handbook of Conducting Polymers*, 2nd ed.; Skotheim, T. A., Elsenbaumer, R. L., Reynolds, J. R., Eds.; Marcel Dekker, Inc.: New York, 1998; pp 311-341.

(12) Rasmussen, S. C.; Straw, B. D.; Hutchinson, J. E. In *Semiconducting Polymers: Applications, Synthesis, and Properties*; Hsieh, B. R, Wei, W., Galvin, M., Eds.; ACS Symposium Series 735, American Chemical Society: Washington, DC, 1999; pp 347-366.

(13) Nayak, K.; Marynick, D. S. *Macromolecules* **1990**, *23*, 2237-2245.

(14) Otto, P.; Ladik, J. *Synth. Met.* **1990**, *36*, 327-335.

(15) Wen, L.; Duck, B. C.; Dastoor, P. C.; Rasmussen, S. C. *Macromolecules.* **2008**, *41*, 4576-4578.

(16) Rasmussen, S. C.; Schwiderski, R. L.; Mulholland, M. E. *Chem. Commun.* **2011**, 11394-11410.

(17) Wen, L.; Rasmussen, S. C.; *Polym. Prepr.* **2007**, *48*, 132.

(18) Wen, L. *PhD Dissertation*, North Dakota State University, Fargo, ND, 2008.

(19) Nyugen, T. P.; Destruel, P. Electroluminescent Devices Based on Organic Materials and Conjugated Polymers. In *Handbook of Luminescence, Display Materials, and Devices,* Inouye, H. S.; Rohwer, L. S., Eds; Organic, American Scientific Publishers, Sevenson Ranch, CA, 2003; Vol 1; p 5.

(20) Amb, C. M.; Chen, S.; Graham, K. R.; Subbiah, J.; Small, C. E.; So, F.; Reynolds, J. R. *J. Am. Chem. Soc.* **2011**, *133*, 10062-10065.

(21) van Mulllekoma, H. A. M.; Vekemans, J. A. J. M.; Havinga, E. E.; Meijer, E. W. *Mater. Sci. Eng. R.* **2001**, *32*, 1-40.

(22) Helgesen, M.; Krebs, F. C. *Macromolecules* **2010**, *43*, 1253-1260.

(23) Steckler, T. T.; Zhang, X.; Hwang, J.; Honeyager, R.; Ohira, S.; Zhang, X.-H.; Grant, A.; Ellinger, S.; Odom, S. A.; Sweat, D.; Tanner, D. B.; Rinzler, A. G.; Barlow, S.; Brédas, J.-L.; Kippelen, B.; Marder, S. R.; Ryenolds, J. R. *J. Am. Chem. Soc.* **2008**, *131*, 2824-2826.

(24) Zhang, X.; Steckler, T. T.; Dasari, R. R.; Ohira, S.; Potscavage, W. J.; Tiwari, S. P.; Coppée, S.; Ellinger, Barlow, S.; Brédas, J.-L.; Kippelen, B.; Reynolds, J. R.; Marder, S. R. *J. Mater. Chem.* **2010**, *20*, 123-134.

(25) Zhang, X.; Shim, J. W.; Tiwari, S. P.; Zhang, Q.; Norton, J. E.; Wu, P.; Barlow, S.; Jenekhe, S. A.; Kippelen, B.; Brédas, J.-L.; Marder, S. R. *J. Mater. Chem.* **2011**, *21*, 4971-4982.

(26) Bundgaard, E.; Krebs, F. C.; *Sol. Energy. Mater. Sol. Cells* **2007**, *91*, 954-987.

(27) Chen, P.; Yang, G.; Liu, T.; Li, T.; Wang, M.; Huang, W. *Polym. Int.* **2006**, *55*, 473-490.

(28) Scherf, U.; List, E. J. W. *Adv. Mater.* **2002**, *14*, 477-487.

(29) Wu, W.-C.; Liu, C.-L.; Chen, W.-C. *Polymer*, **2006**, *47*, 527-538.

(30) Ashraf, R. S.; Hoppe, H.; Shahid, M.; Gobsch, G.; Sensfuss, S.; Klemm, E. *J. Polym. Sci. Part A: Polym. Chem.* **2006**, *44*, 6952-6961.

(31) Snaith, H. J.; Greenham, N. C.; Friend, R. H. *Adv. Mater.* **2004**, *16*, 1640-1645.

(32) Chua, L.-L.; Zaumseil, J.; Chang, J.-F.; Ou, E. C.-W.; Ho, P. K.-H.; Sirringhaus, H.; Friend, R. H. *Nature (London)* **2005**, *434*, 194-199.

(33) Bernius, M. T.; Inbasekaran, M.; O'Brien, J.; Wu, W. *Adv. Mater.* **2000**, *12*, 1737-1750.

(34) Chen, Z.; Bouffard, J.; Kooi, S. E.; Swager, T. M. *Macromolecules*, **2008**, *41*, 6672-6676.

(35) Patel, D. G.; Feng, F.; Ohnishi, Y.-y.; Abboud, K. A.; Shanze, K. S.; Reynolds, J. R. *J. Am. Chem. Soc.* **2012**, *134*, 2599-2612.

(36) Guo, X.; Kim, S. F.; Jenekhe, S. A.; Watson, M. D. *J. Am. Chem. Soc.* **2009**, *131*, 7206-7207.

(37) Carsten, B.; He, F.; Son, H. J.; Xu, T.; Yu, L. *Chem. Rev.* **2011**, *111*, 1493-1528.

(38) Sakamoto, J.; Rehahn, M.; Wenger, G.; Schlüter, A. D. *Macromol. Rapid Commun.* **2009**, *30*, 653-687.

(39) Lafrance, M.; Rowley, C. N.; Woo, T. K.; Fagnou, K. *J. Am. Chem. Soc*. **2006**, *316*, 8754-8756.

(40) Stuart, D. R.; Fagnou, K. *Science*, **2007**, *316*, 1172-1175.

(41) Campeau, L. C.; Bertrand-Laperle, M.; Leclerc, J. P.; Villemure, E.; Gorelsky, S.; Fagnou, K. *J. Am. Chem. Soc.* **2008**¸ *130*, 3276-3277.

(42) Lapointe, D.; Fagnou, K. *Chem. Lett.* **2010**¸ *39*, 1119.

(43) Ackermann, L.; Vicente, R.; Kapdi, A. R. *Angew. Chem. Int. Ed.* **2009**, *48*, 9792-9826.

(44) Do, H. Q.; Daugulis, O. *J. Am. Chem. Soc.* **2008**, *130*, 1128-1129.

(45) Lee, D. H.; Kwon, K. H.; Yi, C. S. *Science* **2011**, *333*, 1613-1616.

(46) Mori, A.; Sekiguchi, A.; Masui, K.; Shimada, T.; Horie, M.; Osakada, K.; Kawamoto, M.; Ikeda, T. *J. Am. Chem. Soc.* **2003**, *125*, 1700-1701.

(47) Mercier, L. G.; Leclerc, M. *Acc. Chem. Res.* DOI: 10.1021/ar3003305.

(48) Wang, Q.; Takita, R.; Kikuzaki, Y.; Ozawa, F. *J. Am. Chem. Soc.* **2010**, *132*, 11420-11421.

(49) Rudenko, A.; Wiley, C. A.; Tannaci, J. F.; Thompson, B. C. *J. Poly. Sci., Part A: Polym. Chem.* **2013**, *81*, 2660-2668.

(50) Blouin, N.; Michaud, A.; Leclerc, M. *Adv. Mater.* **2007**, *19*, 2295-2300.

(51) Zou, Y.; Gendron, D.; Badrou-Aïch, R.; Najari, A.; Tao, Y.; Leclerc, M. *Macromolecules* **2009**, *42*, 2891-2894.

(52) Mulholland, M. E.; Schwiderski, R. L.; Rasmussen, S. C. *Polym. Bull.* **2012**, *69*, 291-301.

(53) Cardona, C. M.; Li, W.; Kaifer, A. E.; Stockdale, D.; Bazan, G. C. *Adv. Mater.* **2011**, *23*, 2367-2371.

(54) Cho, S. Y.; Grimsdale, A. C.; Jones, D. J.; Watkins, S. E.; Holmes, A. B. *J. Am. Chem. Soc.* **2007**, *129*, 11910-11911.

(55) Anuragudon, P.; Newaz, P. P.; Phanichphant, S.; Lee, T. R. *Macromolecules* **2006**, *39*, 3494-3499.

CHAPTER 6. SUMMARY

6.1. Conclusion

Development of new 2nd generation thieno[3,4-*b*]pyrazines (TPs) was continued by synthesis of analogues featuring both electron-donating (ED) and electron-withdrawing (EW) side chains. The previously developed chemistry generating TPs with alkyloxy side chains was further optimized, giving near quantitative yields. The scope of these materials was also expanded by production of both the ethyloxy- and hexyloxy-substituted analogues. Both showed similar optical and electronic properties to previously studied systems. However, altering side chain allows for further tuning of bulk solid state properties in generated polymers.

In the interest at further expanding the electronic tuning of TP-based materials, generation of several TP systems with EW side chains was attempted, featuring both amide and keto functionalities. Attempts at generating the 2,3-(1-octanoyl)TP yielded only monosubstitution. Even attempts at further reacting this product in a second reaction yielded no product. However, the amide system, upon optimization of conditions yielded the product in 50% yield. This system showed the expected stabilization of frontier orbitals, yielding a HOMO at -6.7 eV, 0.5 eV lower than alkyl analogues. Absorption data also showed a significant red shift in the low energy charge transfer (CT) band of ~50 nm. Optimization of dicyanoTP synthesis was also attempted; however, no significant improvement was seen.

Continuing the work of Li Wen, homopolymers of TP units were generated by Grignard metathesis (GRIM) polymerization. This study included the extended chain C_{10}TP and C_{12}TP and alkyloxy OC_2TP and OC_6TP systems. The extended chains were generated in an attempt to increase molecular weight with the idea that longer side chains would cause the growing polymer to be more soluble, however, the opposite trend was seen likely due to side chain crystallization.

Despite the low molecular weight, optical and electronic properties were similar to that of the previously generated C_6TP polymer. Synthesis of the alkyloxy TP polymers were modified due to suspected binding of Mg to the oxygen lone pairs, requiring an additional 0.5 eq. of Grignard. These were successfully generated, showing the expected blue-shift in absorption and, in the case of the higher molecular weight pOC_6TP, a shift to a more negative potential of oxidation similar to effects seen in the monomer systems.

Donor-acceptor (DA) type copolymeric materials combining TPs with thiophene-based comonomers were generated via Stille cross-coupling polymerization. Dithieno[3,2-*b*:2',3'-*d*]pyrroles (DTPs) are a fused ring system featuring high charge carrier mobilities, which have been applied to numerous electronic devices. Combination of *N*-octylDTP with various TP units was performed in an effort to generate polymers featuring reasonable molecular weights with a low band gap and high HOMO. Absorption of these polymers covered most of the visible region and extended into the IR region. Although TPDTP copolymers seemed promising candidates for organic photovoltaics (OPV), upon fabrication of devices no photocurrent was generated. This is believed to be due to the high HOMO, restricting completion of the circuit. A second thiophene-based unit combined with TPs in copolymeric materials was benzo[1,2-*b*:4,5-*b'*]dithiophene. Two such BDTs were used in these copolymers. The first was an unfunctionalized BDT, which was combined with C_{12}TP in good yield and molecular weight (TPBDT1) (9700 Da). The second BDT unit featured phenyl-based 2-dodecylthiophene side chains. This unit was combined with both C_{12}TP and OC_6TP to generate copolymers TPBDT2 and TPBDT3, respectively, also in good yield. These latter two polymers also had molecular weights greater than 10 kDa. All three polymers show absorption covering the majority of the visible region and extending into the IR.

All three were applied to generate OPV devices, with the high efficiency of 0.52 for the polymer TPBDT2 in a polymer:$PC_{61}BM$ blend of 1:3.

A second group of TP DA copolymers were generated with phenyl-based systems including fluorene (FLO), 2,3,1-benzothiadiazole (BTD), and *N*-octylphthalimide (PTH). Two TPFLO copolymers were made with fluorene, using dodecyl and hexyloxy TP-based side chains. Both polymers had reasonable yield and the C_{12}TPFLO copolymer had a molecular weight at 4800 Da. Both were readily soluble several organic solvents. Optical measurements of both polymers were taken giving an onset of ~560 nm for pOC_6TPFLO (E_g = 2.0 eV) and ~640 for pC_{12}TPFLO (E_g = 1.9 eV), showing the expected blue shift, and thus an increase in band gap, going to the alkyloxy analogue. Cyclic voltammetry showed destabilization of the potential of oxidation for pOC_6TPFLO, also expected given the electron-donating nature of the TP-based side chains. An OPV devices was made from pC_{12}TPFLO, with a very low efficiency at 0.027%. However, no optimization of conditions has been attempted. A third terthienylTPFLO copolymer was made with thiophenes between the two units. This polymer contained TP-based –OC_6 side chains. Absorption spectra were taken which showed a further blue shift of the CT band onset (~540 nm) from the pC_{12}TPFLO, thus resulting in a larger band gap (2.3 eV). However, while an increase in band gap is expected, as was seen with pOC_6TPFLO, the degree of this increase is likely due to low molecular weight. Optimization of polymerization would likely result in both a decrease in band gap and increase in potential of oxidation.

Direct (hetero)arylation polycondensation techniques were used to generate the other two copolymers combining C_{12}TP and aryl-based systems. The two aryl groups used for these were BTD and PTH. Conditions were changed slightly between the two polymers where THF was used in the generation of pTPBTD and toluene in the generation of pTPBTD. Although the

molecular weight of pTPPTH was over twice that of pTPBTD, the latter polymer had both superior optical and electronic properties. Absorption of pTPBTD covered most of the visible and into the IR region. Electrochemical studies showed both a clear reduction potential and potential of oxidation. Absorption onset of pTPPTH occurred at 600 nm, giving a larger band gap of 2.0 eV and electrochemical studies showed the polymer to be electrochemically inactive. Due to the optical and electronic properties of pTPBTD, OPV devices were manufactured, however, efficiencies were very low at 0.02 and 0.01%. Much of the low efficiency is likely due to molecular weight issues causing poor film morphology.

6.2. Future Directions

Although the current library of TP materials has been expanded to include both electron-donating and withdrawing groups along with the extensively researched alkyl and aryl analogues, further development of new TP materials is of great interest. Development of TPs featuring EW alkyl side chains is desired as they will introduce the desired electronic effect while maintaining high solubility. A second group of interest for development is that of water solubilizing side chains, involving ionic species including carboxylates. Polymerization of the remaining 2nd generation TPs will allow a more extensive study of the effect of side chain on polymer properties. In this regard the amide TP may be a polymer of particular interest for EW side chains. However, due to potential reaction of a Grignard at the side chain-based carbonyls, alternate polymerization techniques may be required.

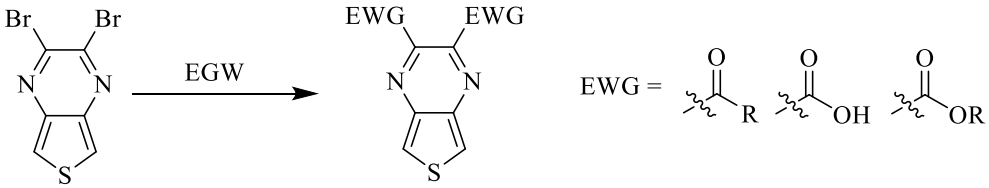

Scheme 6.1. Generation of new TPs featuring EW side chains.

Continuing the generation of new TP-based copolymers would allow for further understanding of structure-function relationships aimed at improving optical, electronic, and film properties for generation of improved device performance. Of particular interest is utilization of TPs featuring EW side chains with both previously investigated and new comonomeric units. Direct (hetero)arylation shows promise in generating TP-based copolymers and so optimizing conditions for this technique may produce materials of higher quality than previously available. In an interest of furthering the scope of TP materials, introduction of vinyl spacer in copolymers is of interest to further increase electron delocalization. Application of new TP-based materials and continuing optimization of existing materials may yield greater efficiency electronic devices, giving further insight into future goals with this unique ambipolar unit.

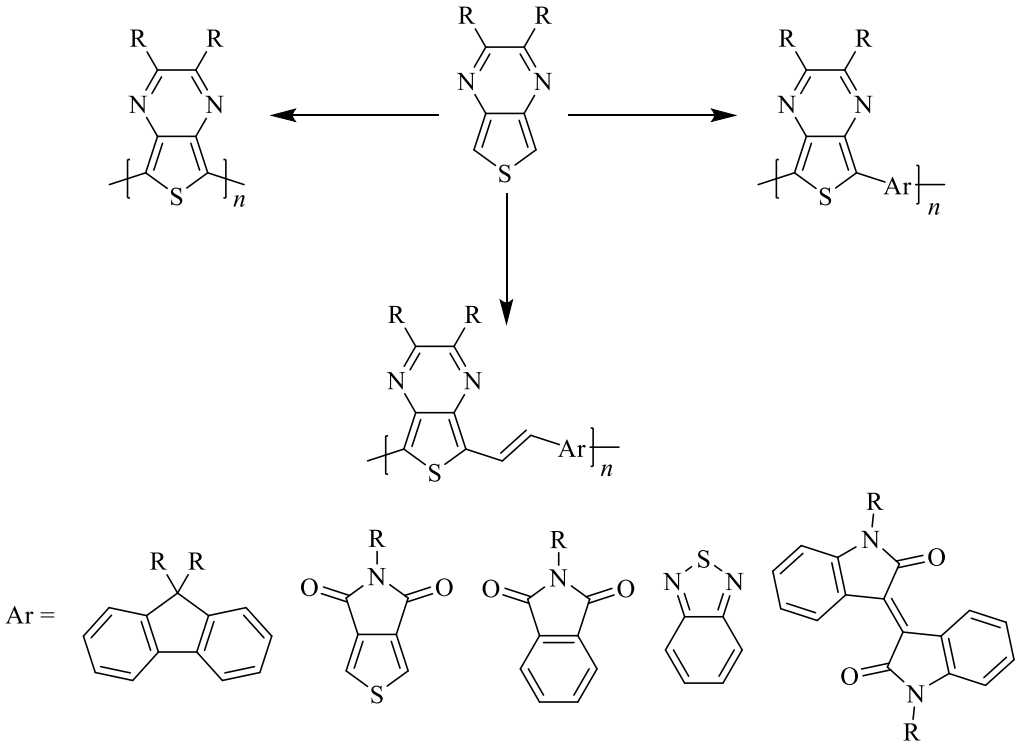

Scheme 6.2. Generalized plan of future work with TP-based materials.